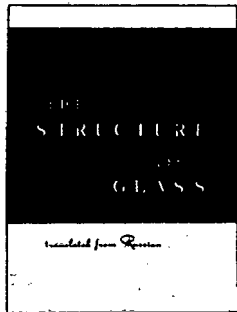# THE SOVIET JOURNAL OF

ATOMIC ENERGY

Атомная энергия

TRANSLATED FROM RUSSIAN

CONSULTANTS BUREAU

THE STRUCTURE OF GLASS

Volume 2

Proceedings of the Third All-Union Conference on the Glassy State, held in Leningrad, November 16-20, 1959.

This notable volume contains papers presented at the conference convened by the Institute of Silicate Chemistry of the Academy of Sciences, USSR, the D. I. Mendeleev All-Union Chemical Society, and the S. I. Vavilov (Order of Lenin) State Optical Institute for discussion of recent experimental studies of various properties of glass, the principal methods for investigating glass structure, and the problem of glass formation.

A complete account is given of research work on the glassy state since the previous conference. The most modern optical, spectroscopic, and electrical techniques were used in studying the structure of glass in all its aspects, and the results are interpreted in the light of contemporary physical theories of the solid state.

Volume 2: $25.00

Volume 1

Proceedings of the Second All-Union Conference on the Glassy State.

". . . The Glass Division of the American Ceramic Society and the National Science Foundation are to be congratulated for making this inspiring collection available . . ." — *Journal of Chemical Education*

"The book should be of great interest to scientific and technical personnel interested in glass technology, ceramics, the states of matter, and any work involving the vitreous state. They should all have the experience of reading this book." — *Chemistry in Canada*

". . . a stimulating experience . . ."
— *Trans. British Ceramic Society*

". . . lively discussions which show the diversity of opinions on every experimental report."
— *The Glass Industry*

". . . the volume is excellent . . . the translation was well worth while . . ."
— *R. W. Douglas, Nature*

Volume 1: $20.00

Volumes 1 and 2: $40.00 per set

492 pages · **illustrated**

296 pages · **illustrated**

Complete contents available upon request

CONSULTANTS BUREAU
227 W. 17 ST., NEW YORK 11, N. Y.

THE SOVIET JOURNAL OF

ATOMIC ENERGY

A translation of ATOMNAYA ÉNERGIYA,
a publication of the Academy of Sciences of the USSR

(Russian original dated August, 1959)

Vol. 7, No. 2   February, 1961

CONTENTS

CONTENTS (continued)

NOTE

The Table of Contents lists all material that appears in Atomnaya Énergiya. Those items that originated in the English language are not included in the translation and are shown enclosed in brackets. Whenever possible, the English-language source containing the omitted reports will be given.

Consultants Bureau Enterprises, Inc.

INDUSTRIAL PRODUCTION OF HEAVY WATER

M. P. Malkov

This article takes up possible methods for producing heavy water on an industrial scale. The most economically competitive methods are described and they are compared in their engineering and economic aspects. Low-temperature distillation and the hydrogen sulfide (dual-temperature exchange) processes are viewed as the best.

Heavy water is an important commodity for nuclear power engineering, where it meets with widespread use as moderator of fast neutrons and as coolant. Heavy water possesses some advantages over other moderators (Table 1).

However, heavy water has one outstanding drawback as moderator: irradiation decomposes it into oxygen and deuterium, which imposes the requirement of special measures to effect the continuous recombination of the oxygen and deuterium evolved.

The following specifications have been set in the USA for reactor-grade heavy water [2]: D_2O content not less than 99.7 wt. % after introducing corrections for O^{18}, and not less than 99.75 wt. % on the average per sample (pH = 6-6.6).

The chemical purity is monitored by measuring the electrical conductivity; the use of heavy water with a resistivity of 15 μohm/cm is permissible.

A nuclear power station of average power rating requires 100-250 tons of heavy water. A power economy based on heavy-water reactors, would thus require the production of thousands of tons. It is therefore, imperative to bring the price of heavy water as low as possible.

The opinion entertained in the USA is that nuclear electric power stations, may become competitive with coal-fired stations, if the cost of 1 kg of heavy water is not higher than 90 dollars. The market price of 1 kg of heavy water stood at 150–200 dollars for a long period [2–5], but is now 62 dollars.

The difficulties attending the production of heavy water are due mainly to the fact, that deuterium is encountered in extremely low abundance in natural hydrogen containing compounds: it constitutes about 1 part per 7 thousand parts of hydrogen. The method used for extracting the deuterium must then be one that combines processing huge amounts of raw hydrogen with low energy input and low capital expenditures.

Much work has been done in various countries to find new methods for isolating deuterium, but only a few of them have proved economically feasible for use on an industrial scale.

Separation of a mixture of hydrogen isotopes is based in practice on the difference in the physical properties of its components; this difference resides in the dimensions of the molecules, their mass, magnetic properties, and on the intermolecular interaction forces.

The following methods have been studied with respect to separation of mixtures of hydrogen isotopes: diffusion through porous membranes and centrifugation; electrolysis of water; chemical isotope exchange; fractional distillation of hydrogen-containing compounds (H_2O, NH_3, etc.), fractional distillation of liquid hydrogen; adsorption, absorption, and ion exchange; thermal diffusion; extraction and fractional crystallization.

Only the following methods were found suitable for industry: electrolysis of water; various modification of chemical isotope-exchange processes; fractional distillation of hydrogen-containing compounds; absorption; fractional distillation of liquid hydrogen.

Some of these methods are now being applied in the industrial production of heavy water.

With respect to the raw feed material used, the methods employed in the production of heavy water may be broken down into two groupings:

1. Methods using intermediate products from another process than the feed (e.g., hydrogen obtained in synthetic ammonia plants or in hydrogenation plants, or

TABLE 1. Properties of Several Moderators [1]

Properties	H_2O	D_2O	Be	C	BeO
Atomic or molecular weight	18	20	9	12	25
Capture cross section at 0.025 ev, barns	0,66	$0,92 \cdot 10^{-3}$	$9 \cdot 10^{-3}$	$4,5 \cdot 10^{-3}$	$9,2 \cdot 10^{-3}$
Scattering cross sec. at 0.025 ev, barns	110	15	6,9	4,8	11,1
Slowing-down constant	67	5820	160	169	180

613
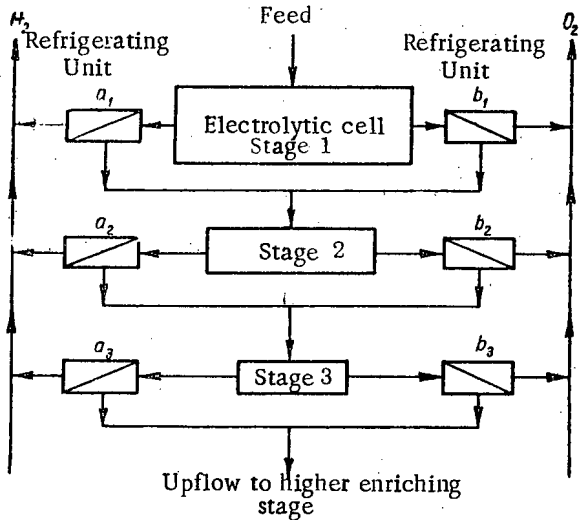
Fig. 1. Flowsheet of electrolytic production of heavy water.

electrolytically produced hydrogen, etc). For example, from the hydrogen processed at synthetic-ammonia plants, 0.21 kg of heavy water per ton of ammonia produced may be extracted, i.e., a plant with an annual capacity of 100,000 tons of ammonia, may yield in excess of 20 tons of heavy water annually [4].

2. Methods using a feed not derived from other processes (e.g., distillation of light water or isotope exchange involving light water). The second grouping has the advantage that the production of heavy water is not limited by the nature of the feed.

We shall now briefly discuss the methods which are of interest on an industrial scale.

Electrolysis of Water. The electrolytic technique for separting the isotopes of hydrogen was discovered as far back as 1932. The essence of the approach consists in the presence of an enhanced yield of heavy water (three to eight times that in the feed material) in the undecomposed residue, upon electrolysis of ordinary water. The hydrogen fraction with lower deuterium content is given off with the gas in electrolysis, and a buildup of the heavy isotope of hydrogen takes place in the electrolyte. Until the Second World War, electrolysis was considered the sole technically feasible method for the production of heavy water on a large scale (used by the Norsk-Hydro company at Rjukan, Norway).

Figure 1 shows a flowsheet of a continuously operating bank of electrolyzers. The constant level of the liquid in the principal electrolytic cell (stage one) is maintained by addition of makeup water. The water condensing as the hydrogen and oxygen are dried in the refrigerating units a_1 and b_1 enters the second stage as feed. Cooling units a_2 and b_2 feed the third stage, and so forth. The dimensions of the electrolytic cells are tapered off as the deuterium concentration in the water increases.

This type of cascade of cells is not feasible for the production of heavy water in high concentration, since hydrogen heavily enriched in deuterium is obtained from

the last stages, as a result of which the degree of extraction of deuterium falls in the arrangement. In order to raise the degree of extraction of deuterium, the gas may be burned from the cells, which yields hydrogen with enriched deuterium content, and the water forming in the cells containing a corresponding concentration of deuterium in the electrolyte may be recycled. The percentage of hydrogen and oxygen produced for chemical purposes is reduced in that method, and the production costs for heavy water are increased.

The degree of separation of heavy water by simple electrolysis is quite low (~ 8–10%) [4]. If the entire supply of electric power were to be consumed solely in
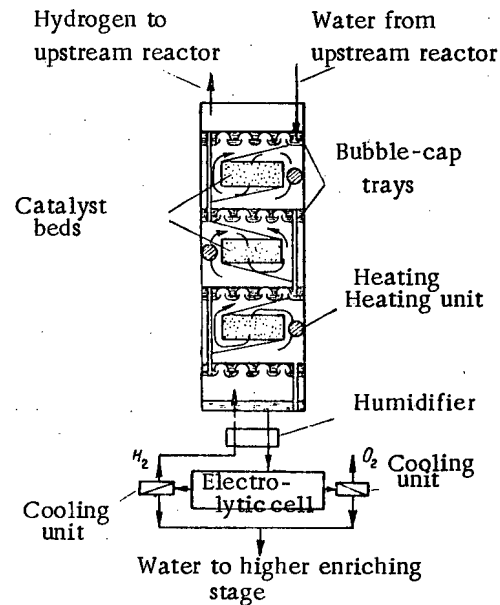
Fig. 2. Flow diagram of joint operation of electrolytic cells and isotope-exchange reactor.

the production of heavy water in that process, as an example, this would amount to 120–150 thousand kw-hr per kg of heavy water. Production of heavy water by simple electrolysis is thus shown to be highly uneconomical. The degree of separation of deuterium may be increased in the electrolytic process without resorting to burning the hydrogen, however. To do this, the deuterium is extracted from the deuterium-enriched hydrogen stream in the final stages of the electrolysis sequence by means of catalytic isotope exchange with the condensed water of the preceding stages. The heavy-hydrogen isotope accumulates in the water, which yields the possibility of the deuterium to the liquid phase.

Figure 2 shows a flowsheet for this variant of joint operation of an electrolyzer stage with an isotope-exchange reactor. Water from the previous electrolytic stage is fed to the top of the reactor. Water enriched in deuterium from the gaseous phase is allowed to flow in successively from one tray to the next and is admitted to the electrolytic cells. Hydrogen from those cells proceeds to the bottom of the reactor where it is mixed

614

with water vapor. Phase exchange takes place on the catalyst bed placed between the trays, as a result of which the deuterium from the hydrogen is converted to steam (K > 1) and later condensed on the trays.

A similar flowsheet for operation of an isotope-exchange reactor in series with each electrolysis stage has been devised. The degree of separation of deuterium may be increased considerably over that resulting from the simple electrolytic technique.

The combination of the electrolytic and isotope exchange arrangements is widely used in industry.

Chemical Isotope Exchange. From the viewpoint of practicability, the following reactions are of greatest interest:

$$H_2O + HD \rightleftarrows HDO + H_2 \begin{bmatrix} K = 2,69 & at & 100° C \\ K = 3,62 & at & 25° C \end{bmatrix};$$

$$H_2O + HDS \rightleftarrows HDO + H_2S \begin{bmatrix} K = 1,92 & at & 100° C \\ K = 2,34 & at & 25° C \end{bmatrix};$$

$$NH_3 + HD \rightleftarrows NH_2D + H_2 \quad [K = 5,83 \quad at \quad 25° C].$$
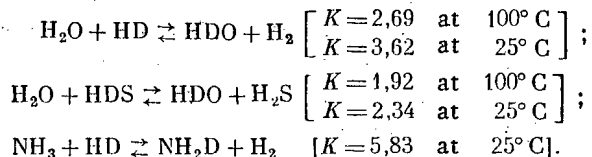
The method of separation is based on the fact that the equilibrium ratio of deuterium and hydrogen in those reactions is different in one pair ($H_2O + HDO$) from the same ratio in the other pair ($H_2 + HD$). If the substances are contacted in countercurrent, the deuterium may be separated in the same manner as in an absorption process.

Two exchange processes are known:

1) the simple equilibrium chemical exchange at some optimum temperature, constituting a conversion of a compound enriched in deuterium (e.g., the deuterium of HDO goes over into HD);

2) the "dual-temperature" exchange process in which some hydrogen-containing compound is used in a closed cycle. The isotope exchange is carried through at two different temperature levels and, consequently, at different equilibrium ratios, which provides the conditions for continuous concentration of the deuterium.

Simple exchange of isotopes proves to be economically feasible only for the water vapor–hydrogen reaction. It is possible to design a cascade of reactors with platinum or chrome-nickel catalysts where the exchange reaction proceeds in the vapor phase, while each succeeding reactor is fed by the water from the preceding stage. As indicated above, simple isotope exchange is being successfully employed in combination with electrolysis of water.

The most promising approach is the dual-temperature process. Many isotope-exchange reactions find successful application in this process: of particular interest is the reaction $HDS + H_2O$, which proceeds at a rather rapid rate without benefit of catalyst. The simplest scheme for this reaction is shown in Fig. 3.

The feed water passes down through two bubble-cap towers A and B in series, the top tower operating at a temperature of 25°C, and the downstream unit at 100°C. The equilibrium constant of the exchange reaction be-
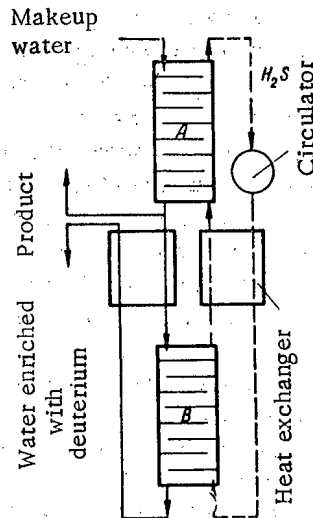
Fig. 3. Flow scheme of a "dual-temperature" exchange process.

tween hydrogen sulfide and water at 25°C is 2.34, and at 100°C is 1.92. In both columns, the hydrogen sulfide and the water circulate in countercurrent. Deuterium begins to accumulate in the streams between the two columns in line with the equilibrium constants. The intermediate heat exchangers recover the heat from the streams passing from one column to the next. The degree of separation of deuterium by this method is about 15% [4].

The simplicity of the scheme and the comparatively low energy input make this process the most promising one. The disadvantage inherent in the method is corrosion of the associated equipment. These difficulties seem to have been surmounted in the USA so that the method described is widely used on an industrial scale in the USA for the production of heavy water, and proves to be highly economical [4, 5, 7].

The method may in principle become still more economical if gaseous hydrogen sulfide, which requires comparatively high-powered compressors to get it to circulate, is replaced by some liquid compound with suitable equilibrium constants for the reaction with water. Aside from the choice of some such compound, difficulties arise here in connection with the establishment of a satisfactory reaction rate for isotope exchange between liquid phases.

In the dual-temperature process, the $H_2O + HD$ system is characterized by more favorable constants than the $H_2O + HDS$ system. The engineering of this process requires an expensive tower with catalysts, and the maintenance of different pressure levels in the cold and hot towers. However, the operating conditions of this system may be significantly improved by using a catalyst in the form of a sol or slurry [8]. Suitable catalysts are provided by metals of the platinum group and nickel deposited on activated charcoal or chromium oxide to increase the active area. An advantage of this system over the dual-temperature hydrogen sulfide process is also found in

615

the fact that water circulates with the catalyst in the closed cycle, instead of hydrogen sulfide, so that the amount of energy consumed in circulation is greatly reduced. The source of deuterium for this process may be hydrogen produced in some other manner, e.g., the gas used in the production of synthetic ammonia, or hydrogen used in hydrogenation processes.

As calculation have demonstrated [8], the circulating flow in that system will be four to five times less than in the H_2S system. Calculations based on equilibrium constants with the process rate accounted for show that the temperature of the cold tower may be 30°C, while that of the hot tower is 200°C. The process proceeds better at a pressure of 200 atmos. When the production of large quantities of heavy water is called for, this process must be highly economical [8]. At the present time it has not yet been developed for industrial-scale use, and only pilot-plant and design research is in progress.

To sum up, different modifications of the dual-temperature exchange process, must be acknowledged to be the most promising methods for separating deuterium, while one of the variants, the hydrogen sulfide process, has already been applied on an industrial scale, and may become one of the most economical methods.

Fractional Distillation of Hydrogen-Containing Compounds. This method is based on the possibility of distillation, when there is a sufficiently large difference between the vapor tensions of the hydrogen and deuterium compounds.

Table 2 lists data giving the ratios of the vapor tensions of the most commonly encountered hydrogen compounds and corresponding deuterium compounds at the triple point and at the boiling point, under normal conditions.

TABLE 2. Vapor-Pressure Ratios of Hydrogen and Deuterium Compounds under Different Conditions

Compounds	At triple point	At boiling point under normal conditions
H_2O/HDO	1,12	1,026
NH_3/NH_2D	1,08	1,036
CH_4/CH_3D	1,0016	0,9965
H_2/HD	3,6	1,7

The method of fractional distillation of water is exceptionally simple in its arrangement, and reliable in operation. Industrial plants based on this method were build in the USA during the Second World War.

As a result of the relatively low value of the separation factor the number of trays for producing the end product is very large, more than 700, which then brings about a need for a large number of very high towers.

Figure 4 shows a simplified flowsheet of the first two stages of a facility for separating heavy water by a distillation procedure. In each stage, the towers operate

in series and thus comprise, as it were, a single tower unit. The water is pumped from tower to tower.

The advantage of this method is the unlimited supply of raw material. A disadvantage in this method is that the relative difference in the vapor tensions of H_2O and HDO drops sharply as the temperature goes up, so that operation at low pressures and, consequently, with towers of larger diameter is necessitated. No small amount of difficulty is occasioned by the small vapor-pressure drop along the height of the column. The degree of separation of deuterium by the fractional-distillation method is small (~ 3-4%). In the USA, such facilities were closed down as unprofitable after a prolonged operating experience. The cost of a single kg of heavy water produced at those plants was 300-500 dollars. The economic competitiveness of the process of extracting deuterium by the water-distillation method may be enhanced by using heat pumping action, i.e., by secondary compression of steam for heating the column still, and utilizing other improvements.

It is obvious that this method may become profitable only on condition that costs of the low temperature heat sources be exceptionally low. Such conditions may be had, e.g., in geyser regions. According to available information [4], a combine consisting of a facility for extraction of heavy water by the distillation method and an electric-power generating station operated on the heat from geothermal vapors is being built.
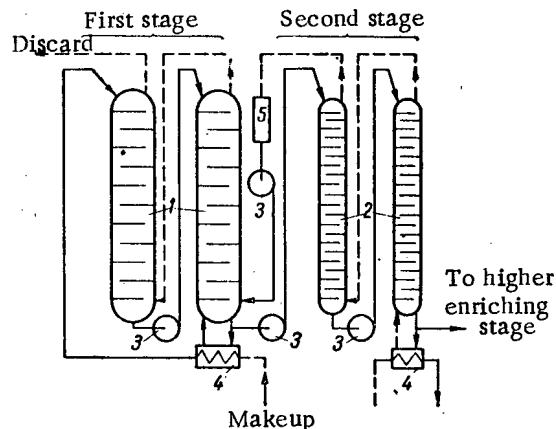
Fig. 4. Flowsheet of facility for extracting heavy water by the water-distillation method.

The fractional distillation of liquid ammonia has attracted great interest. It is quite true that this process must be carried to completion under more exacting conditions than the process of fractional distillation of water. The scales of the industrial enterprises processing ammonia are limited. The rectification process may be combined with an ammonia–water isotope-exchange process, but this results in much higher costs.

The British "CJB" firm has developed a process for producing heavy water in which a hydrogen-ammonia isotope-exchange step is combined with subsequent rectification of liquid ammonia. In the first isotope-exchange

column, operating at a pressure of 250 atmos. and a temperature of -40°C, the deuterium concentration in the ammonia is quintupled. This ammonia is admitted to the system of two columns, whose operation is based on the dual-temperature process. The cold tower operates at a temperature of -40°C, while the hot tower runs at +100°C. Hydrogen serves as a gaseous circulating medium. At this point, the concentration of deuterium in the ammonia is again quintupled. The hydrogen-ammonia isotope-exchange process takes place only in the presence of a catalyst suspended in the liquid ammonia. Ammonia enriched 20-25 times in deuterium thus enters the system of rectifying towers. To improve the economic performance of this rectification process the heat pump principle is resorted to: the overhead ammonia vapors drawn from the top of the column are compressed by a compressor and fed to the column still coils for reheating.

According to the data of the company, the cost of 1 kg of heavy water obtained by this process is ~ 48 dollars; capital outlay comes to ~ 230,000 dollars, scaled to the production of one ton of heavy water annually.

Methane is not suitable as feed since the relative volatilities of CH_4 and CH_3D are close to unity. The same reason rules out the successful use of other more complex hydrogenous compounds.

Absorption. This approach is based on the differential solubility of gaseous H_2 and HD in the absorbing medium. A large assortment of solvents have been studied experimentally and theoretically [6]: NH_3, SO_2, CH_4, H_2S, NO, CO_2, A, N_2, Ne. These studies were performed over a wide range of pressures (1-200 atmos.) and temperatures (27°-239°K). It was found, that in almost all cases HD dissolves better than H_2. The ratio of the Henry coefficients may be used as a measure of the possibility of separation. For most absorbents, this ratio lies within the range 1.03-1.2; for liquid neon, it is very high (~ 3.24). Using the best solubility of HD in liquid, it is possible to set up a scheme of continuous extraction of deuterium from some gas containing hydrogen (e.g., from a gas such as synthesis gas used in the production of ammonia) by scrubbing it with liquid absorbent (nitrogen or neon) in passage through the tower. Calculations based on such schemes have shown that the energy input per kg of D_2O must amount to 8-15,000 kw-hr [6]. Making this process a reality involves great engineering difficulties and no way has yet been found to surmount them.

Fractional Distillation of Liquid Hydrogen. The search for cheaper ways of manufacturing deuterium led to the study of the possibility of extracting the heavy isotope of hydrogen directly by rectification of liquid hydrogen.

Such a method is entirely possible in principle, since the boiling point of deuterium is 23.5°K and that of hydrogen 20.38°K, i.e., the difference in the boiling points attains 3.12°K. In practice, because what is

present in the hydrogen is not D_2, but HD whose boiling point lies between that of hydrogen and deuterium (22.13°K to be exact, the difference does not exceed 1.75°K. This difference in boiling points suffices to provide a very high enrichment factor of 1.7.

The feasibility of enriching deuterium by a simple evaporation of liquid hydrogen was first proven under laboratory conditions in 1932 [9]. In 1933, a small tower was used on a laboratory scale for enriching liquid hydrogen with deuterium [10].

As calculations demonstrated, this method for producing heavy water requires rather low capital expenditures and involves relatively low input [2,4,5,11,12], e.g., in order to extract 1 kg of D_2O, 4-5000 kw-hr of energy must be supplied.

The method of fractional distillation of liquid hydrogen thus comprises one of the cheapest and most efficient methods of deuterium separation. However, this interesting method is so novel and so unusual from the engineering standpoint (i.e., fractional distillation of liquid hydrogen and the attendant secondary processes), that much preparatory research work would have to be carried out to make it a reality.

Plans and designs for large-scale heavy-water separation facilities based on this approach were actually worked out in the USA in 1950-1951; but while all of the experts acknowledged the economic soundness of the method, American specialists were unable to solve all of the scientific and engineering problems standing in the way, and the facilities were not constructed.

In processing hydrogen by the refrigeration method, the decisive point is the removal of impurities from the hydrogen. For example, when the hydrogen contains appreciable amounts of oxygen and nitrogen, these substances freeze and plug up the tubes when cooled to the boiling point of hydrogen, thus impairing the normal operation of the separation units. It is known that oxygen impurities may be readily removed by catalytic hydrogenation, as is done with melanges in synthetic-ammonia plants and in the liquefication of hydrogen [13].

When the hydrogen contains appreciable nitrogen impurities (over 3-4%), as does, for example, a melange (25% N_2 and 75% H_2), removal of the first batches of impurities is carried out with relative ease: when the starting mixture is cooled down, the nitrogen liquefies and is continuously rejected, while the entire hydrogen fraction remains in the gaseous phase. The nitrogen residues may be frozen out in reversible heat exchangers, or else absorbed in refrigerated absorbent [2,4,5,12,14,15].

Figure 5 shows a flow diagram for the separation of deuterium from hydrogen by the refrigeration method. The initial hydrogen, at a pressure of 2-3 atmos after cooling in the heat exchangers (not shown in the diagram) to a temperature close to the saturation point, i.e., close to ~ 25°K, is admitted to the midsection of the rectifying tower L. The reflux from this column is high-pressure recycled hydrogen which is cooled in the

617

heat exchanger and in the coils of the still of column I, after which the hydrogen stream is throttled and admitted in liquid form to the top of the column. The recycled hydrogen is simultaneously used for balancing off the cold losses of the entire facility, for which purpose it is compressed to high pressures. To compensate for cold losses, reciprocating or turbo-driven expansion engines may also be used. A concentrate containing 5-10% HD is drawn off from the still of column. The degree of separation of HD in the column may be stepped up to 90-95%. This unit, which may be termed the first separation stage, is basic both with respect to energy consumption and with respect to equipment costs, in the entire process of extraction of deuterium from hydrogen. The second enrichment stage consists in obtaining ~ 100% HD from the 5-10% concentrate. To achieve this, the concentrate produced in the first stage is fed to the fractionating column II. The semifinished overhead product from this column is then recycled to column I of the first stage in order to recover the remaining HD. All the ~100% HD drawn off from the still of column II is passed through heat exchanger T-1 and fed to the contacting unit P where the reaction

$$2\ HD \rightleftharpoons H_2 + D_2$$
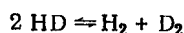
takes place.

After the HD is passed through the contacting unit, a ternary mixture containing ~ 50% HD, 25% D_2, and 25% H_2 is formed. In order to separate out 100% deuterium, this mixture is then passed through heat exchanger T-1 and fed to the fractionating column III, which works in a manner similar to column II. The product taken off the top of the column, which may be viewed as discard from this stage, is recycled to column II as feedstock for the extraction of HD and D_2. The second stage, and particularly the third stage, are tapered off in dimensions, being incommensurably smaller than the first stage.

It should be noted that the scheme described reflects only the general operating principles of the arrangement, and the concentrations of the intermediate products referred to may therefore take on other values,
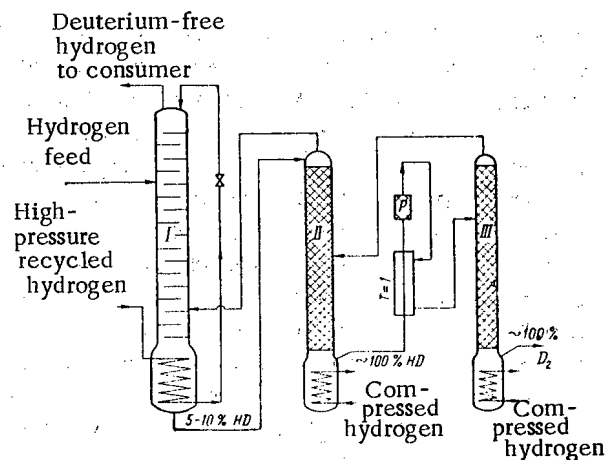
Fig. 5. Flowsheet for separation of deuterium by the refrigeration method.

just as a different combination of the operation of the discrete stages is also possible.

The feedstock used in this method depends on the sources of the hydrogen used (synthetic-ammonia plants, hydrogenation plants, etc.), so that while the sources of feed are quite ample, they are not unlimited. Production could be rendered independent of the source of raw hydrogen by introducing a closed hydrogen cycle, the deuterium content of which would be renewed continuously by isotope exchange with water vapor at high temperatures [5]. Capital and operating costs would naturally rise.

In the Soviet Union, the method of low-temperature distillation in deuterium production, has been realized on an industrial scale. Details on the technique were reported in a paper submitted to the Second International Conference on the Peaceful Uses of Atomic Energy [12]. Prolonged operational experience in production based on this method has completely confirmed all of the design data, with no complications of any kind hindering the successful carrying out of the process. Thus, the USSR was the first to achieve the transition, on an industrial scale, from the region of temperatures of around 80°K, widely used for separating air, to the region

TABLE 3. Comparative Data on Several Industrial-Scale Methods Used in the Production of Heavy Water

Parameter	Fractional distillation of water	Hydrogen–water isotope exchange in combination with electrolysis	Fractional distillation of liquid hydrogen	Hydrogen sulfide method combination with fractional distillation and electrolysis of water
Input of electric power (kw-hr) or steam (tons) per 1 kg D_2O	178 tons of steam (lower isotherm)	70,000 kw-hr	4-5000 kw-hr	> 65 tons steam plus ~ 400 kw-hr
Plant costs based on capacity of 1 kg D_2O per year, $ thousands	1100	400	300-350	360
Operating unit cost of 1 kg D_2O (capital expenses not included) dollars	340	132	35	30
Equilibrium settling time	4-5 mos.	15-18 mos.	20-50 mos.	--
Degree of separation of D_2O, %	3,7	43	90-95	< 18

of 20°K, for the separation of hydrogen isotopes.

In late 1958, the Hochst and Linde firms started up (in Frankfurt am Main, Germany) a pilot plant for the production of deuterium by the low-temperature distillation method from gases by-produced at a nitrogen fertilizer works [16]. This plant is designed for a capacity of 6 tons of D_2O annually, with a future scale-up to 10 tons proposed. The L'Aire Liquide Corporation (Toulouse, France) is also inaugurating a pilot plant with a capacity of 4000 cubic meters per hour of gas as feed to synthetic-ammonia plants [17].

In several cases, the simultaneous exploitation of various enrichment processes, may prove to be economical in the production of heavy water. For example, the USA's largest heavy-water plant, at Savannah River, uses three methods [7]: 1) the dual-temperature hydrogen sulfide process for producing 15% D_2O; 2) vacuum distillation of water to produce 90% D_2O; 3) electrolysis to obtain 99.75% reactor-grade D_2O.

In India, a plant based on an electrolytic processing facility [18], where hydrogen samples with deuterium content three times that found in nature will be produced, has been proposed, and the hydrogen so obtained will be processed further through the low-temperature distillation method to extract the remaining deuterium. According to calculations, the cost per kg of heavy water will not exceed 60 dollars.

Comparative data on several industrial methods in heavy-water production are entered in Table 3 above [2, 7].

To sum up, fairly reliable and economical methods have been worked out on an industrial scale for the production of heavy water at the present time. The most sophisticated of those methods are agreed upon as the low-temperature fractional-distillation method and the dual-temperature hydrogen-sulfide-exchange process. There is every justification for the assumption that, with future improvements in existing processes and the elaboration of new ones, unit costs of heavy water can be reduced and the economic performance of nuclear power reactors using heavy water can be improved at the same time.

LITERATURE CITED

1. R. Stephenson, Introduction to Nuclear Engineering (McGraw-Hill, N.Y., 1954).
2. P. Selak and J. Finke, Chem. Eng. Prog. 50, 221 (1954).
3. G. M. Murphy (editor), Production of Heavy Water (McGraw-Hill, N.Y., 1955).
4. W. Becker, Angew. Chem. 68, No. 1 (1956).
5. M. Benedict, "Survey of heavy-water production processes," P/819, Vol. 4, Geneva 1958.
6. D. Augood, Trans. Inst. Chem. Eng. 35, 394 (1957).
7. W. Bebbington and V. Thayer, "Concentration of heavy water by distillation and electrolysis," P/1065, Vol. 4, Geneva 1958.
8. E. Becker, R. Hübener, and R. Kessler, Chem.-Ing. Tech. 5, 288 (1958).
9. H. Urey, F. Brickwedde, and G. Murphy, Phys. Rev. 39, 864 (1932); 40, 464 (1932).
10. W. Keesom, H. van Dijk, and J. Heantyes, Commun Kamerlingh Onnes Lab. Univ. Leiden 20, 1 (1933).
11. K. Clusius and K. Starke, Z. Naturforsch 4a, 549 (1949).
12. M. P. Malkov, A. G. Zel'dovich, A. B. Fradkov, and I. B. Danilov, P/2323, Vol. 4 Geneva 1958.
13. G. Koplen, J. Amer. Rocket Soc. 22, 6 (1952).
14. W. Denton, B. Shaw, and D. Ward, Trans. Inst. Chem. Eng. 36, 179 (1958).
15. B. Bailey, "Some aspects of heavy-water production by distillation of hydrogen," P/1063, Vol. 4, Geneva 1958.
16. Chem. Ind. 10, 712 (1958).
17. Chem. Eng. Progr. 54, 126 (1958).
18. D. Gami, D. Gupta, N. Prasad, and K. Sharma, "Production of heavy water in India," P/1649, Vol. 4 Geneva 1958.

SORPTION METHODS OF SEPARATING BARIUM AND RADIUM, ALUMINUM AND GALLUM, AND ZIRCONIUM AND HAFNIUM

B. N. Laskorin, V. S. Ul'yanov, R. A. Sviridova, A. M. Arzhatkin, and A. I. Yuzhin

Chromatographic methods of separating elements with very similar properties have now been developed. However, a number of these methods are difficult to use industrially as their throughput is low. The efficiency of chromatographic separation methods could be increased considerably by using appropriate complex formers, which decrease the effective concentration of the ions being separated, and, in the first approximation, this is equivalent to a decrease in the amount of elements being separated. The difference in the formation constants of the complex compounds increases the separation coefficient. By investigating chromatographic separation with the use of various complex formers, we found the optimal conditions for separating barium and radium, zirconium and hafnium, and aluminum and gallium. The throughput of these methods, with respect to the macroelement was 15-60 kg/ hr per m² of column cross section.

Separation of Barium and Radium

Barium and radium have been separated chromatographically [1]. An ammonium citrate solution was used as eluant. The investigations were carried out with milligram amounts of substance of Dowex-50 cationite. It was shown that it is possible in principle to separate barium and radium, though insufficient grounds were given for the selection of the conditions and separation method.

We investigated the statics and dynamics of the separation of barium and radium, using various complex formers, to find the optimal conditions for their chromatographic separation.

The main value characterizing the sorption of an ion by a cationite or anionite is the distribution coefficient K_d. The ratio of the distribution coefficients of two ions gives the separation coefficient K_s.

Table 1 gives the values of the distribution and the separation coefficients of barium and radium on various ion-exchange resins.

Sulfonate cationites with the greatest percent of cross-linkage, have the maximum distribution and separation coefficients. The data obtained agreed qualitatively with the results given in [2-4].

For the separation it is advantageous to have the maximum value of K_s. However, with an increase in the percent of cross-linking, the diffusion coefficient of the ion within the ion-exchanger falls, and as a result the desorption band is not sharp, and the separation deteriorates. An increase in K_s is also possible by using complex formers. It is known, that the stability of complex compounds decreases in the series calcium-radium,

TABLE 1. Values of K_d and K_s of Barium* and Radium for Various Resins in a Hydrochloric Acid Solution

Cationite	Swelling, ml/g	K_d of barium	K_d of radium	K_s
Dowex 50 x 10.	2,22	23,8	36,0	1,51
Dowex 50 x 8	2,38	16,2	22,9	1,41
Calcite	2,48	22,6	34,5	1,47
KU- 2 x 8	2,32	16,2	22,9	1,41
KU- 2 x 5	3,18	10,5	14,6	1,39
Espatite-1	2,38	3,0	4,06	1,35
SBS-R	2,45	2,37	3,20	1,35
RF.	—	0,20	0,30	—
KMT x 5.	--	17,9	22,4	1,35

* The barium concentration in the solution was 0.03 M.

while radium is retained most strongly by a cationite. When a complex former is used, the separation coefficient is determined in the first approximation by the expression

$$K_s^{comp} = K_s^{without\ comp} (K_{form}^{Ra} / K_{form}^{Ba}).$$

Table 2 gives the logarithms of the formation constants of some complex compounds of alkali earth elements. The most suitable of all the acids were citric, nitrilotriacetic (NTA), and ethylenediaminatetraacetic (EDTA) acids.

620

TABLE 2. Formation Constants of Complex Compounds of Alkali Earth Elements

Acid	Logarithms of formation constants			
	Ca	Sr	Ba	Ra
Citric...........	—	—	2,54	2,34
Malonic.........	—	—	1,36	0,95
Tartaric.........	1,8	1,65	1,62	1,24
Acetic...........	1,00	0,97	0,93	—
Malic..........	2,66	—	2,19	—
Polyphosphoric	3,00	2,8	3,0	—
Iminodiacetic.....	3,41	3,4	1,67	—
Uramil-N, N-diacetic	8,77	7,6	6,8	—
Ethylenediamine-tetraacetic......	10,59	8,63	7,76	—
Propylenediamine-tetraacetic.....	7,12	5,18	4,24	—
Nitrilotriacetic.....	6,41	4,94	4,82	—
1,2-diaminocyclo-hexanetetraacetic .	12,5	—	—	—

Fig. 1. Relation of distribution coefficients of alkali earth elements to hydrochloric acid concentration.

The use of hydrochloric acid as eluant. Figure 1 shows the relation of the distribution coefficients of alkali earth elements to hydrochloric acid concentration for a KU-2 cationite. The working range of acid concentrations was limited to 0-4 M solutions. With an increase in concentrations to 7 M, the separation coefficient fell to 0 and then barium sorption was mainly observed. In this concentration range, barium and radium could not be eluted with small volumes of hydrochloric acid as the distribution coefficients were above 25.

The following optimal conditions were found from the experiments on the separation of barium and radium with hydrochloric acid: KU-2 cationite with 8% cross-linking, grain size of 100-200 mesh, temperature 90°, a gradually increasing acid concentration from 0.5 to 5.0 M at the end of the experiment, and an elution rate of 2 cm/min. The barium and radium were sorbed in the upper section of the column. The height of the cationite layer saturated with barium was 10% of the total height of the sorbent layer. The results of the separation under these conditions are shown in Fig. 2.

Elution with ammonium citrate solutions. Preliminary experiments were first carried out using citric acid as complex former to obtain the maximum separation coefficient. The relation of the distribution and separation coefficient to the pH of a 5% ammonium citrate solution was investigated for 0.03 M solutions of barium on a KU-2 cationite. Table 3, gives the results of these investigations. The optimal value for the pH was in the range 7-9 in which all the acid hydrogen was neutralized.

Table 4 gives the distribution and separation coefficients for various types of cationite in the optimal pH range. The experimental values of the separation coefficients were somewhat lower than expected from the data on the stability constants of the complex compounds.
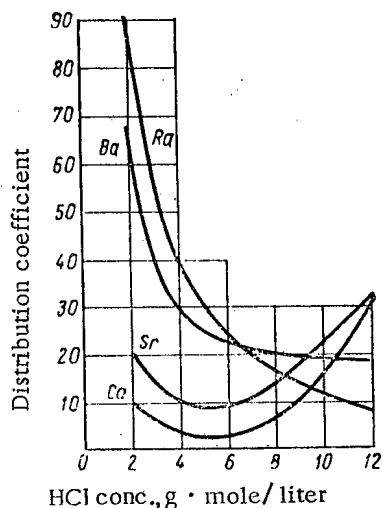
Investigations of the relation of the distribution coefficients to the ion concentration in the solution showed that in the concentration range from 0.001 to 0.1 M, K_d depended little on concentration. In this connection it was interesting to check the applicability of the "plate theory" [5] to the separation of barium and radium.

Figure 3 shows theoretical and experimental data on the elution of barium and radium from a column 7 cm in height and filled with KU-2 cationite with a grain size of 100-200 mesh.

A 5% ammonium citrate solution with pH = 7.6 was used for desorption. The position of the maxima on the curve and the course of the elution agree well with the theoretical curve (continuous line). The height of the "theoretical plate" under these conditions was 0.54 mm.

The use of ammonium citrate solutions for elution made it possible to separate barium and radium completely on 50 cm columns with barium saturating the upper 10 cm of layer. The solutions used for the elu-
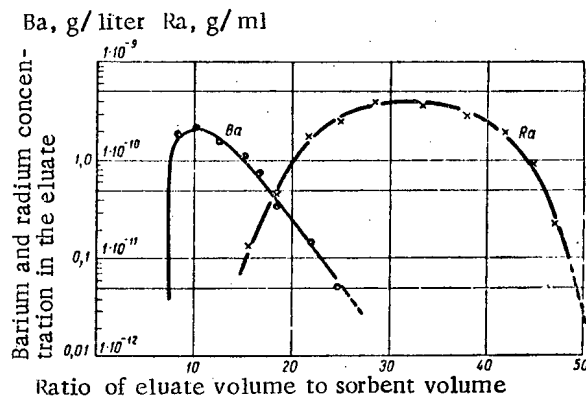
Fig. 2. Barium and radium separation with hydrochloric acid elution.

621

TABLE 3. Relation of K_d and K_s to pH of a Citric Acid Solution

pH	K_d Barium	K_d Radium	K_s
5,4	16,6	28,6	1,72
6,5	6,2	12,4	2,00
7,6	6,1	12,8	2,11
9,4	5,8	11,9	2,05

TABLE 4. K_d and K_s Values of Barium and Radium for Citric Acid

Cationite	Barium K_d	Radium K_d	K_s
Dowex 50 X 10. . . .	6,3	16,0	2,54
Dowex 50 X 8	6,15	13,5	2,20
KU-2 x 8	6,08	12,8	2,11
Espatite-1.	2,70	4,1	1,51
SBS-R.	1,20	1,8	1,50
RF.	3,2	4,6	1,44

Ba, g/ liter   Ra, counts/ min
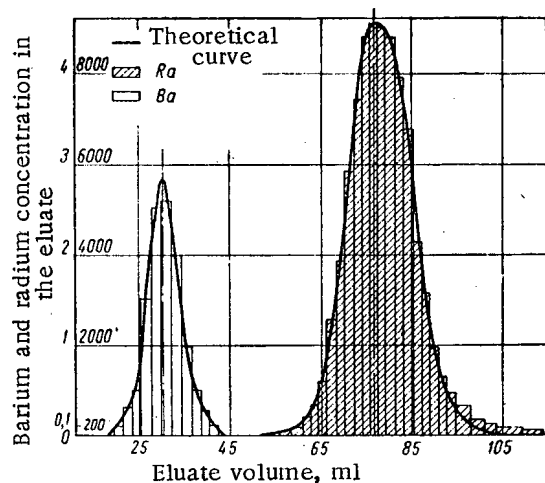
Fig. 3. Theoretical and experimental data on the elution of barium and radium.

Ba, g/ liter   Ra, g/ ml

Fig. 4. Barium and radium separation with ammonium citrate.

tion had an increasing concentration of ammonium citrate (from 0 to 5%).

In further experiments, the usual procedure of chromatographic separation was changed somewhat. Barium and radium were sorbed not from chlorides, but from a 5% ammonium citrate solution with a molar ratio of barium to citrate anion of 1:1. This procedure made it possible to dispense with elution with solutions of varying concentrations and decrease the volumes.

In this case, the optimal separation conditions were KU-2 cationite with a grain size of 100-200 mesh, 20% of the height of the sorbent layer spent, elution rate 2 cm/ min, and 5% ammonium citrate with pH = 8.0 used as the regenerating solution.

The results of separating barium and radium under these conditions are shown in Fig. 4.

Use of ethylenediaminetetraacetic acid. Among the practically accessible complex formers, EDTA forms complexes of alkali earth elements with the greatest difference in stability constants. The relation of the distribution and separation coefficients to the pH of a 4% EDTA solution for a KU-2 cationite is given in Table 5.

The maximum separation coefficient was obtained at pH = 6.2; with an increase in the pH of the solution, the distribution coefficient fell sharply.

From the data obtained, we calculated the formation constant of the radium–EDTA complex and its logarithm was found to be 7.2.

Different results were obtained in the separation of radiochemical amounts of radium and barium. An increase in the amount of barium lead to a change in pH along the axis of the column during elution. Due to the strong dependence of the distribution coefficients on pH, there was no separation. In order to avoid a change in pH along the front of the elution curve, the column was first completely saturated with barium not containing radium, and a solution of a complex of barium and radium with EDTA, with the optimal pH value was filtered through the column. Due to the lower stability of its complex compound, the radium was completely adsorbed by the resin under these conditions, while the eluant contained only barium. In this type of experiment, barium plays the part of the "retaining ion".

The technological scheme for separating barium from radium, using EDTA solutions, consists of the following: the starting solution, with pH = 6.5, containing 20 g/ liter of barium (the radium content depended on the initial raw material and varied over a wide range, but was generally a factor of tens of thousands less than barium) and 40 g/ liter of EDTA was filtered successively through a series of columns filled with KU-2 cationite

622

TABLE 5. K_d and K_s Values of Barium and Radium for a KU-2 Cationite in Relation to the pH of EDTA Solutions

pH	Barium K_d	Radium K_d	K_s
5,00	48,6	90,0	1,85
5,25	—	—	—
5,50	24,7	72,4	2,93
5,75	17,6	56,7	3,22
6,00	8,40	42,0	5,00
6,25	4,55	23,1	5,08
6,50	2,90	14,6	5,05
·7,00	0,5	2,05	5

with a grain size of 100-200 mesh. The solution volume equaled 13-14 column volumes and the filtration rate was 3-4 cm/min. Regeneration was then carried out with an EDTA solution with pH = 10. The last fractions of the regeneration solution contained 99% of the initial amount of radium. The EDTA was precipitated from the regeneration solutions with hydrochloric acid and returned to the process. Two concentrations stages gave a radium enrichment of 5000-6000 times. Separation of radium from 100 kg of barium, required columns with a total sorbent volume of 0.5 m³. The solution volume was 8 m³. The throughput of this method equals that of contemporary technological methods, and was 50 kg/hr per m² of column cross section.

0.01 kg of EDTA, 1.5 kg of sodium hydroxide and 1.2 kg of hydrochloric acid were consumed per kg of barium separated.

Separation of Zirconium and Hafnium

Efficient industrial methods of obtaining zirconium free from hafnium are a pressing problem due to the creasing use of zirconium as a construction material in atomic technology. Numerous methods of separating

zirconium and hafnium have been described in the literature. In [6] and [7] hafnium was separated from zirconium on anion-exchange resins in mixtures of the acids HF and HCl. In [8], zirconium and hafnium were separated by eluting mixtures of these elements from sulfonate cationite with hydrochloric acid. There are a number of other papers which are of less interest. In [9] there is a review of separation methods and their throughput is evaluated. The authors evaluated the throughput of an ion-exchange method based on data given in [10] as 0.5 kg/hr per m² of column cross section. The throughputs of distillation and extraction methods were 30 and 100 kg/hr per m² of apparatus cross section, respectively.

As a result of investigating the separation of zirconium and hafnium on cation-exchange resins with a mixture of sulfuric and hydrofluoric acids, we developed a scheme for separating zirconium and hafnium chromatographically that would be applicable industrially.

We used KU-2 sulfonate cationite with a low percentage of cross-linking. The relation of the distribution coefficients of zirconium and hafnium to the concentrations of zirconium and hydrofluoric and sulfuric acids was investigated (Figs. 5 and 6).

The separation coefficient for zirconium and hafnium in a suitable range of K_d values varied from 1-5. Quite efficient chromatographic separation was possible at a K_s value of 5. Further experiments were carried out under dynamic conditions.

Chromatography on a stationary ionite layer gave the following optimal conditions, which take into account kinetic factors: 20-30 g/liter of zirconium (calculated on zirconium dioxide), 0.65-0.75 M of sulfuric acid and a molar ratio of fluorine to zirconium of 0.7-1.0, 10% by weight of the resin in the column spent, KU-2 cationite with a grain size of 60-100 mesh, a sorbent layer height of 2-2.5 m and a solution filtration rate of 1.5-2 cm/min.
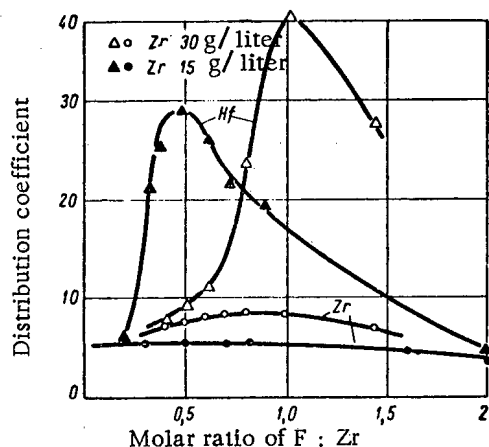

Fig. 5. Relation of distribution coefficients of zirconium and hafnium to the fluorine ion concentration for a solution containing 0.65 M sulfuric acid.
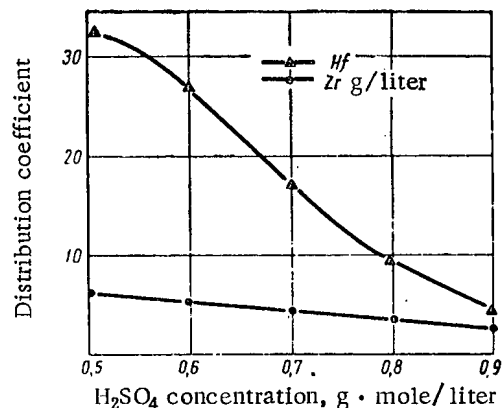
Fig. 6. The effect of sulfuric acid concentration on the distribution coefficients of zirconium and hafnium.

The starting solution whose composition is given above was filtered through a cationite layer. The hafnium was completely adsorbed by the cationite while the zirconium remained in the solution. When the column had been saturated with hafnium, the column was regenerated with 0.65 M sulfuric acid. Zirconium hydroxide was precipitated from the eluted fraction which contained less than 0.01-0.08% of hafnium in relation to zirconium. The intermediate fraction which contained some zirconium contaminated with hafnium was recovered and added to the starting solution. The hafnium fraction was filtered through a layer of RF phosphate cation-exchange resin. The hafnium was completely adsorbed by the sorbent, while the solution was recovered and used as a regenerating substance in the starting cycle. Ammonium oxalate was used to remove the hafnium from the phosphate resin. Hafnium hydroxide was precipitated from the regeneration solution with ammonia. This operation made it possible to increase the hafnium concentration by a factor of 30 in one operation and to return part of the solutions to the process. Hafnium concentrates with 99% purity were obtained.

The scheme described above had a throughput of 15-20 kg/hr per m^2 of the column cross section. To separate one kg of hafnium-free zirconium using metal hydroxides prepared from fluozirconates as starting material required 5 kg of sulfuric acid, 5 kg of ammonia, and 0.2 kg of 40% hydrofluoric acid. This method gave 100 kg of hafnium-free zirconium as well as pure hafnium preparations.

Isolation of Gallium from an Anode Melt

The main difficulty in the technical isolation of gallium from an anode melt is the separation of gallium from aluminum. Technical solutions contain hundreds of times more aluminum than gallium. The known methods of isolating gallium are quite complicated and therefore, the development of a method for separating it chromatographically seemed promising.

An efficient separation of small amounts of gallium from large amounts of aluminum and a series of other
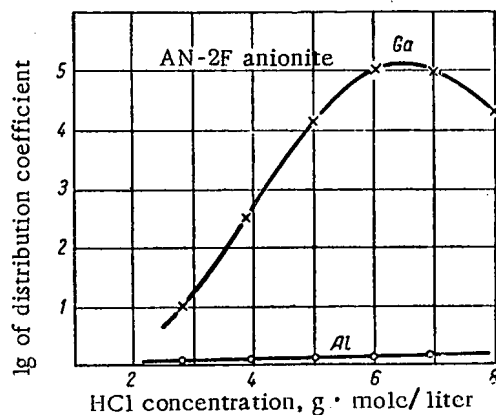
TABLE 6. Purification of Gallium by Ion-Exchange Separation

Element	Conc. in starting solution, g/liter	Conc. in regeneration solution, g/liter
Aluminum	23	0,00
Gallium	0,3	2,64
Copper	0,025	0,00
Iron	7,4	0,12
Manganese	0,014	0,00

elements required conditions under which gallium would be adsorbed by a sorbent, while the aluminum and other impurities remained in the solution. Cation-exchange resins do not fulfill this requirement, although aluminum and gallium may be separated on cationites.

We investigated the sorption of gallium and aluminum by anion-exchange resins in various media. The maximum distribution coefficients were obtained in hydrochloric acid solutions. Aluminum was hardly adsorbed from hydrochloric acid solutions. Figure 7 shows a graph of the relation of the distribution coefficient of gallium to hydrochloric acid concentration in the outer solution. Due to the high value of the distribution coefficient gallium may be separated from aluminum by filtration of the solution through an anionite at a definite acidity.

We developed a technological scheme for separating gallium from an anode melt on the basis of the experimental results described.

The starting material, which was an anode melt pulverized to 0.3 mm, was dissolved in hydrochloric acid. The copper in the solution obtained was cemented with aluminum or iron filings; the iron was simultaneously reduced to the divalent state. The solution was acidified to 3.7 M and filtered through a sorbent layer. The anionite was washed with 5 M hydrochloric acid. Gallium was desorbed with 0.5 M hydrochloric acid. The solution was neutralized with alkali and the gallate electrolyzed to obtain metallic gallium.

Table 6 gives the composition of a starting solution and regeneration solution after ion-exchange separation of impurities.

The throughput of the apparatus was 50 kg/hr of aluminum per m^2 of the column cross section.

Fig. 7. Relation of the distribution coefficient of gallium to hydrochloric acid concentration.

LITERATURE CITED

1. E. Tompkins, J. Am. Chem. Soc. 70, 3520 (1948).
2. H. Gregor, J. Am. Chem. Soc. 73, 642 (1951).
3. E. Gluckauf, Proc. Roy. Soc. 214, 207 (1952).
4. B. Soldano, J. Am. Chem. Soc. 77, 1134 (1955).
5. S. Mayer and E. Tompkins, J. Am. Chem. Soc. 69, 2866 (1947).

6. K. Kraus and G. Moore, J. Am. Chem. Soc. 71, 3263 (1949).

7. E. Huffman and R. Lilly, J. Am. Chem. Soc. 73, 2902 (1951).

8. K. Street and G. Seaborg, J. Am. Chem. Soc. 70, 4268 (1948).

9. F. Hudswell and J. Hutcheon, "Chemistry of nuclear fuel," Reports of foreign scientists to the International Conference on the Peaceful Uses of Atomic Energy (Geneva, 1956).

10. B. Lister and R. McDonald, Atomic Energy Research Establ. (Gt. Brit.) C/R-545 (1950).

HYDROGEN CONDENSATION PUMP WITH BUILT-IN LIQUEFIER

E. S. Borovik, B. G. Lazarev, and I. F. Mikhailov

A hydrogen pump with a capacity of $3.7 \cdot 10^4$ liters/sec and a built-in liquefier is described. The pump produces a limiting vacuum of the order of $10^{-8}-10^{-9}$ mm Hg. The total required power (including the power used in obtaining the liquid hydrogen) is 17 kw, which is less than the power required for an oil-diffusion pump of the same capacity.

At the temperature of boiling hydrogen (20.4°K) the vapor pressure of most materials is extremely low, so that a surface which is cooled to this temperature will, even in a rough vacuum ($p \leq 10^{-8}$ mm Hg) condense almost all molecules which strike it. The refrigerated surface is the basic element of the hydrogen condensation pump [1]. At high pumping rates (each square centimeter of the refrigerated surface provides an air pumping rate of approximately 11 liters/sec) the pump produces a good limiting vacuum, approximately $10^{-8}-10^{-9}$ mm Hg.

In the design described in [1], the cooling is accomplished by filling the condensation element with liquid hydrogen. Although this design is simple, it has a number of disadvantages: it can be used only when a source of liquid hydrogen is available and the cooling effect of the hydrogen vapor is not used; the use of this refrigerating effect would make it possible to improve the refrigerating efficiency of the cooling apparatus by a large factor.

These disadvantages can be avoided if the hydrogen is cooled directly in the pump. Below, we describe a design in which this feature is used and report on experimental results.

It is not useful to use a liquefier on a pump of low capacity; for this reason the design is applied to a pump with nominal capacity of $40 \cdot 10^{-3}$ liters/sec. A diagram of the pump is shown in Fig. 1.

The basic operating element of the pump is a thin-walled (2 mm) copper chamber 1, which is filled with liquid hydrogen. When the liquid hydrogen is at the bottom of the tank, the temperature at the upper portions of the walls does not differ from the temperature of liquid hydrogen by more than 0.1° K.

With an outer surface area for the tank of approximately 5000 cm², the theoretical pumping rate is approximately 55,000 liters/sec. This pumping rate is reduced somewhat, because of the input resistance. The chamber 1 is located in an iron tank 2 of diameter 900 mm in which there is a cylindrical shield 5 made from sheet copper 1.5 mm thick, which is cooled by nitrogen. The rear part of the shield 5 is covered by another shield 7,
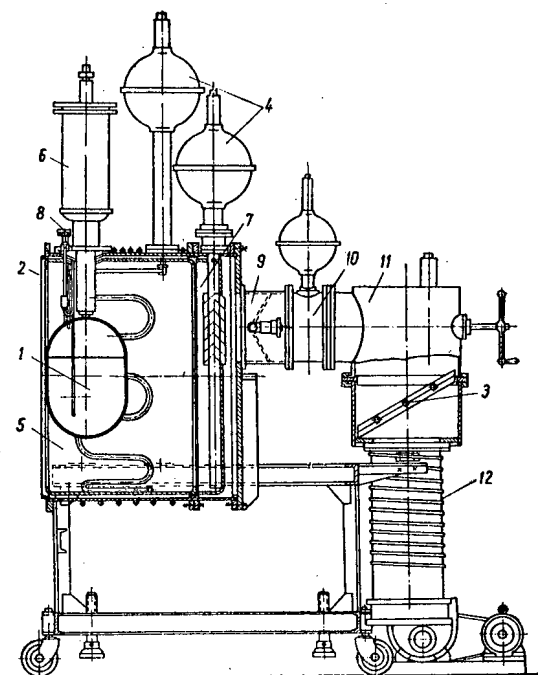
Fig. 1. Diagram of the hydrogen condensation pump.

which is cooled by nitrogen. The nitrogen used for cooling the shields 5 and 7 is stored in the dewars 4.

The liquid hydrogen is obtained in the liquefier 6 by throttling the cooled compressed hydrogen through valve 8.

In order to reduce the thermal losses, the outer surfaces of the tank 1 and the shields 5 and 7 are polished. The shields 5 and 7 serve two purposes: on the one hand, they partially shield tank 1 against thermal radiation and reduce the consumption of liquid hydrogen; on the other, they condense the water vapors and certain other adsorbed gases which evolve from the walls of the reservoir. It has been shown in [1 and 2] that the chief obstacle to obtaining a good vacuum is the gas which is desorbed by the walls; hence, it is desirable, in the hydrogen condensation pump, to have large surfaces which are cooled to the temperature of liquid nitrogen.

626

In order to evacuate the noncondensable gases (He, Ne, H_2), the pump is furnished with an M-2500 diffusion pump 12. In order to prevent the entrance of oil vapors and products of the oil decomposition into the compression space, there is a venetian-blind baffle (water cooled) 3, a venetian-blind trap 10 (cooled by liquid air), and venetial-blind baffles which overlap the aperture in the shield 7. The diffusion pump 12 is isolated from the apparatus by the valve 11. A gasketless valve 9 is provided in order to prevent contamination of the apparatus in time periods when the trap 10 is allowed to warm up.

Figure 2 shows a section of a liquefier. The hydrogen which is compressed by the compressor, enters in tube 4 (3 x 4 mm); after cooling in the heat exchangers it is throttled in valve 3 and partially liquefied. The liquid hydrogen enters the tank 1. The nonliquefied gas and the hydrogen which evaporates from the tank 1 are returned to the compressor input through tube 4 (8 x 10 mm); in passing through the heat exchangers, this hydrogen serves to cool the incoming high-pressure hydrogen.

The incoming high-pressure hydrogen is cooled in tank 2 by liquid nitrogen, which boils at reduced pressure at a temperature of 64°K. The evaporating nitrogen is exhausted through tube 6 and is used for cooling the high-pressure hydrogen.

The upper heat exchanger consists of 13 coils (tubes 4, 5, and 6) which are soldered to provide good thermal contact; tube 6 in the heat exchanger is flattened in such a way that its small diameter is 14 mm, while the large diameter is 25.4 mm. The coils in the upper heat exchanger are located outside the nitrogen tank 2, but do not touch it. After cooling in the upper heat exchanger, the high-pressure hydrogen is cooled to a temperature of 64°K in the 4-5 coils of the spiral of tube 4 of length 2 m, which is soldered to the outside of the nitrogen tank.

In the next stage, the high-pressure hydrogen is cooled in the lower heat exchanger, which consists of tubes 4 and 5 (5.5 m in length) which are soldered together; the hydrogen is then throttled. The heat exchangers are in vacuum. In order to reduce the radiation losses the upper heat exchanger is covered by shield 7, which is made from aluminum foil, while the lower heat exchanger is covered by shield 8, which is made from polished copper. Shield 8 is soldered to the nitrogen tank 2. The nitrogen tank 2 is suspended from the upper flange of the liquefier on tube 9, which is made of German silver; the lower part of the nitrogen tank carries the hydrogen tank 1, which is suspended on tube 10 and is also made of German silver. Tube 11 serves for pouring the liquid nitrogen, while tubes 12 and 13 serve for measurements of the level of the liquid in tanks 1 and 2.

The liquefier is designed to operate with a compresser with a capacity of 10 m^3/hr, but has adequate heat-exchanging surfaces to be able to operate with a com-
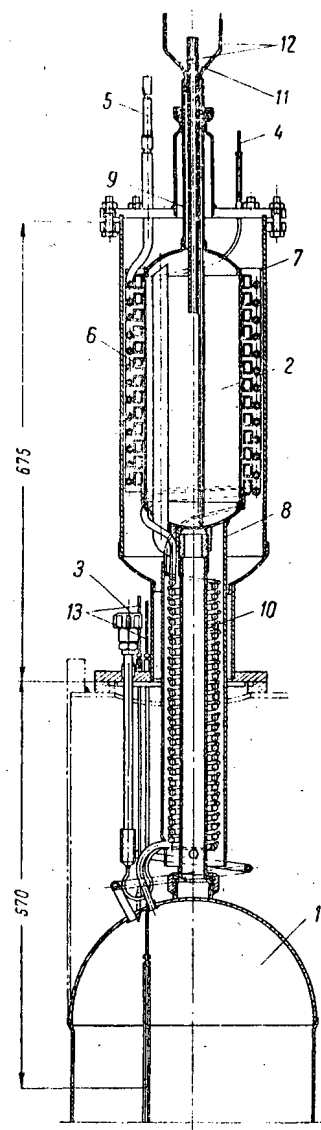
Fig. 2. Section of the hydrogen liquefier.

pressor with a capacity of 17 m^3/hr, with which all tests were carried out.

The pump has been tested in evacuating an iron tank with a volume of approximately 1.5 m^3, which is connected to it as a reservoir. The tank is an element of an apparatus designed for melting metals and has inner strengthening ribs, a large number of flanges with rubber gaskets, and a number of other elements which impede evacuation. This is the reason for the relatively low limiting vacuum ($5 \cdot 10^{-8}$ mm Hg) obtained in tests of the pump.

In Fig. 3 is shown a part of the curve which gives the time dependence of the pressure in the reservoir. The arrow indicates the time at which the liquefier is switched on. Before it is switched on, the apparatus is processed continuously for 14 hr with the nitrogen-cooled shield. This processing period is necessary because of the elements in the reservoir indicated above. The beginning of liquefaction is denoted on the curve by the

627
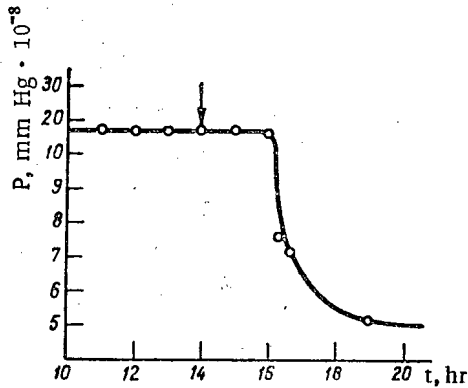
Fig. 3. Dependence of pressure in the reservoir on time. The arrow denotes the time at which the liquefier is switched on.

Fig. 4. Curve showing the dependence of hydrogen consumption on time under conditions of strong outgassing. The operating pressure is $1.4-1.2 \cdot 10^{-6}$ mm Hg.

sharp drop in pressure. The hydrogen starts to fill up the tank two hours after the liquefier is set into operation. Three hours after the operation starts, a pressure of $5 \cdot 10^{-8}$ mm Hg is achieved.

The measurements of the pumping rate of the pump were carried out in the pressure range $10^{-7}-10^{-5}$ mm Hg. The pumping rate for air is $W = 37 \cdot 10^3$ liters/sec and is independent of pressure. This result is in agreement with the results of measurements in [1].

The pumping rate of the diffusion pump 12 (cf. Fig. 1) for noncondensable components was determined with hydrogen. The pumping rate for hydrogen in the pressure range $10^{-5}-10^{-7}$ mm Hg is $W_{H_2} \approx 1000$ liters/sec. The evaporation rate of hydrogen in the first hours of operation of the pump (in the time periods during which the surface of the hydrogen tank is still clean) is approximately 0.4 liters/hr of liquid. It has been shown earlier [1] that in a vacuum of the order of $5 \cdot 10^{-8}$ mm Hg, during the course of several days, the consumption of hydrogen remains essentially unchanged.

In order to investigate the possibility of operating the hydrogen pump under conditions of strong outgassing and contamination of the condensation surface, we have investigated the dependence of hydrogen consumption on the evacuation time of the reservoir in an experiment in which a powerful apparatus for vacuum distillation of metals was operated. In order to provide shielding from the direct radiation of the incandescent parts of the apparatus, venetian-blind baffles were placed between the pump and the reservoir. The baffles reduce the pumping rate to $17 \cdot 10^3$ liters/sec. During the evaporation of the metal (iron), the pressure usually is maintained at a level of $1-1.5 \cdot 10^{-6}$ mm Hg. The dependence of hydrogen consumption on time is shown in Fig. 4.

It should be noted that each time the apparatus is started up (after being operated and allowed to come to room temperature), the hydrogen consumption is increased because of the accumulation on the condensation element of a residue of evaporated metal, material from the crucible, etc. Hence, after operation of the appara-

tus for a month, it is necessary to clean the condensation surface, an operation which requires 1-1.5 hr. The maximum consumption of liquid hydrogen at the end of the operation period is never greater than 2 liters/hr.
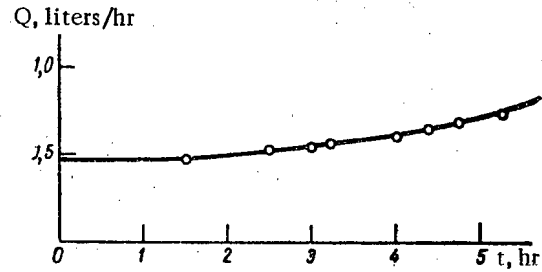
In Fig. 5 is shown the dependence of the liquefier capacity with a compressor having a capacity of 17 m³/hr on pressure. The tests were carried out under conditions in which the evaporation of liquid hydrogen in tank 1 (cf. Fig. 1) due to the flow of heat was approximately 1.5 liters/hr. The consumption of liquid hydrogen tends to increase the cooling capacity of the apparatus for the following reason: with a small heat load on the condensation element (low hydrogen evaporation) almost all of the hydrogen which is liquefied after throttling remains in the collector. When the heat load is increased, there is an increase in the amount of evaporating hydrogen and this improves the cooling of the high-pressure hydrogen and increases the liquefaction factor.

A calculation for an ideal liquefier shows that the liquefaction factor is several times larger for total evaporation of the liquefied hydrogen. In particular, at a pressure of 60 atmos. the liquefaction factor and consequently, the cooling capacity of the apparatus, should increase by a factor of 2.2 as compared with the cooling capacity with no evaporation.
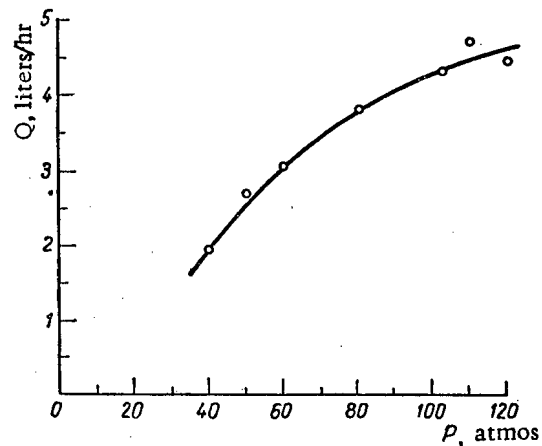
Fig. 5. Curve showing the dependence of liquefier capacity on pressure.
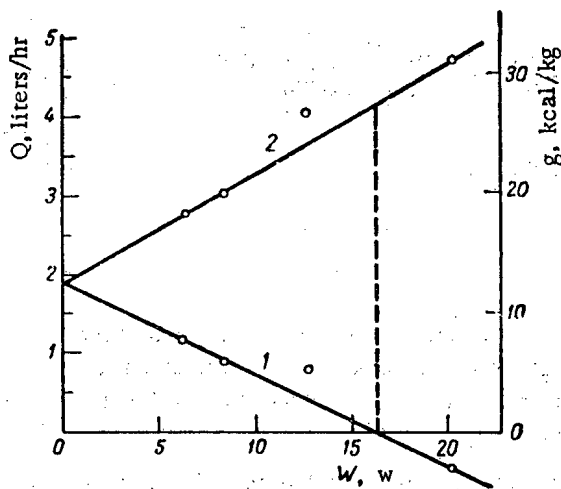
Fig. 6. Dependence of liquefier capacity on heat load W:
1) rate of accumulation of liquid hydrogen in the col-
lector; 2) total amount of liquefied hydrogen (cooling
capacity of the system).

The dependence of cooling capacity of the liquefier
on the heat load, i.e., on the amount of hydrogen evap-
orated from the tank 1 (cf. Fig. 1), is shown in Fig. 6
(for a pressure of 60 atmos). Curve 1 delineates the rate
of accumulation of liquid hydrogen in the collector as
a function of the heat load, i.e., the difference between
the amounts of liquefied and evaporated hydrogen.
Negative values on this curve mean that the amount of
evaporated hydrogen is greater than the amount of lique-
fied hydrogen. Operation in this mode is possible be-
cause of the excess liquid hydrogen accumulated in the
collector. Curve 2 represents the total amount of hy-
drogen liquefied after throttling. It is given as the sum
of the amount of hydrogen accumulated in the collector
and the hydrogen evaporated from it. The latter quantity
is found by the heat of evaporation of liquid hydrogen as

the heat load. Curve 2 characterizes the cooling capac-
ity of the liquefier.

The portion of the curve which is of practical sig-
nificance is that part corresponding to a heat load less
than 15 w, at which liquid hydrogen does not accumulate
in the collector. Thus, the maximum capacity of the
liquefier at a pressure of 60 atmos is approximately 4
liters of liquid hydrogen per hour; converted to opera-
tion with a compressor with a capacity of 10 m^3/hr, this
is 2.5 liters of liquid per hour. The maximum evapora-
tion in the system, as indicated above, is 2 liters/hr.
Consequently, a compressor with a capacity of 10 m^3/hr
at a pressure of 60 atmos is adequate for the system. A
unit which meets these specifications is the KVD air
compresser, which is as small as the VN-1 forepump;
with some minor modification, this unit can be used for
compressing hydrogen.

CONCLUSION

The total power of all the units in the pump de-
scribed here (with a capacity of $3.7 \cdot 10^4$ liters/sec) and
the electrical power required for liquefying the nitrogen
for operating the liquefier is approximately 13 kw; if
the nitrogen used for cooling the shield is considered,
this figure is 17 kw. This power is smaller than the power
required by an oil diffusion pump of the same capacity.

A shortcoming of the condensation pump is that
constant observation of the operation of the liquefier and
compressor, is required.

In conclusion, the authors wish to thank B. P. Batra-
kov and V. I. Sharonov for help in these measurements.

LITERATURE CITED

1. B. G. Lazarev, E. S. Borovik, M. F. Fedorova, and
   N. M. Tsin. Ukrain. Fiz. Zhur. 2, 175 (1957).
2. E. S. Borovik, B. G. Lazarev, M. F. Fedorova, and
   N. M. Tsin, Ukrain. Fiz. Zhur. 2, 88 (1957).

THE PROBLEM OF STABILITY OF NUCLEAR POWER PLANTS

A. S. Kochenov

This article presents an investigation of the stability of nuclear power plants, consisting of an aqueous reactor with a negative temperature coefficient of reactivity, a steam generator producing saturated steam, and a turbine. It is assumed that the system has only two regulators: a throttling regulator before the turbine and a regulator for maintaining a constant water level in the steam generator.

One-group kinetics equations are used and a single group of delayed neutrons is considered. The investigation was performed for small excitation parameters. Nonlinear equations are linearized. Conclusions with respect to plant stability are given.

Let us consider the stability of a nuclear power plant, the schematic diagram of which is shown in Fig. 1. The power source is an aqueous reactor 1 which has a negative temperature coefficient of reactivity. It is assumed that the effective neutron multiplication factor is a linear function of the average temperature of water in the reactor. Changes in thermal resistance in the steam generator, caused by transient processes, mainly depend on variations of the heat-exchange coefficient in boiling. However, since the thermal resistance connected with boiling is small, it is assumed that the heat-exchange coefficient per unit length of a single steam-generator tube is constant.
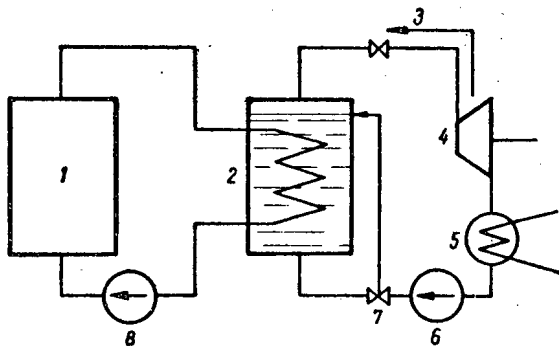
Fig. 1. Schematic diagram of the plant. 1) Reactor; 2) steam generator; 3) throttle; 4) turbine; 5) condenser; 6) second loop pump; 7) valve; 8) first loop pump.

Saturated vapor enters turbine 4 with throttling regulator 3 (the turbine power is determined only by the electric load). A valve 7 is provided for maintaining a constant water level in the steam generator.

In the derivation of equations describing the time relations in the reactor and steam-generator operation, we shall consider that the time of the water passage through the reactor and the steam generator is equal to zero.

The behavior of the reactor in time is described by the following equations:

$$
\left.
\begin{aligned}
&\frac{dn}{d\tau} = \frac{k-1}{l}\,n - \frac{k\beta_i n}{l} + \sum_i \lambda_i c_i, \\[4pt]
&\frac{dc_i}{d\tau} = -\lambda_i c_i + \frac{k\beta_i n}{l}, \\[4pt]
&N = G_1 c_{p_1}(t_r^{out} - t_r^{in}), \\[4pt]
&k - 1 = \alpha\,\frac{t_{r_0}^{in} + t_{r_0}^{out}}{2} - \alpha\,\frac{t_r^{in} + t_r^{out}}{2}, \\[4pt]
&N = N_0 n,
\end{aligned}
\right\}
\tag{1}
$$

where n is the total number of neutrons in the reactor, c_i is the over-all number of type-i fragments emitting delayed neutrons, λ_i is the decay constant of type-i fragments, β_i is the portion of type-i fragments, l is the lifetime of prompt neutrons, k is the effective neutron multiplication factor, α is the temperature coefficient of reactivity, N is the power level reactor, G_1 is the water consumption in the first loop, c_{p_1} is the specific heat of water in the first loop, t_r^{in} is the water temperature at the reactor inlet, and t_r^{out} is the water temperature at the reactor outlet. (The index 0 indicates that a given quantity pertains to the initial moment.)

In the system (1) the first two equations describe the change in the number of neutrons in the reactor [1]; the third equation relates the reactor power to water consumption and its heating; the fourth equation defines the dependence of the effective neutron multiplication factor on the average temperature of water in the reactor; the fifth equation relates the number of neutrons to the reactor power level, where the number of neutrons at the initial moment is normalized to unity, i.e., $n(0) = 1$.

630

Let us consider a single group of delayed neutrons. In this case, the reactor equations will assume the following form:

$$\frac{dn}{d\tau} = \frac{k-1}{l}n - \frac{k\beta n}{l} + \lambda c,$$
$$\frac{dc}{d\tau} = -\lambda c + \frac{k\beta n}{l},$$
$$N = G_1 c_{p1}(t_r^{out} - t_r^{in}),$$
$$k - 1 = \alpha \frac{t_{r_0}^{in} + t_{r_0}^{out}}{2} - \alpha \frac{t_r^{in} + t_r^{out}}{2},$$
$$N = N_0 n.$$
$$\tag{2}$$

The steam generator operation is described by the equations

$$G_1 c_{p1}(t_{sg}^{in} - t_{sg}^{out}) =$$
$$= G c_{p2}\frac{dt_2}{d\tau} + G_2(i'' - i_{cw}),$$
$$t_{sg}^{out} - t_2 = (t_{sg}^{in} - t_2)\exp\left(-\frac{K_l L}{G_1 c_{p1}}\right),$$
$$\tag{3}$$

where t_{sg}^{in} is the temperature of water in the first loop at the steam-generator inlet, t_{sg}^{out} is the temperature of water in the first loop at the steam-generator outlet, t_z is the temperature of water in the second loop in the steam generator, g is the steam-generator weight, c_{p2} is the specific heat of the steam generator (water and metal), G_2 is the water consumption in the second toop, i" is the enthalpy of saturated steam, i_{cw} is the enthalpy of water supplied from the condenser, K_l is the heat-exchange coefficient per unit length of a single steam-generator tube, and L is the total length of piping in the steam generator.

The first steam-generator equation characterizes the heat balance between the first and the second loops; the second equation expresses the dependence of water temperature in the first loop at the steam-generator inlet and outlet on the water temperature in the second loop.

The turbine power is related to steam parameters by the expression

$$N_T = \frac{3600 G_2 H_0 \eta_T}{860},$$
$$\tag{4}$$

where H_0 is the available adiabatic heat drop, and η_T is the turbine efficiency.

The available adiabatic heat drop depends on the saturated steam enthalpy i", the steam pressure p_1 before the turbine (after the throttling valve), and the steam pressure p_2 in the condenser. Since the pressure in the condenser does not change, the indicated relation $H_0 = H_0(i'', p_1, p_2)$ can be written in the form of the following linear relation:

$$H_0 = \frac{\partial H_0}{\partial i''}i'' + \frac{\partial H_0}{\partial p_1}p_1 + C_1,$$
$$\tag{5}$$

where $\partial H_0/\partial i''$, $\partial H_0/\partial p_1$, and C_1 are positive numbers.

From the theory of steam turbines, it is known that the relation between steam consumption and steam pressure is of the following form:

$$\frac{G_2}{G_{20}} = \sqrt{\frac{p_1^2 - p_2^2}{p_{10}^2 - p_{20}^2}}\sqrt{\frac{T_{20}}{T_2}},$$
$$\tag{6}$$

In the investigation of transient processes it is also necessary to know the dependence of turbine efficiency on steam consumption and the dependence of saturated-steam enthalpy on temperature. The character of the indicated dependences is shown in Figs. 2 and 3. These nonlinear dependences can be replaced by approximate linear expressions:

$$\eta_T = \frac{d\eta_T}{dG_2}G_2 + C_2,$$
$$\tag{7}$$

$$i'' = \frac{di''}{dt_2}t_2 + C_3.$$
$$\tag{8}$$

By substituting (5), (7), and (8) in (4), and by using (6), we obtain the following nonlinear equations for turbine power:

$$N_T = \frac{3600}{860}G_2\left[\frac{\partial H_0}{\partial i''}\left(\frac{di}{dt_2}t_2 + C_3\right) + \right.$$
$$\left. + \frac{\partial H_0}{\partial p_1}p_1 + C_1\right]\left(\frac{d\eta_T}{dG_2}G_2 + C_2\right),$$
$$\frac{G_2}{G_{20}} = \sqrt{\frac{p_1^2 - p_2^2}{p_{10}^2 - p_{20}^2}}\sqrt{\frac{T_{20}}{T_2}}.$$
$$\tag{9}$$

Here, we consider small oscillations and, therefore, we linearize the equations. For each variable we shall introduce the following deviation from the initial value:

$$\Delta x(\tau) = x(\tau) - x_0.$$
$$\tag{10}$$

We shall express the variables in terms of deviations from the initial values, substitute them in the reactor
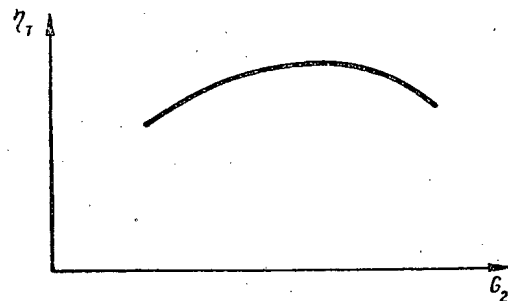
Fig. 2. Character of the turbine efficiency dependence on steam consumption.

631

equations (2), steam-generator equations (3), and turbine-power equations (9), and we shall neglect the terms containing deviations of orders higher than one and the products of deviations. If we subtract the corresponding statics equations from the obtained equations, assume that $\Delta N_m = 0$, and eliminate all variables except Δt_r^{in}, Δt_r^{out}, Δt_{sg}^{in}, and Δt_{sg}^{out} from the obtained equations, we shell obtain the following equations

$$G_1 c_{p1} \frac{l}{\lambda} \frac{d^2 \Delta t_r^{out}}{d\tau^2} + \left[\left(\frac{\beta}{\lambda} + l \right) G_1 c_{p1} + \right.$$
$$\left. + \frac{1-\beta}{2\lambda} \alpha N_0 \right] \frac{d\Delta t_r^{in}}{d\tau} + \frac{\alpha N_0}{2} \Delta t_r^{out} =$$
$$= G_1 c_{p1} \frac{l}{\lambda} \frac{d^2 \Delta t_r^{in}}{d\tau^2} + \left[\left(\frac{\beta}{\lambda} + l \right) G_1 c_{p1} - \right.$$
$$\left. - \frac{1-\beta}{2\lambda} \alpha N_0 \right] \frac{d\Delta t_r^{in}}{d\tau} - \frac{\alpha N_0}{2} \Delta t_r^{in}, \qquad (11)$$

$$G c_{p2} \frac{d\Delta t_{sg}^{out}}{d\tau} + \left\{ G_1 c_{p1} \left[1 - \exp\left(-\frac{K_L L}{G_1 c_{p1}} \right) \right] + \right.$$
$$+ \frac{di''}{dt_2} G_{20} - \frac{A_2}{A_1} (i_0'' - i_{cw}) \left. \right\} \Delta t_{sg}^{out} =$$
$$= G c_{p2} \exp\left(-\frac{K_L L}{G_1 c_{p1}} \right) \frac{d\Delta t_{sg}^{in}}{d\tau} +$$
$$+ \left\{ G_1 c_{p1} \left[1 - \exp\left(-\frac{K_L L}{G_1 c_{p1}} \right) \right] + \right.$$
$$+ \left[\frac{di''}{dt_2} G_{20} - \frac{A_2}{A_1} (i_0'' - i_{cw}) \right] \times$$
$$\times \exp\left(-\frac{K_L L}{G_1 c_{p1}} \right) \left. \right\} \Delta t_{sg}^{in}, \qquad (12)$$

where $A_1 = \frac{3600}{860} \left[H_{00} \eta_{r0} + \frac{\partial H_0}{\partial p_1} \eta_{r0} p_{10} + \right.$
$$\left. + \frac{d\eta_r}{dG_2} G_{20} H_{00} \right],$$
$$A_2 = \frac{3600}{860} G_{20} \eta_{r0} \left[\frac{\partial H_0}{\partial i''} \frac{di''}{dt_2} + \frac{1}{2} \frac{\partial H_0}{\partial p_1} \frac{p_{10}}{T_{20}} \right].$$

In usable form, these equations will be represented as:

$$G_1 c_{p1} \frac{l}{\lambda} S^2 \Delta t_r^{out} + \left[\left(\frac{\beta}{\lambda} + l \right) G_1 c_{p1} + \right.$$

$$+ \frac{1-\beta}{2\lambda} \alpha N_0 \right] S\Delta t_r^{* out} + \frac{\alpha N_0}{2} \Delta t_r^{* out} =$$
$$= G_1 c_{p1} \frac{l}{\lambda} S^2 \Delta t_r^{* in} + \left[\left(\frac{\beta}{\lambda} + l \right) G_1 c_{p1} - \right.$$
$$\left. - \frac{1-\beta}{2\lambda} \alpha N_0 \right] S\Delta t_r^{* in} - \frac{\alpha N_0}{2} \Delta t_r^{* in}, \qquad (13)$$

$$G c_{p2} S\Delta t_{sg}^{* out} + \left\{ G_1 c_{p1} \left[1 - \exp\left(-\frac{K_L L}{G_1 c_{p1}} \right) \right] + \right.$$
$$+ \frac{di''}{dt_2} G_{20} - \frac{A_2}{A_1} (i_0'' - i_{cw}) \left. \right\} \Delta t_{sg}^{* out} =$$
$$= G c_{p2} \exp\left(-\frac{K_L L}{G_1 c_{p1}} \right) S\Delta t_{sg}^{* in} +$$
$$+ \left\{ G_1 c_{p1} \left[1 - \exp\left(-\frac{K_L L}{G_1 c_{p1}} \right) \right] + \right.$$
$$+ \left[\frac{di''}{dt_2} G_{20} - \frac{A_2}{A_1} (i_0'' - i_{cw}) \right] \exp\left(-\frac{K_L L}{G_1 c_{p1}} \right) \left. \right\} \Delta t_{sg}^{* in}. \qquad (14)$$

(Asterisks denote functions obtained by means of Carson's transformation

$$\Delta t^*(S) = S \int_0^\infty \Delta t(\tau) \exp(-S\tau) d\tau.)$$

We shall call the relation $W_r = \Delta t_r^{* out} / \Delta t_r^{* in}$ the transfer function of the reactor, and the relation $W = \Delta t_{sg}^{* out} / \Delta t_{sg}^{* in}$ will be called the transfer function of the steam generator.
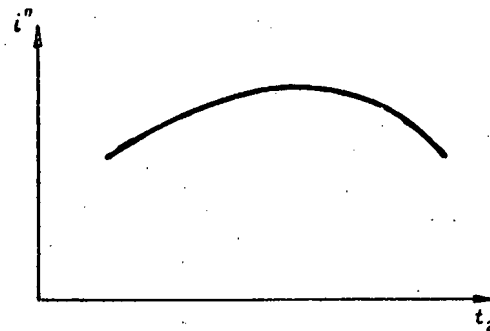
Fig. 3. Character of the saturated-steam enthalpy dependence on temperature.

From (13) and (14), we obtain

$$W_r = \frac{G_1 c_{p1} \frac{l}{\lambda} S^2 + \left[\left(\frac{\beta}{\lambda} + l \right) G_1 c_{p1} - \frac{1-\beta}{2\lambda} \alpha N_0 \right] S - \frac{\alpha N_0}{2}}{G_1 c_{p1} \frac{l}{\lambda} S^2 + \left[\left(\frac{\beta}{\lambda} + l \right) G_1 c_{p1} + \frac{1-\beta}{2\lambda} \alpha N_0 \right] S + \frac{\alpha N_0}{2}}, \qquad (15)$$

$$W_{sg} = \frac{G c_{p2} \exp\left(-\frac{K_L L}{G_1 c_{p1}} \right) S + G_1 c_{p1} \left[1 - \exp\left(-\frac{K_L L}{G_1 c_{p1}} \right) \right] + \left[\frac{di''}{dt_3} G_{20} - \frac{A_2}{A_1} (i_0'' - i_{cw}) \right] \exp\left(-\frac{K_L L}{G_1 c_{p1}} \right)}{G c_{p2} S + G_1 c_{p1} \left[1 - \exp\left(-\frac{K_L L}{G_1 c_{p1}} \right) \right] + \frac{di''}{dt_2} G_{20} - \frac{A_2}{A_1} (i_0'' - i_{cw})}. \qquad (16)$$

In investigating the plant stability it is necessary to take into account the heat-carrier lag, which is caused by the piping. It can be considered that, approximately,

$$t_{sg}^{in}(\tau) = t_r^{out}(\tau - \tau_1),$$
$$t_r^{in}(\tau) = t_{sg}^{out}(\tau - \tau_2),$$
$$\tag{17}$$

where τ_1 and τ_2 are the lag times. In this case, the transfer function for the "reactor steam-generator" piping will be of the form

$$W_{r, sg} = \exp(-S\tau_1), \tag{18}$$

and the transfer function for the "steam-generator—reactor" piping will be given by

$$W_{sg, r} = \exp(-S\tau_2). \tag{19}$$

The system under consideration consists of four elements connected in series: 1) reactor, 2) "reactor-steam-generator" piping, 3) steam generator (together with the turbine)*, and 4) "steam-generator—reactor" piping.

Let us disconnect the system before the reactor inlet. The transfer function of the open system (W_{os}) is equal to the product of the transfer functions of individual elements

$$W_{os} = W_r W_{r, sg} W_{sg} W_{sg, r} = \frac{G_1 c_{p1} \frac{l}{\lambda} S^2 + \left[\left(\frac{\beta}{\lambda} + l\right) G_1 c_{p1} - \frac{1-\beta}{2\lambda}\alpha N_0\right] S - \frac{\alpha N_0}{2}}{G_1 c_{p1} \frac{l}{\lambda} S^2 + \left[\left(\frac{\beta}{\lambda} + l\right) G_1 c_{p1} + \frac{1-\beta}{2\lambda}\alpha N_0\right] S + \frac{\alpha N_0}{2}} \times$$

$$\times \frac{G c_{p2} \exp\left(-\frac{K_L L}{G_1 c_{p1}}\right) S + G_1 c_{p1}\left[1 - \exp\left(-\frac{K_L L}{G_1 c_{p1}}\right)\right] + \left[\frac{di''}{dt_2}G_{20} - \frac{A_2}{A_1}(i_0'' - i_{cw})\right]\exp\left(-\frac{K_L L}{G_1 c_{p1}}\right)}{G c_{p2} S + G_1 c_{p1}\left[1 - \exp\left(-\frac{K_L L}{G_1 c_{p1}}\right)\right] + \frac{di''}{dt_2}G_{20} - \frac{A_2}{A_1}(i_0'' - i_{cw})} \times$$

$$\times \exp[-S(\tau_1 + \tau_2)]. \tag{20}$$

In (20), the factor $\exp[-S(\tau_1 + \tau_2)]$ takes into account the heat-carrier lag in the piping. Assuming that $\tau_1 + \tau_2 = 0$, we obtain the lag-free transfer function of the system (W_{ls}). In the theory of control, such systems are called limiting systems. Before analyzing the problem of a stable system with a lag, we shall consider the stability of a limiting system. The equation for an open limiting system will be of the following form:

$$\frac{\Delta t_{sg}^{*out}}{\Delta t_r^{*in}} = W_{ls} \tag{21}$$

Assuming that $\Delta t_r^{*in} = \Delta t_{sg}^{*out}$, we obtain the equation for a closed limiting system:

$$W_{ls} - 1 = 0. \tag{22}$$

By substituting the value of the transfer function of the limiting system in (22), we obtain the following characteristic equation:

$$a_0 r^3 + a_1 r^2 + a_2 r + a_3 = 0, \tag{23}$$

where

$$a_0 = \frac{l}{\lambda}G c_{p2}\left[1 - \exp\left(-\frac{K_L L}{G_1 c_{p1}}\right)\right];$$

$$a_1 = \frac{l}{\lambda}\delta\left[1 - \exp\left(-\frac{K_L L}{G_1 c_{p1}}\right)\right] +$$

$$+ \left(\frac{\beta}{\lambda} + l\right)G c_{p2}\left[1 - \exp\left(-\frac{K_L L}{G_1 c_{p1}}\right)\right] +$$

$$+ \frac{\alpha(1-\beta)\Delta T_0}{2\lambda}G c_{p2}\left[1 + \exp\left(-\frac{K_L L}{G_1 c_{p1}}\right)\right];$$

$$a_2 = \left[\frac{\alpha(1-\beta)N_0}{\lambda} + \left(\frac{\beta}{\lambda} + l\right)\delta\right] \times$$

$$\times \left[1 - \exp\left(-\frac{K_L L}{G_1 c_{p1}}\right)\right] +$$

$$+ \frac{\alpha\Delta T_0}{2}\left[\frac{1-\beta}{\lambda}\delta + G c_{p2}\right]\left[1 + \exp\left(-\frac{K_L L}{G_1 c_{p1}}\right)\right];$$

$$a_3 = \alpha N_0\left[1 - \exp\left(-\frac{K_L L}{G_1 c_{p1}}\right)\right] +$$

$$+ \frac{\alpha\Delta T_0}{2}\delta\left[1 + \exp\left(-\frac{K_L L}{G_1 c_{p1}}\right)\right];$$

$$\delta = \frac{di''}{dt_2}G_{20} - \frac{A_2}{A_1}(i_0'' - i_{cw});$$

ΔT_0 is the preheating of water in the reactor.

---

* The lag in the "steam-generator—turbine" piping is not taken into account here, i.e., it is assumed that throttle 3) (see Fig. 1) is located at the beginning of this piping, and that the signal indicating a change in the number of revolutions of the turbine shaft reaches the throttle instantaneously.

633

As is known from the theory of control [2], it is necessary and sufficient that in order that a system of the third order be stable, the following conditions be satisfied:

$$a_0 > 0, \qquad (24)$$
$$a_1 > 0, \qquad (25)$$
$$a_3 > 0, \qquad (26)$$
$$a_1 a_2 - a_0 a_3 > 0. \qquad (27)$$

Generally speaking, two cases are possible: 1) $\delta \geq 0$, and 2) $\delta < 0$.

If $\delta \geq 0$, all the stability conditions (24)-(27) are satisfied, and the limiting system is stable.

If $\delta < 0$, the stability of the limiting system depends on the degree of water preheating in the reactor. For certain cases of preheating, the plant can be stable, and for other cases, it can be unstable. A limiting system will be stable if the intensity of water preheating in the reactor satisfies the conditions (25)-(27)[†]. The inequalities (25) and (26) can be rewritten in the following form:

$$\Delta T_0 > \frac{\frac{l}{\lambda}|\delta| - \left(\frac{\beta}{\lambda} + l\right) G c_{p2}}{\frac{\alpha(1-\beta)}{2\lambda} G c_{p2}} \times$$

$$\times \frac{1 - \exp\left(-\frac{K_L L}{G_1 c_{p1}}\right)}{1 + \exp\left(-\frac{K_L L}{G_1 c_{p1}}\right)} \equiv \Delta T_1, \qquad (28)$$

$$\Delta T_0 < \frac{2N_0}{|\delta|} \frac{1 - \exp\left(-\frac{K_L L}{G_1 c_{p1}}\right)}{1 + \exp\left(-\frac{K_L L}{G_1 c_{p1}}\right)} \equiv \Delta T_2. \qquad (29)$$

Let us now determine for which cases of preheating (27) is satisfied. We rewrite this expression thus:

$$A \Delta T_0^2 + B \Delta T_0 + C > 0. \qquad (30)$$

It is obvious from (27) that for all

$$\Delta T_0 > \Delta T^* =$$
$$= \frac{2\left(\frac{\beta}{\lambda} + l\right)|\delta|}{\alpha G c_{p2}} \frac{1 - \exp\left(-\frac{K_L L}{G_1 c_{p1}}\right)}{1 + \exp\left(-\frac{K_L L}{G_1 c_{p1}}\right)}$$

(27) is valid. Consequently, for any parameters of the system, $A > 0$. It remains to be determined whether the equation

$$A \Delta T_0^2 + B \Delta T_0 + C = 0 \qquad (31)$$

has real roots.

If $B^2 - 4AC > 0$, the equation has two real roots: ΔT_3 and ΔT_4, where $\Delta T_3 < \Delta T_4$. The inequality (27) holds for $\Delta T_0 < \Delta T_3$ and $\Delta T_0 > \Delta T_4$. In this case the limiting system is stable if $\Delta T_1 < \Delta T_0 < \Delta T_3$ or $\Delta T_4 < \Delta T_0 < \Delta T_2$ (Fig. 4).

If $B^2 - 4AC = 0$, (31) has one real root: ΔT_5. In this case, the inequality (27) holds for all $\Delta T_0 \Delta T_5$, and the limiting system is stable for $\Delta T_1 < \Delta T_0 < \Delta T_2$ with the exception of $\Delta T_0 = \Delta T_5$.

If $B^2 - 4AC < 0$, the equation has no real roots, (27) is satisfied for any ΔT_0, and the limiting system is stable if $\Delta T_1 < \Delta T_0 < \Delta T_2$.

Let us consider the stability of the system by taking into account the lagging elements. We shall write the transfer function of the limiting system in the form

$$W_{ls}(j\omega) = W_0(\omega) \exp[j\theta(\omega)], \qquad (32)$$

where $W_0(\omega)$ is the modulus, $\theta(\omega)$ is the argument, and $j = \sqrt{-1}$. The transfer function of a system where the lagging elements have been taken into account is of the following form

$$W(j\omega) = W_0(\omega) \exp\{j[\theta(\omega) - (\tau_1 + \tau_2)\omega]\}. \qquad (33)$$

In order that a system with delays be stable, it is necessary and sufficient [3] that the point $(1, j0)$ lies outside the contour of the vector hodograph:

$$W(j\omega) = W_0(\omega) \exp\{j[\theta(\omega) - (\tau_1 + \tau)\omega]\}.$$
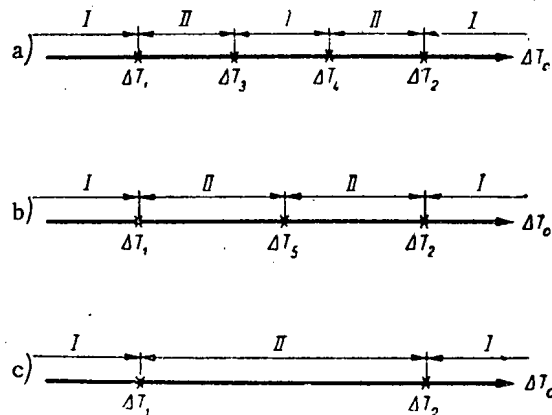
Fig. 4. Stability regions of the plant for $\delta < 0$. a) $B^2 - 4AC > 0$; b) $B^2 - 4AC = 0$; c) $B^2 - 4AC < 0$; I) instability region; II) stability region. (At the points ΔT_1, ΔT_2, ΔT_3, ΔT_4, and ΔT_5, the system is unstable.)

[†] Condition (24) is always satisfied.

The moduli of vectors $W_{1s}(j\omega)$ and $W(j\omega)$ for each frequency are identical and equal to $W_0(\omega)$. Let us evaluate the value of $W_0(\omega)$:

$$W_0(\omega) = W_{r_0}(\omega) W_{sg_0}^r(\omega),\tag{34}$$

where $W_{r_0}(\omega)$ and $W_{sg_0}(\omega)$ are the moduli of transfer functions of the reactor and the steam generator.

$$W_{r_0}(\omega) = \frac{\left(G_1 c_{p1}\frac{l}{\lambda}\omega^2+\frac{\alpha N_0}{2}\right)^2+\left[\left(\frac{\beta}{\lambda}+l\right)G_1 c_{p1}-(1-\beta)\frac{\alpha N_0}{2\lambda}\right]^2\omega^2}{\left(G_1 c_{p1}\frac{l}{\lambda}\omega^2+\frac{\alpha N_0}{2}\right)^2+\left[\left(\frac{\beta}{\lambda}+l\right)G_1 c_{p1}+(1-\beta)\frac{\alpha N_0}{2\lambda}\right]^2\omega^2}.\tag{35}$$

It is obvious from (35) that $W_{r_0}(\omega) = 1$ only for $\omega = 0$; for all $\omega \neq 0$, $W_{r_0} = (\omega) < 1$.

Thus, $\tag{36}$

$$W_{r_0}(\omega) \leqslant 1,$$

$$W_{sg_0}(\omega) = \frac{\left\{G_1 c_{p1}\left[1-\exp\left(-\frac{K_L L}{G_1 c_{p1}}\right)\right]+\delta\exp\left(-\frac{K_L L}{G_1 c_{p1}}\right)\right\}+G^2 c_{p2}^2\exp\left(-\frac{2K_L L}{G_1 c_{p1}}\right)\omega^2}{\left\{G_1 c_{p1}\left[1-\exp\left(-\frac{K_L L}{G_1 c_{p1}}\right)\right]+\delta\right\}^2+G^2 c_{p2}^2\omega^2}.\tag{37}$$

From (37), it is obvious that

$$W_{sg_0}(\omega) < 1.\tag{38}$$

By taking into account (34), (36), and (38), we obtain

$$W_0(\omega) < 1.$$

Since the modulus of the transfer function is less than 1, the point $(1, j0)$ will lie outside the contour of the vector hodograph for any lag time. Consequently, a system with delays will be stable, if the limiting system is stable, i.e., if (25)-(27) are satisfied.

CONCLUSIONS

On the basis of investigations performed on the considered nuclear power plant, we can arrive at the following conclusions: 1) $\delta = di^*/dt_2[G_{20}-(A_2/A_1)(i_0^* - i_{cw})] \geq 0$, the system is stable for any intensity of water preheating in the reactor;

2) If $\delta < 0$, then, for certain given preheating intensities, instability regions appear (see Fig. 4), and the number of such regions and their size are determined by the following relations:

$$\Delta T_0 > \frac{\frac{l}{\lambda}|\delta|-\left(\frac{\beta}{\lambda}+l\right)Gc_{p2}}{\frac{\alpha(1-\beta)}{2\lambda}Gc_{p2}}\times$$

$$\times\frac{1-\exp\left(-\frac{K_L L}{G_1 c_{p1}}\right)}{1+\exp\left(-\frac{K_L L}{G_1 c_{p1}}\right)}=\Delta T_1,$$

$$\Delta T_0 < \frac{2N_0}{|\delta|}\frac{1-\exp\left(-\frac{K_L L}{G_1 c_{p1}}\right)}{1+\exp\left(-\frac{K_L L}{G_1 c_{p1}}\right)}=\Delta T_2,$$

$$A\Delta T_0^2+B\Delta T_0+C > 0.$$

The roots of the quadratic trinomial are ΔT_3 and ΔT_4; $A > 0$.

The indicated relations make it possible to determine the stability of a system for any values of the plant parameters. However, in actual plants, the system parameters are such that $\Delta T_1 < 0$, $\Delta T_3 < 0$, and $\Delta T_4 < 0$, and the stability region lies in the $0 < \Delta T_0 < \Delta T_2$ interval, where ΔT_2 is equal to $\sim 10^3\,°C$, i.e., it considerably exceeds the actual preheating of water in the reactor.

It should be noted that, if the reactor has a positive temperature coefficient of reactivity, the system of inequalities defining the stability conditions is incompatible and the plant is unstable.

Thus, actual plants of the considered type are stable if the reactor has a negative temperature coefficient of reactivity.

The author extends his thanks to S. M. Feinberg and Ya. V. Shevelev for their discussion of a number of problems encountered in the work.

LITERATURE CITED

1. Material of the USA Atomic Energy Commission. Nuclear Reactors, part I: Nuclear Reactor Physics.
2. A. A. Voronov, Elements of Automatic Control Theory [in Russian] (Voenizdat, 1954).
3. Ya. Z. Tsypkin, Avtomatika i Telemekhanika 7, 107 (1946).

THE NUCLEAR REACTOR CIRCULATION CIRCUIT
AS A RADIATION SOURCE

Yu. S. Ryabukhin and A. Kh. Breger

The solution of the problem of circulation circuits with a single radioisotope, which has been found earlier [1], is applied to the general case where several radioisotopes having radioactive progeny are formed in the substance to be activated. The problems of the absolute maximum circuit power and the consumption of neutrons per unit power for a number of elements which can be used as substances to be activated in the circuit are considered. From among them, the most promising are indium and its alloys.

Special attention is paid to a circulation circuit where the substance to be activated contains a fissionable isotope ("uranium" circuit). It is shown that the specific power of such a circuit, all other conditions being equal, is considerably lower than the specific power of circuits with metallic indium or its alloys. As a particular case of a "uranium" circuit, the circulation from the reactor into the radiation unit, and the reverse, of fuel elements which have not burned up completely is considered. It is shown that, in this case, the power of the unit can be increased two- to fourfold in comparison with the power of a unit, which makes a single use of completely burned-up fuel elements.

INTRODUCTION

A circuit where a single radioisotope without radioactive progeny is formed in the substance to be activated has been considered in [1].[*] However, more complex cases are possible. In the first place, several radioisotopes can be formed as a result of activation; in the second place, the daughter products of these primary radioisotopes can be radioactive; in the third place, the primary radioisotopes themselves as well as their radioactive and stable decay products can be activated, thus forming new radioisotopes. Finally, there is a special case where a fissionable isotope is contained in the substance to be activated ("uranium" circuit).

Consequently, the formation of a very complex mixture of isotopes, the components of which can be either independent or genealogically related to each other, is possible. The calculation of such a circuit with the values t_r, t_a, and t_B, changing from one cycle to another is difficult and hardly rational.[†] Therefore, in this case it is natural to limit ourselves to the consideration of a circuit where t_r, t_a, and t_B are constant.

Circuit with Constants t_r, t_a, and t_B

The over-all power of such a circuit is obviously equal to the sum of powers of isotopes emitting γ radiation

If a radioactive family is available, the specific power (i.e., the power per liter of substance to be activated) of an ideal circuit, which corresponds to the $\underline{m}$th isotope in the chain (designating the isotope to be activated by zero), is equal to[‡]

$$P_m^{id} = A_m \prod_{q=1}^{m} \lambda_q \sum_{q=1}^{m} \frac{[1-\exp(-\tau_q)][1-\exp(-\nu_q)]}{(\tau_q+\nu_q)\lambda_q \prod_{j=1}^{m} (\lambda_j - \lambda_q) \left[1-\exp[-(\tau_q+\nu_q)]\right]} \left[1 - \frac{1-\exp[-n(\tau_q+\nu_q)]}{n[\exp(\tau_q+\nu_q)-1]}\right],\qquad(1)$$

where $A_m = \varphi \sigma N \Gamma_m$, and the condition $\lambda_j - \lambda_q = 1$ holds with respect to $\prod_{j=1}^{m} (\lambda_j - \lambda_q)$.

We also derived ‡ the equation for the energy of γ radiation stored at the moment $\underline{t}$ of the period t_a, which

---

[*] While [1] was in preparation, we had the opportunity of studying the report by R. Gordon ("Project of an Irradiation Loop"), which was presented at the Conference on Nuclear Science and Technology (Chicago, March, 1958). A certain number of problems considered in [1] are treated in this paper. The results obtained by Gordon agree with the results obtained in the corresponding parts of our work [1].

[†] For notation, see [1].

[‡] See Appendix.

636

is equal to the number of atoms of a given isotope multiplied by the energy of γ radiation emitted by these atoms:

$$U_m^{id} = A_m \prod_{q=1}^{m-1} \lambda_q \sum_{q=1}^{m} \frac{\left[1-\exp[-n(\tau_q+\nu_q)]\right][1-\exp(-\tau_q)]\exp(-\lambda_q t)}{\lambda_q \prod_{j=1}^{m}(\lambda_j-\lambda_q)\left[1-\exp[-(\tau_q+\nu_q)]\right]}. \qquad (2)$$

This equation is simpler than the similar equation derived in [2].

By using (1) and (2), the specific power can be calculated also in the case where any of the isotopes in the family, for instance the pth, is activated. Such an isotope can be designated as the zero isotope in a new family, and the specific power of the m'-th isotope can also be determined from (1), where, in the expression for $A_{m'} = \varphi\sigma_r N_r \Gamma_{m'}$, the magnitude of N_r is calculated from (2).

For an actual circuit, the expressions for specific power and stored decay energy are of the following form:

$$P_m = A_m \prod_{q=1}^{m} \lambda_q \sum_{q=1}^{m} \frac{[1-\exp(-\tau_q)][1-\exp(-\nu_q)]\exp(-\eta_q)}{\left(\tau_q+\nu_q+\varepsilon_q-\frac{\vartheta_q}{n}\right)\lambda_q \prod_{j=1}^{m}(\lambda_j-\lambda_q)\left[1-\exp[-(\tau_q+\nu_q+\varepsilon_q)]\right]} \times$$

$$\times \left[1-\frac{1-\exp[-n(\tau_q+\nu_q+\varepsilon_q)]}{n[\exp(\tau_q+\nu_q+\varepsilon_q)-1]}\right];$$

$$U_m = A_m \prod_{q=1}^{m-1} \lambda_q \sum_{q=1}^{m} \frac{\left[1-\exp[-n(\tau_q+\nu_q+\varepsilon_q)]\right][1-\exp(-\tau_q)]\exp[-\lambda_q(t+t_{ra})]}{\lambda_q \prod_{j=1}^{m}(\lambda_j-\lambda_q)\left[1-\exp[-(\tau_q+\nu_q+\varepsilon_q)]\right]}. \qquad (3)$$

In order to determine the optimum power conditions, it is necessary to find the maximum of the sum of specific powers with respect to each isotope. In its general form this problem is very complicated, and, in practice, it is more convenient to use an approximate and, therefore, simpler method of selecting operating conditions. In this, one should be guided by the following considerations.

If a simple isotope mixture is available, only the shortest-lived and the longest-lived isotopes, whose contribution to the over-all specific power is the greatest, are considered.

A decrease in specific power in comparison with 1/4 A due to the finiteness of t_B and the fact that t_r and t_a are not at their optimum values is more strongly pronounced in the case of short-lived isotopes (see (4) and (5) in [1]); a decrease in specific power due to unsaturation with respect to activity will be more strongly pronounced in long-lived isotopes. The magnitudes of functional parts in the expression for the specific power of all other isotopes lie between the magnitudes of functional parts in the expression for specific power corresponding to these two isotopes.

In the case of an isotope chain, the specific power corresponding to the mth isotope will be determined by the accumulation and decay of atoms of the preceding members of the chain. If the decay constants of individual chain members differ very much among themselves, i.e., $\lambda_a \gg \lambda_b \gg \lambda_c \ldots \gg \lambda_d$, the operating conditions will be mainly determined by that term of the sum in (3) where the decay constant is the smallest. If there are two or more terms where λ differ little from each other, then, on the basis of the fact that the product of each term of the sum in (3) and $\lambda_q \prod_{j=1}^{m}(\lambda_j-\lambda_q)$ changes

little in relation to λ (see (5) [1]), such products can be considered as being equal; the corresponding components of the sum in (3) can be added, and the considerations mentioned before can be used.

Having chosen the operating conditions, it is possible to calculate with accuracy the specific power corresponding to each isotope and to prove that the conditions have been correctly chosen.

Substances Which Can Be Used in the Circuit

Table 1 provides some data on elements which can be used as substances to be activated.

In this table, C_i is the share of the i th isotope in a natural mixture of isotopes with the activation cross section $\sigma_{i\,act}$; σ_{abs} is the cross section of neutron absorption by the natural mixture of isotopes of a given element.†† The fourth column gives the absolute maximum power per atom of the element in question, and the fifth column provides the maximum power per one consumed neutron. The table contains only those elements for which: 1) the half life of γ-emitting isotopes does not exceed 100 days; 2) $\sum_i C_i \sigma_{i\,act} \Gamma_i \geqslant 2\,\text{barn·Mev}$; 3) $\dfrac{\sum_i C_i \sigma_{i\,act} \Gamma_i}{\sigma_{abs}} \geqslant 0,5\,\text{Mev}$.

The data in the table show that the most suitable elements with respect to the absolute maximum power per atom are In, Ir, Sc, Mn, and La. The actually attainable absolute maximum powers depend, of course, on the physical and chemical properties of the substances.

With respect to the most efficient use of neutrons consumed in activation, Na, which is the best element, is followed by La, Sc, In, Mn, and Ga. The actual efficiency of neutron utilization depends on the absorption

†† The values for σ_{act}, σ_{abs}, and C are taken from [3]; the values for Γ are taken from [4-6].

637

Element	Isotopes emitting γ rays	Half life	$\sum_i C_i \sigma_{i\,act} \Gamma_i$, barn·Mev	$\dfrac{\sum_i C_i \sigma_{i\,act} \Gamma_i}{\sigma_{abs}}$, Mev
Na	Na^{24}	15,1 hr	2,1	4,1
Sc	Sc^{46}	85 days	44	2,0
Mn	Mn^{56}	2,58 hr	21,5	1,6
Ga	Ga^{72}	14,3 hr	3,7	1,4
Br	Br^{82} Br^{80}	1,5 days 18 min	4,9	0,76
In	In^{116}	53,9 min	344	1,8
Sb	Sb^{122} Sb^{124}	2,8 days 60 days	3,6	0,66
La	La^{140}	1,66 days	19	2,2
Ir	Ir^{192}	74,3 days	220	0,5

cross section of a given substance and on the operating conditions of a given circuit.

Table 2 lists the absolute maximum powers for some substances whose application seems to be most promising. The calculations were performed for $\varphi = 10^{13}$ neutron·cm^{-2}·sec^{-1}.

In this table, indium and its alloys are the best substances with respect to specific power, and sodium has a good neutron utilization efficiency. Thus, in developing actual systems, it is possible to select a circulating substance which is most suited to satisfy the necessary requirements.

The following factors should be taken into account in selecting a circulation circuit for an actual nuclear reactor. In comparing specific powers, it is assumed that the introduction of the substance to be activated in the activation zone will not disturb the neutron flux to a great extent. The same assumption has been made also in [1] in the selection of an optimum circuit. Such an assumption is connected not only with the fact that the amount of the substance to be activated is considered to be small in many cases, but also with the fact that it is impossible to find a general expression for reducing the flux in the activation zone when a certain volume of the substance to be activated is introduced. The reduction

of the flux depends in every case on geometric factors. However, if the flux reduction is significant we can consider that, for a given average flux in volume V_r, the volume V_r is also given, and we can find the relatively optimum operating conditions (see [1]). A comparison of substances with respect to the power per neutron absorbed in 1 sec is important in the case where neutrons are used for other purposes, i.e., when they have a certain "value". The most efficient use of neutrons is secured in a circuit where V_a is infinitely large with respect to V_r. In this case, the power per each neutron absorbed in 1 sec will be twice that indicated in Table 2. It is obvious that such a circuit will be extremely inefficient with respect to the power liberated in the unit per liter, i.e., with respect to volumes circulating in the circuit.

It is of interest to compare the obtained results with the corresponding data characterizing the use of the Co^{60} isotope as a source of γ radiation. The quantities

$$\sum_i C_i \sigma_{i\,act} \Gamma_i, \text{ and } \frac{\sum_i C_i \sigma_{i\,act} \Gamma_i}{\sigma_{abs}}$$ for cobalt are equal to

90 barn·Mev and 2.5 Mev, respectively; in the case of a circuit containing pure cobalt, $P_{a\,max}$ (for $\varphi = 10^{13}$ neutron·cm^{-2}·sec^{-1}) is equal to 3160 w/liter. However, the average specific power for a time acceptable in prac-

Elements to be activated	Substance state	$P_{a\,max}$, w/liter	Power per neutron absorbed in 1 sec, w × 10^{-13}	Melting temperature, °C
Na	Liquid metal	20	3,16	97
Mn, Br	3 M solution of MnBr$_2$	23	0,96	
In, Ga	Liquid alloy: 24%-In alloy	1200	1,42	16*
In	Liquid metal	5100	1,44	156
In	Liquid alloy: 56% In; 34% Bi; 10% Pb	3300	1,44	73 [8]
In	Liquid alloy: 52% In; 30% Bi; 18% Sn	2900	1,44	60 [8]
In	1 M solution of In$_2$(SO$_4$)$_3$	165	1,44	

* See, for example, [7].

638

tice is much lower. Actually, by using (4b) of [1], it is easily found that for K = 1 year, $t_r = t_a$ = 0.5 year , and t_B = 0; the average power of a Co^{60} specimen with a volume of 1 dm^3 is P^{id} = 0.032A = 405w.

In this case the efficiency of neutron utilization will be 0.25 w/neutron, i.e., it will be 5.8 times lower than that for the In-Ga alloy (see Table 2).

"Uranium" Circuit

The consideration of a circulation circuit where a substance containing a fissionable isotope is used for the "transfer" of γ radiation to the radiation unit is undoubtedly of great interest [9]. The solution of the problem of selecting optimum operating conditions of a circuit with respect to the attainable specific power of the radiation unit, can serve as a basis for the development of such circuits for homogeneous as well as for heterogeneous nuclear reactors. Moreover, the "uranium" circuit theory must serve as a basis in calculating the conditions for a complete or partial utilization of burn-up elements in different radiation units, which is also of great practical importance (see, for example, [10-13].

The main difficulty in solving this problem is connected with the fact that the data on the γ radiation of fragments and, particularly, of fragments of short-lived isotopes are incomplete and often inaccurate. Nevertheless, we attempted to calculate the maximum specific power of a "uranium" circuit by borrowing data on iso-
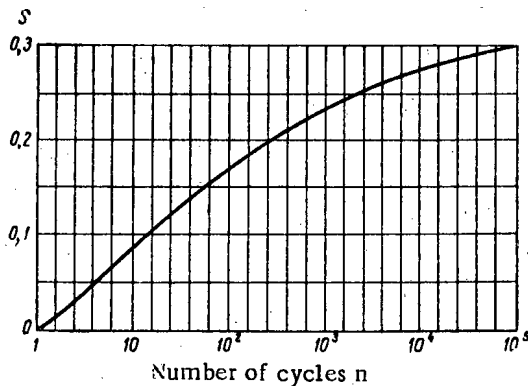
Fig. 1. Graph of the S(n) function.

Fig. 2. Graph of the $Q(\xi)$ function for different numbers of cycles $\underline{n}$.

topes from [4-6] and data on U^{235} fission-product yields from [14].

By summing up the specific powers with respect to each isotope, we obtain

$$P^{id}_{a \cdot max} = \frac{1}{4} \sum_m A_m = \frac{1,6}{4} \varphi \sigma_U N_U \text{ Mev/sec·liter.} \tag{4}$$

For the circulation of a 1.26 M aqueous solution of the $UO_2 (NO_3)_2$ natural uranium salt for $\varphi = 10^{13}$ neutron $\cdot cm^{-2} \cdot sec^{-1}$, we have $P^{id}_{a \, max}$ = 1.9 w/liter.

This magnitude is apparently lower than the actual one, since many short-lived isotopes have not been taken into account.

Therefore, we thought it convenient to use a different method in this case: the Way-Wigner equation for the energy of γ radiation emitted by fragments per unit time at the time $\underline{t}$ sec after fission. This equation can be used in the $10 \le t \le 10^7$ sec interval [15]:

$$\frac{dE}{dt} = 1,26 \ t^{-1,2} \text{ Mev/sec·fission.} \tag{5}$$

Considering, as before, that t_r and t_a are constant, we obtain

$$P_c = \frac{7,88f \sum_{k=0}^{n-1} \left(1 - \frac{k}{n}\right) \{(g_c + t_a)^{0,8} - g_c^{0,8} - (g_c + t_a + t_r)^{0,8} + (g_c + t_r)^{0,8}\}}{t_r + t_a + t_n - \frac{t_{ar}}{n}} ,$$

where f is the number of fissions per sec in 1 liter, and $g_c = k (t_r + t_a + t_B) + t_{ra}$.

It should be noted that (6) as well as the corresponding equations in [1] are symmetrical with respect to t_r and t_a, i.e., for the optimum condition $t_r = t_a$ for a given t_B.

The problem of finding the sum in (6) in a form con-

venient for practical use and with a good approximation at the same time remains unsolved. ‡‡

However, the necessary equations can be obtained for certain particular cases.

_____

‡‡ In principle, this can be done by using Euler's equation, however, the resultant expression would be unwieldy.

639

1. If $\underline{n}$ is so small, that a term-by-term summation can be done in practice, this summation would provide a general solution of the problem, i.e., a solution for any t_r, t_a, t_{ra}, and t_{ar}.

2. Let $t_r = t_a$ and $t_{ra} = t_{ar}$.

Then, for $\xi \leq 1$, with an accuracy of $\pm 2\%$, we have[***]

$$P_c = \frac{7,88/\xi^{0,2}}{t_{ra}^{0,2}\left[2(1+\xi)-\frac{\xi}{n}\right]}\left[2(\xi+1)^{0,8}-\xi^{0,8}-(\xi+2)^{0,8}+\frac{S(n)}{(1+\xi)^{1,2}}\right], \quad (7)$$

where $S(n)$ is found from Fig. 1.

Let us denote $P_c\, t_{ra}^{0,2}/f$ by $Q(\xi, n)$. The $Q(\xi, n)$ curve is shown in Fig. 2. As can be seen from the figure, the value $\xi \approx 0.08$ corresponds to the optimum operating conditions for any $\underline{n}$. Like (5), (6) and (7) are applicable in the time interval from 10 to 10^7 sec.

Calculations according to (7), show that the specific power of a circulation circuit where the substance to be activated is, for instance, a 1.26 M solution of uranyl nitrate (for $\varphi = 10^{13}$ neutron$\cdot$cm$^{-2}\cdot$sec^{-1}, $t_r = t_a = 140$ sec, $t_{ra} = t_{ar} = 10$ sec, and K = 100 days) is equal to 3.2 w/liter, i.e., it is 1.7 times greater than the corresponding value obtained from (4) for the ideal optimum circuit.

However, with respect to specific power, such a circuit is considerably inferior to those considered earlier (Table 2).

For the sake of comparison, we shall mention that even if metallic uranium circulates in the circuit, the specific circuit power (for the same conditions) amounts to only 190 w/liter.[†††] This is the limit for this type of circuit (for the above-mentioned neutron flux).

It is easy to evaluate by how much the "uranium"
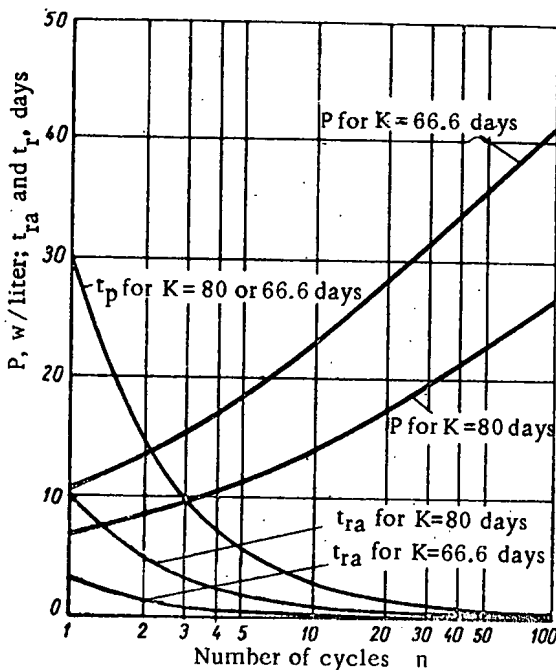
circuit power can be increased in approaching the ideal optimum circuit with n = ∞. It is known that the total γ-radiation energy emitted by fragments amounts to ~ 6 Mev/fission. At the same time, it can be easily found from (5) that an energy of

$$\int_{10}^{10^7} 1,26t^{-1,2}\,dt = 3,85 \quad \text{Mev/fission}$$

is emitted in the interval from 10 to 10^7 sec.

Hence, it follows that even in the ideal case the power can be increased approximately 1.5-fold.

However, it should be kept in mind that the number of delayed neutrons emitted in the radiation unit per unit time will greatly increase in approaching the indicated ideal circuit. For each isotope emitting neutrons, the number of such neutrons per 1 liter is determined from an equation which is similar to (4a) in [1]:

$$M = \frac{Df\left[1-\exp(-\tau)\right]\left[1-\exp(-v)\right]\exp(-\eta)}{(\tau+v)\left[1-\exp\left[-(\tau+v+\varepsilon)\right]\right]},$$

where D is the yield of delayed neutrons of a certain group per fission. For instance, for the above data used in the calculation of specific "uranium" circuit power, the over-all specific number of neutrons in all groups is $1.5 \cdot 10^{10}$ neutron/sec $\cdot$ liter^{-1}.

Utilization of Fuel Elements in Radiation Units

Equation (7) can be applied also for determining the operating conditions and for calculating the specific power of radiation units where completely (n = 1) or partially (n > 1) burned-up fuel elements are used as radiation sources.[‡‡‡]

In using completely burned-up fuel elements, it is understood that the cooling must be done in a special radiation unit. As an example, we calculated according to (7), the specific power for completely burned-up fuel elements for different burn-up times (t_r = 10, 20, 30, and 45 days) and for different feed rates of fuel elements from the reactor to the radiation unit ($0.3 \leq t_{ra} \leq 10$ days). The calculation results indicate a) the average specific power of the unit can be considerably increased (1.5- to 3-fold) and, for natural uranium, it can be increased from 4-7 to 13-14 w/liter for $\varphi = 10^{13}$ neutron$\cdot$cm$^{-2}\cdot$sec^{-1} (throughout the operational period of fuel elements) by reducing the conveyance time of fuel elements from 10 to 1-2 days; b) if the transport of fuel

[***] See Appendix.
[†††] The data pertain to unenriched uranium.
[‡‡‡] By completely burned-up fuel elements, we mean such elements which were present in the reactor during a normal operation cycle. Afterwards, they are usually cooled and reprocessed.

640

elements lasts 1-2 days, the average specific power of the unit is almost independent of the burn-up time (within ± 5%) and is equal to 13-14 w/liter for the above conditions.

As will be seen from the following, a considerably more efficient irradiation will be achieved by using fuel elements which are partially burned-up in the reactor (during time t_r) and then transferred to the radiation unit where, during time t_a, they are used as sources of γ radiation and then returned to the reactor. Obviously, this process can be repeated many times until the fuel elements have burned up completely.

Figure 3 shows some calculation results for two cases with different durations K of operation of the whole "circuit" for a neutron flux equal to $\varphi = 10^{13}$ neutron· ·cm^{-2}·sec^{-1}. The calculation was performed for 1 dm^3 of a conventional fuel element consisting of pure unen-

riched uranium. The duration nt_r of a full cycle of the fuel element operation in the reactor is taken to be 30 days. It is assumed that $t_a = t_r$. The time t_{ra} required for transporting the fuel element from the reactor to the unit and the time t_{ar} required for the reverse process, were determined by taking into account the following conditions: $t_{ra} = t_{ar}$ and $nt_{ra} = 10$ days (for K = 80 days), and $nt_{ra} = 3.3$ days (for K = 66.6 days). It is obvious from the curves in Fig. 3 that if partially burned-up fuel elements are used many times (n > 1), the specific power of the unit can be increased manifold in comparison with the power of a unit, where completely burned-up fuel elements are used only once (n = 1).

Equation (7) and the curves shown in Figs. 1 and 2 provide the possibility of performing calculations for other cases of "circulation" of fuel elements if $t_r = t_a$ and $t_{ra} = t_{ar}$.

APPENDIX

Derivation of Equations (1) and (2)

Let us first determine the decay energy of the mth isotope (considering the isotope to be activated as the zero isotope) stored until time t of the period t_{ai}; due to activation over the period t_{rc}:

$$U_m^{ik} = \Gamma_m \sum_{r=1}^{m} \left\{ N_r \prod_{q=r}^{m-1} \lambda_q \sum_{q=r}^{m} \frac{\exp[-\lambda_q(t_r+t_a)(i-k)-\lambda_q t]}{\prod\limits_{j=r}^{m}(\lambda_j-\lambda_q)} \right\}, \tag{1A}$$

where

$$N_r = N_0 \prod_{q=1}^{r-1} \lambda_q \sum_{q=0}^{r} \frac{\exp[-\lambda_r t_r]}{\prod\limits_{j=0}^{r}(\lambda_j-\lambda_q)} \tag{2A}$$

is the number of atoms of the rth isotope available at the end of period t_{rc}, due to activation during this time only. In (1A) and (2A) the following conditions hold: $\prod\limits_a^b \lambda_q = 1$, if b < a, $\lambda_0 N_0 = \varphi \sigma_0 N_0$, but $\lambda_0 = 0$ in the exponent, and, in $\lambda - \lambda_g[1/(\lambda-\lambda_g)]=1$. Equations (1A) and (2A) are obtained by modifying the equation for the number of radioactive atoms of the mth element in the chain (see, for instance, [16]). By substituting (2A) in (1A), we obtain

$$U_m^{ik} = A_m \prod_{q=1}^{m-1} \lambda_q \sum_{r=1}^{m} \left\{ \sum_{q=0}^{r} \frac{\exp[-\lambda_q t_r]}{\prod\limits_{j=0}^{r}(\lambda_j-\lambda_q)} \sum_{q=r}^{m} \frac{\exp[-\lambda_q(t_r+t_a)(i-k)-\lambda_q t]}{\prod\limits_{j=r}^{m}(\lambda_j-\lambda_q)} \right\}$$

Let us simplify the expression under the summation sign $\sum\limits_{r=1}^{m}$. For this, we shall note that as a result of

multiplying the $\sum\limits_{q=0}^{r}$ and $\sum\limits_{q=r}^{m}$ sums, three kinds of products are obtained: 1) products containing only

$\exp \lambda_a[-(t_r + t_a)(i-k)-t]$; 2) products containing $\exp[-\lambda_a t_r] \exp \lambda_a[-(t_r + t_a)(i-k)-t]$; 3) products containing

$\exp[-\lambda_a t_r] \times \lambda_b[-t_r + t_a)(i-k)-t]$, $a \neq b$. The sums containing the products of the first, second, and third kinds are reduced to the following expressions, respectively:

$$1)\ \sum_{q=1}^{m} \frac{\exp \lambda_q[-(t_r+t_a)(i-k)-t]}{\lambda_q \prod_{j=1}^{m}(\lambda_j-\lambda_q)}\ ; \qquad 2)\ \sum_{q=1}^{m} \frac{\exp \lambda_q[-t_r-(t_r+t_a)(i-k)-t]}{\prod_{j=0}^{m}(\lambda_j-\lambda_q)} \qquad 3)\ 0.$$

Hence

$$U_m^{ik} = A_m \prod_{q=1}^{m-1} \lambda_q \sum_{q=1}^{m} \frac{\exp \lambda_q[-(t_r+t_a)(i-k)-t]}{\lambda_q \prod_{j=1}^{m}(\lambda_j-\lambda_q)}[1-\exp(-\lambda_q t_r)].$$

For the stored decay energy of the mth isotope at the moment t of the t_a period of the nth cycle (i.e., $i = n$), we obtain

$$U_m^{id} = \sum_{h=1}^{n} U_m^{ik} = A_m \prod_{q=1}^{m-1} \lambda_q \sum_{q=1}^{m} \frac{[1-\exp[-n(\tau_q+\nu_q)]]\,[1-\exp(-\tau_q)]\exp(-\lambda_q t)}{\lambda_q \prod_{i=1}^{m}(\lambda_j-\lambda_q)\,[1-\exp[-(\tau_q+\nu_q)]]}.$$

The energy emitted by the mth isotope during the ith cycle due to activation during the kth cycle is only

$$E_m^{ik} = \int_0^{t_a} \lambda_m U_m^{ik}\,dt = A_m \prod_{q=1}^{m} \lambda_q \sum_{q=1}^{m} \frac{[1-\exp(-\lambda_q t_p)]\,[1-\exp(-\lambda_q t_a)]\exp[-\lambda_q(t_r+t_a)(i-k)]}{\lambda_q^2 \prod_{j=1}^{m}(\lambda_j-\lambda_q)}.$$

The specific power corresponding to the mth isotope for n cycles is

$$P_m^{id} = \frac{\sum_{i=1}^{n}\sum_{h=1}^{i} E_m^{ik}}{n(t_r+t_a)} = A_m \prod_{q=1}^{m} \lambda_q \sum_{q=1}^{m} \frac{[1-\exp(-\tau_q)]\,[1-\exp(-\nu_q)]}{(\tau_q+\nu_q)\lambda_q \prod_{j=1}^{m}(\lambda_j-\lambda_q)\,[1-\exp[-(\tau_q+\nu_q)]]} \times$$

$$\times \left[1 - \frac{1-\exp[-n(\tau_q+\nu_q)]}{n[\exp(\tau_q+\nu_q)-1]}\right].$$

Derivation of the Equation for the Specific Power of a "Uranium" Circuit

If the number of fissions per sec is f, then, by using (5), it can be written that the energy liberated during the t_{ai} in the time interval from Δt_{ai} to $\Delta t_{ai} + dt_{ai}$ as a result of fissions which occurred during the period t_{rc} in the time interval from Δt_{rc} to $\Delta t_{rc} + dt_{rc}$ is equal to

$$dE_{ic} = 1,26 f \cdot dt_{rc}[(i-k)(t_r+t_a+t_u)+t_{ra}+\Delta t_{ai}+(t_{rc}-\Delta t_{rc})]^{-1,2}\,dt_{ai},$$

whence

$$E_{ic} = \int_{\Delta t_{ai}=0}^{t_{ai}} \int_{\Delta t_{rc}=0}^{t_{rc}} dE_{ic} = 7,88 f\,\{(g_{ic}+t_a)^{0,8}-g_{ic}^{0,8}-(g_{ic}+t_a+t_r)^{0,8}+(g_{ic}+t_r)^{0,8}\}.$$

where

$$g_{ic} = (i-k)(t_r+t_a+t_u)+t_{ra}$$

and

$$P_c = \frac{\sum_{i=1}^{n}\sum_{k=1}^{i} E_{ik}}{n\,(t_r + t_a + t_B) - \dfrac{t'_{ar}}{n}} = \frac{7{,}88f\sum_{k=0}^{n-1}\left(1-\dfrac{k}{n}\right)\{(g_c + t_a)^{0,8} - g^0{}_c{}^{,8} - (g_c + t_a + t_r)^{0,8} + (g_c + t_r)^{0,8}\}}{t_r + t_a + t_B - \dfrac{t'_{ar}}{n}},$$

where $g_c = k(t_r + t_a + t_B) + t_{ra}$.

If $t_r = t_a$ and $t_{ra} = t_{ar}$, (3A) can be rewritten in the following manner:

$$P_c = \frac{7{,}88f\xi^{0,2}\sum_{k=0}^{n-1}\left(1-\dfrac{k}{n}\right)\{2\,[2k\,(1+\xi)+\xi+1]^{0,8} - [2k\,(1+\xi)+\xi]^{0,8} - [2k\,(1+\xi)+\xi+2]^{0,8}\}}{t_{ra}^{0,2}\left[2\,(1+\xi)-\dfrac{\xi}{n}\right]}.$$

The sum $\sum_{k=0}^{n-1}$ is rewritten

$$\sum_{k=0}^{n-1} = 2\,(\xi+1)^{0,8} - \xi^{0,8} - (\xi+2)^{0,8} + \sum_{k=1}^{n-1}1.$$

It can be shown that if $\xi \leq 1$, then, with an accuracy $\leq \pm 3\%$,

$$\sum_{k=1}^{n-1} \approx \frac{S\,(n)}{(1+\xi)^{1,2}},$$

where

$$S\,(n) = \sum_{k=1}^{n-1}\left(1-\frac{k}{n}\right)\{2\,(2k+1)^{0,8} - (2k)^{0,8} - (2k+2)^{0,8}\}.$$

The S(n) curve is shown in Fig. 1. The error in calculating S(n) does not exceed 3%. Finally, if $\xi \leq 1$ with an accuracy of $\pm 2\%$, we have

$$P_c = \frac{7{,}88f\xi^{0,2}}{t_{ra}^{0,2}\left[2\,(1+\xi)-\dfrac{\xi}{n}\right]}\left[2\,(\xi+1)^{0,8} - \xi^{0,8} - (\xi+2)^{0,8} + \frac{S\,(n)}{(1+\xi)^{1,2}}\right].$$

LITERATURE CITED

1. Yu. S. Ryabukhin and A. Kh. Breger, Atomnaya Énergiya 5, 533 (1958).[2]
2. C. Lock, "Mathematics of fission-product formation in reactors with circulating fuel", Atomic Energy Research Establ. (Gt. Brit.).
3. D. Hughes and J. Harvey, Neutron Cross Sections (N.Y., 1955, McGraw-Hill).
4. N. G. Gusev, Manual for Radioactivity and Protection Against Radioactivity [in Russian] (Medgiz, 1956).
5. A. N. Nesmeyanov, A. V. Lapitskii, and N. P. Rudnenko, Production of Radioactive Isotopes [in Russian] (Goskhimizdat, 1954).
6. G. T. Seaborg, I. Perlman, and J. M. Hollander, Table of Isotopes (1953).
7. W. Svirbely and S. Selis, J. Phys. Chem. 58, 33 (1954).
8. A. Smith and J. Everhart, U. S. Patent No. 2,649,368, American Smelting and Refining Co.
9. A. Kh. Breger, Problemy Fiz. Khim. No. 1, 61, 1958.
10. C. Stackman, D. Harmon, and H. Heff, Nucleonics 15, 94 (1957).
11. Nucleonics 15, 173 (1957).
12. L. Johnson, H. Adams, and M. Barzam, Rubber World No. 1, 137 (1957).
13. W. Francis and J. Marsden, Nucleonics 15, 80 (1957).
14. J. Prawitz and J. Rydberg, Acta Chem. Scand. 12, 369 (1958).
15. R. Murray, Introduction to Nuclear Techniques [Russian translation] (IL, 1955) p. 275.
16. S. E. Bresler, Radioactive Elements [in Russian] (Gostekhizdat, 1952) p. 65.

---

[1] The expression under the sum sign is omitted for brevity.

[2] Original Russian pagination. See C. B. translation.

DOSIMETRY METHOD FOR β RADIATION BASED ON INVESTIGATIONS
OF THE ELECTRON SPECTRA IN THE FIELDS OF β EMITTERS

K. K. Aglintsev and V. P. Kasatkin

A method has been developed for β-ray dosimetry based on the investigation of the effective electron spectra in the fields of β emitters. The β spectra was investigated with the help of a scintillation spectrometer. It was shown, that the value of the dose $D = N\left(\overline{\dfrac{dE}{dx}}\right)$, where N is the number of β particles penetrating an infinitesimal volume around the point being considered; $\left(\overline{\dfrac{dE}{dx}}\right)$ is the value of the ionization loss averaged over the spectrum. It was established that the quantity $\left(\dfrac{dE}{dx}\right)$ is determined by the maximum energy of the β spectrum of the isotope and may be considered to be independent of the depth of the medium and of the source diameter. Curves of depth doses for S^{35}, Tl^{204}, Y^{91}, and $Ce^{144} + Pr^{144}$ are given and criteria for selecting isotopes to provide optimal conditions of irradiation are established.

In the course of its development, β-ray dosimetry is falling behind γ-ray dosimetry. The computational methods for γ-ray dosimetry are based on a simple and accurate exponential law and the absorption and scattering coefficients are reliably established. In contrast to this, β-ray dosimetry has at its disposal only a few empirical relations, valid for a limited number of special cases. In the area of experimental methods, γ-ray dosimetry has at its disposal universal and convenient rules for measuring doses, based on the use of the Bragg-Gray principle for ionization in a cavity and for monitors with tissue-equivalent absorbers, while β dosimetry is compelled to restrict itself to a measuring apparatus adapted to a few special cases [1, 2]. This situation is paradoxical as the mechanism of the action of γ rays is, undoubtedly, more complex that that of β rays, since it involves an additional stage—the absorption of the γ rays and the production of secondary electrons.

The fact that γ emitters often give monochromatic radiation, while β rays give a continuous spectrum of β particles does not explain the above contradiction. Moreover, if we compare measurements of a dose of monoenergetic electrons, with that of a continuous spectrum of x rays, the result of such a comparison is not in favor of electron dosimetry.

Apparently, the decisive factor is the ratio of the lengths of path of the β particles and the γ quanta and the extent of the irradiated medium. Sharp changes in the strength of the dose and the spectral composition of the β radiation take place from point to point in the

field of β emitters. That is why spectral investigations are of decisive importance to β-ray dosimetry.

We have developed a method of β-ray dosimetry, based on investigations of the effective electrons in the spectra, at various depths of the irradiated medium in fields of β emitters, differing in their radiochemical compositions and source dimensions.

Knowledge of the shape of the β spectrum allows one to find the value of the β-ray dose. If an electron possessing an energy E penetrates some infinitesimal volume of the medium about a certain point, then the dose given to the volume will be proportional to the value of the ionization loss of the electron.

Let us consider, the dose received from a stream of electrons possessing different energies. The mean dose given by one electron is equal to the value of the ionization loss $\overline{dE/dx}$ averaged over the spectrum of the electrons penetrating the given volume. Thus, the dose given this volume by the stream of electrons is

$$D = N\left(\overline{\frac{dE}{dx}}\right), \qquad (1)$$

where N is the number of electrons entering the given volume.

We shall give a more rigorous proof of (1). Let us consider a sphere of radius a, and let us assume, that this sphere is penetrated by a parallel stream of β particles. If n is the number of β particles crossing an area 1 cm^2,

the total number of β particles penetrating the sphere is equal to $n\pi a^2$. Since the mean path of the β particles through the sphere is 4/3 a, then, on the average, a β particle penetrates a layer of matter 4/3 aρ (ρ is the density of the matter) and the total energy given up by all the β particles to the sphere is $4/3\pi na^3 \rho(\overline{dE/dx})$. Dividing this expression for the energy by the mass of the sphere, $4/3\pi a^3\rho$, we obtain the dose given the sphere by the stream of β particles:

$$D = \frac{n\pi a^2\, {}^4/_3\, a\rho\left(\overline{\frac{dE}{dx}}\right)}{{}^4/_3\,\pi a^3\rho} = n\left(\overline{\frac{dE}{dx}}\right).$$

If we add the streams corresponding to all possible directions of the β particles through the sphere, we obtain (1), where $N = \Sigma_n$.

We now denote by N(E)dE, the number of electrons whose energy is contained in the interval from E to E + + dE; then

$$N = \int_0^{E_{max}} N(E)\,dE.$$

Obviously, the dose is

$$D = \int_0^{E_{max}}\left(\frac{dE}{dx}\right) N(E)\,dE.$$

We thus obtain, in agreement with (1), the mean dose D_1 for one β particle:

$$D_1 = \frac{D}{N} = \frac{\int_0^{E_{max}}\left(\frac{dE}{dx}\right) N(E)\,dE}{\int_0^{E_{max}} N(E)\,dE} = \left(\overline{\frac{dE}{dx}}\right).$$

$$(2)$$

The dose D_1 and $(\overline{dE/dx})$ are expressed in units of Mev/g · cm². In order to express the dose D_1 in rads or REP it is necessary to multiply $(\overline{dE/dx})$ by a factor equal to

$$\frac{1,6\cdot 10^{-6}}{100} \quad\text{or}\quad \frac{1,6\cdot 10^{-6}}{93},$$

respectively, where $1.6 \cdot 10^{-6}$ is the factor for converting a million electron-volts into ergs. Hence

$$D_1 = 1.6\cdot 10^{-8}\left(\overline{\frac{dE}{dx}}\right)\frac{\text{rad}}{\beta\ \text{particle}} =$$
$$= 1.72\cdot 10^{-8}\left(\overline{\frac{dE}{dx}}\right)\frac{\text{REP}}{\beta\ \text{particle}} \qquad (3)$$

To determine the dose from (1)-(3), we used a scintillation spectrometer [3] consisting of a stilbene crystal in the shape of a flattened hemisphere 35 mm in diameter, a photomultiplier tube, and electronic equipment for analysis and recording of the pulses.

The value of the dose at a given point in the β-emitter field may be found from (2), if the values of N and $(\overline{dE/dx})$ are known. The number of β particles is measured directly and the average value of the ionization loss $(\overline{dE/dx})$ for a given spectrum is found from the well-known relation between (dE/dx) and the electron energy. The method described here has considerable advantages over existing scintillation methods, which employ both thick crystals with complete absorption and thin crystals. In scintillation dosimeters with thick crystals there takes place an averaging of the dose over the entire crystal volume, in particular, over the thickness, i.e., over a direction in which, the value of the dose changes particularly rapidly. The measurement of the spectral distribution, and the use of ionization-loss curves permit one to avoid the averaging over the thickness. The scintillation dosimeters with thin crystals are, in principle, quite suitable for dosage measurements, but their use is connected with great difficulties. In practice, it is impossible to prepare a sufficiently thin scintillator to work with soft and medium β emitters, while the spectrometric method described here gives results corresponding to the use of an infinitely thin crystal.

The investigations were carried out with sources prepared from S^{35}, W^{185}, Tl^{204}, Y^{91}, $Sr^{90} + Y^{90}$, P^{32}, and $Ce^{144} + Pr^{144}$ of diameters 1, 8, 25, and 50 cm. The beta-active substances were placed on tracing paper set on a plexiglas base 10 mm thick. Separate experiments were made with thin sources of small dimensions placed on a colloidal film (~ 50 μg/cm²). The sources were placed at a distance of 2-6 cm from the crystal.

Figure 1 shows the β spectra of the S^{35}, Tl^{204}, and $Sr^{90} + Y^{90}$ sources (1 cm diameter) placed on a film with a plexiglas base; each spectrum refers to a given depth of a tissue-equivalent medium, for which sheets of filter paper were used.

The data presented indicate that as the depth of the medium increases, the curves shift to the left and flatten out and the area under them decreases. This corresponds to a decrease in the number of electrons falling on the crystal and a decrease in their energy. The shape of the β spectrum changes, owing to the fact that β particles which have undergone scattering, i.e., a change in the direction of motion, do not fall on the crystal. Moreover, the slower electrons, which traverse a path less than the thickness of the layer of medium also do not fall on the crystal.

The general character of the curves for sources of different diameter is similar, but the distance between neighboring curves in the case of large-diameter sources is greater than in the case of sources of small diameter.

645
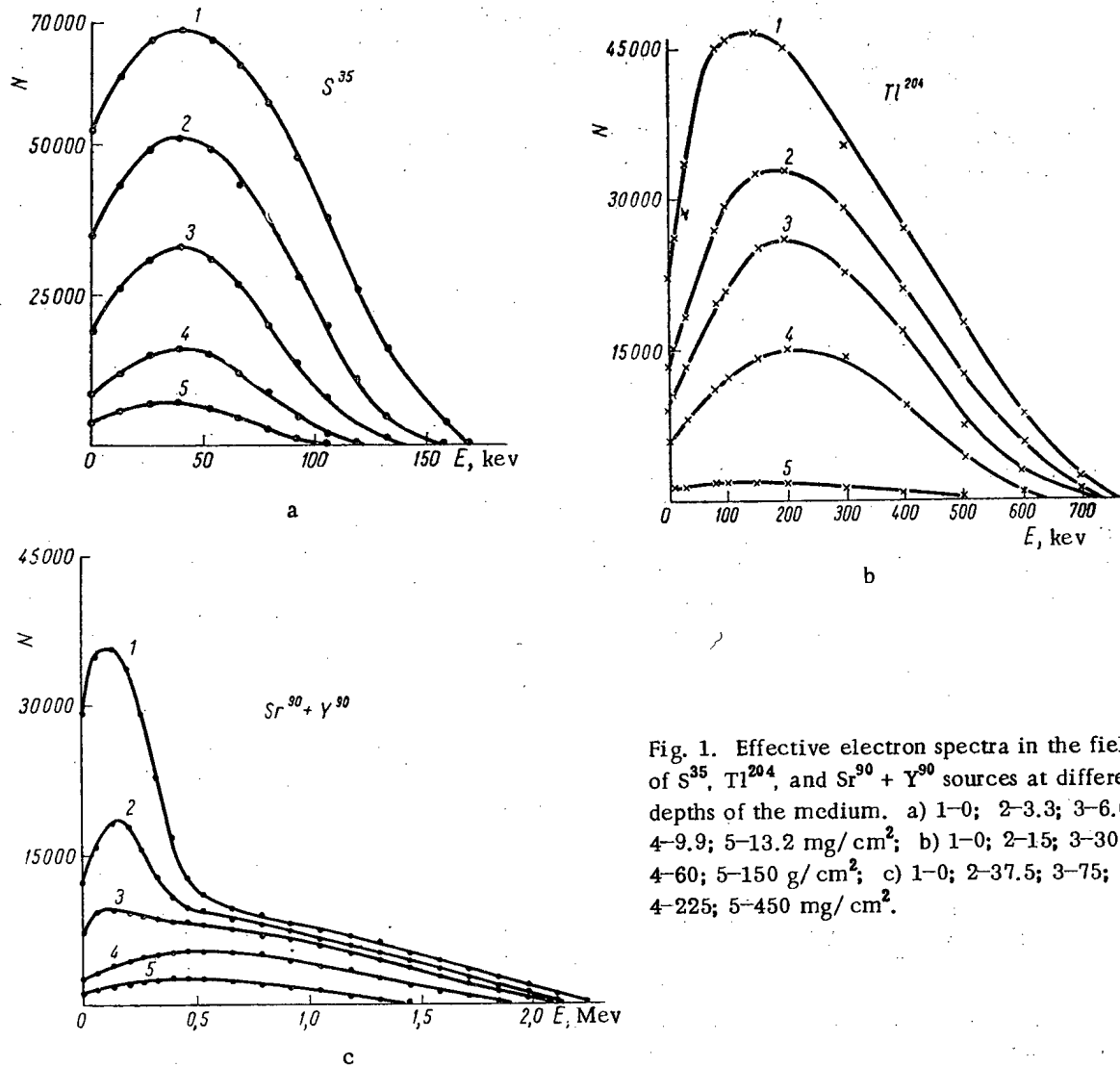
Fig. 1. Effective electron spectra in the field of S^{35}, Tl^{204}, and $Sr^{90} + Y^{90}$ sources at different depths of the medium. a) 1–0; 2–3.3; 3–6.6; 4–9.9; 5–13.2 mg/cm^2; b) 1–0; 2–15; 3–30; 4–60; 5–150 g/cm^2; c) 1–0; 2–37.5; 3–75; 4–225; 5–450 mg/cm^2.

This is explained by the fact that extended sources have β particles travelling obliquely, which leads to a greater path being traversed in the irradiated medium.

The spectral investigation permit one to determine the contribution of β particles of various energies to the dose. This question is of particular importance since the linear density of ionization along the β-particle tracks depends on their energy, and, in turn, are of great interest for a comparison of the biological effectiveness of β particles of different energies. Figure 2 shows data obtained from S^{35}, Tl^{204}, and Y^{91} sources for the surface of the medium.

In each of the investigated sources, the greatest contribution to the dose comes from the softest β particles, which are slowed down the most in the medium. As the maximum energy of the β spectrum increases, the contribution to the dose by particles of higher energy increases. The linear density of ionization, of course, decreases as one goes toward isotopes, whose β spectra have higher maximum energies (E_{max}).

The investigations showed that the shape of the curves representing the contribution for a given isotope changes little with a change in the depth of the medium.

Most important, is the question of the relation between the number of β particles and the doses given to different depths of the irradiated medium in the fields of sources of different diameters. As a result of our measurements, it was established that for a source of a given type (on a 10 mm thick plexiglas base), and independently of the source diameter and depth of medium, the ratio of the size of the dose D to the number of β particles, N remains within 10% of a constant value D_1, depending on the maximum energy of the β spectrum. It thus follows that the dose D_1 for one β particle for a given isotope and given type of source base will have a definite value, regardless of the thickness of the medium and dimensions of the source. Experiments with small-diameter sources placed on a lead base 3 mm thick, gave the same value of D_1 as sources of greater diameter.

646
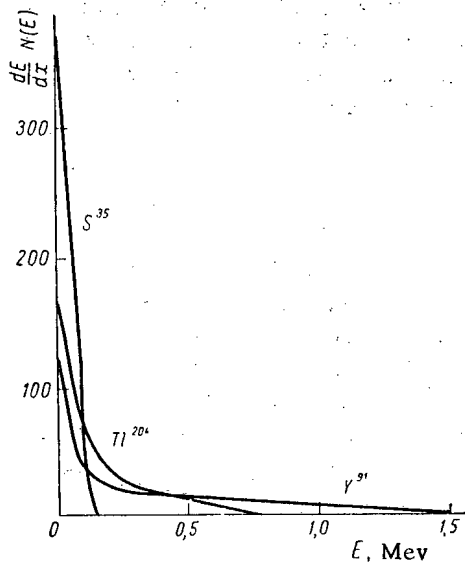
Fig. 2. Relative contribution to the dose by β particles of various energies for S^{35}, Tl^{204}, and Y^{91} sources.

The constancy of the value of D_1 for a given isotope, regardless of the thickness of the medium $\underline{h}$ and the source diameter $\underline{d}$, is an empirically found law. It might be supposed that the value D_1 depends not only on E_{max}, but also on the values of $\underline{h}$ and $\underline{d}$; however, experiments indicate that partial derivaties of the function D_1 (E_{max}, $\underline{h}$, $\underline{d}$) with respect to $\underline{h}$ and $\underline{d}$ are very small and, evidently, not constant in sign. Therefore, one may consider D_1 to be dependent only on one parameter, the maximum energy of the β spectrum for the isotope.

The values of D_1 which we found are given in Fig. 3.

The curve of Fig. 3 is similar in shape to the curve of ionization loss vs. electron energy, but it extends somewhat higher. This is explained by the fact that there is a considerable number of slow electrons in β spectra, for which the ionization loss dE/dx is very high.

The data presented directly solves one of the fundamental problems of β-ray dosimetry: it permits an in-

dication of the value of the surface dose of β radiation when the isotope from which the source was prepared and the number of β particles falling on the surface of the medium are known.
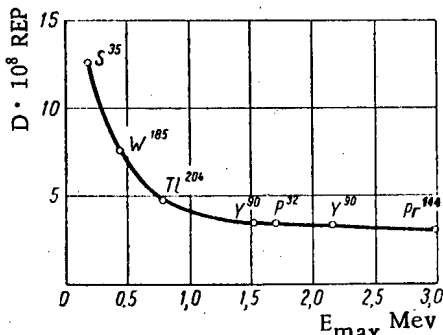
The statement that the size of the dose for one β particle is independent of the source diameter and depth of the medium is correct only for sources with simple β spectra. In the case of isotopes with complex spectra or sources consisting of two (or more) isotopes, e.g., Sr^{90} + Y^{90}, Ce^{144} + Pr^{144}, the size of D_1 will not be constant. This follows from the fact that as the dimensions of the source or the thickness of the medium increase, the softer β spectra will undergo greater filtering; the ratio of the number of β particles belonging to spectra of different hardness will change in favor of the harder spectra. Thus, for example, in the case of the Sr^{90} + Y^{90} source at very small filtration (thickness of 1 mg/cm^2 and less), the value of D_1 for one β particle will equal half the sum of the values of doses for Sr^{90} and Y^{90}, i.e., it will be approximately equal to $4.5 \cdot 10^{-8}$ REP. As the softer β rays of Sr^{90} are filtered out, the value of D_1 rapidly approaches the value for Y^{90}: $3.6 \cdot 10^{-8}$ REP. For the Ce^{144} + Pr^{144} source, the value of D_1 in the absence of a filter and with the filtering out of the Ce^{144} β spectrum will be $6.5 \cdot 10^{-8}$ and $3.1 \cdot 10^{-8}$ REP, respectively.

The investigations we conducted also allow us to solve a second basic problem in β-ray dosimetry: to fix the value of the dose at different depths of the medium irradiated by a given number of β particles of a given isotope.

Figure 4 shows the curves for deep doses calculated for one β particle falling on 1 cm^2 of surface of the medium for S^{35}, W^{185}, Tl^{204}, Y^{91}, and Ce^{144} + Pr^{144} sources of 1 cm diameter.

The curve for Ce^{144} + Pr^{144} drops steeply right away, owing to the absorption of the soft Ce^{144} spectrum.

The curves of deep doses for different isotopes cross one another. Any point of intersection for two curves corresponds to equal values of doses for two emitters,

Fig. 3. Relation between size of dose D_1 for one β particle and maximum energy of the β spectrum.
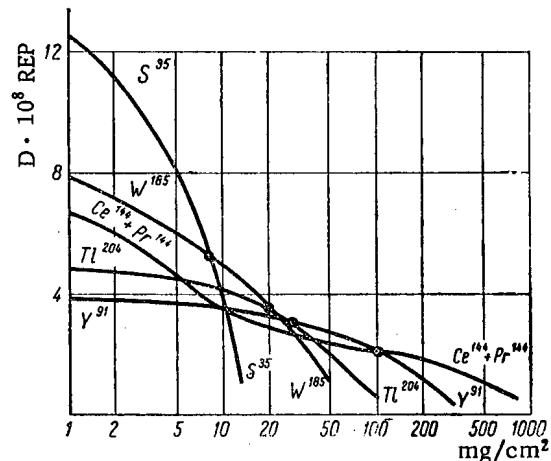
Fig. 4. Deep doses in the field of S^{35}, W^{185}, Tl^{204}, Y^{91}, and Ce^{144} + Pr^{144} sources.

647

one harder and the other softer. At smaller depths, the greater value of the dose is obtained in the field of the softer emitters, since their mean ionization loss is greater. Thus, at small depths, for the same number of β particles, the softer emitters give a greater dose than the harder ones. Naturally, at greater depths, it is more convenient to use harder emitters. According to the data given in Fig. 4, it is easy to fix the region of most suitable use for each of the emitters we have investigated. For the isotopes S^{35}, W^{185}, Tl^{204}, Y^{91}, Pr^{144}, the regions are 0-8, 8-20, 30-100, and greater than 100 mg/cm^2, respectively.

The experimental data and the considerations presented above indicate that spectral investigations of the effective electrons from the spectra of β emitters allow one to fix not only the absolute value of the β radiation dose, but also to establish a simple relation between the doses and the number of β particles. Moreover, spectral investigations provide the possibility of drawing conclusions as to the relative values of the linear ionization density.

LITERATURE CITED

1. K. K. Aglintsev, Dosimetry of Ionizing Radiation [in Russian] (Moscow, Gost. 1957).
2. G. J. Hine and G. L. Brownell, Radiation Dosimetry [Russian translation] (IL, Moscow, 1958).
3. K. K. Aglintsev, V. P. Kasatkin, and V. V. Smirnov, Report at the UNESCO Conference on the Use of Radioactive Isotopes (1957) [in Russian].

FINE STRUCTURE OF THE YIELD-MASS CURVE
FOR U²³³ FISSION FRAGMENTS

V. K. Gorshkov and M. P. Anikina

The yields of Ba^{138}, Sr^{88}, Sr^{90}, Y^{89}, and five isotopes of zirconium produced in the fission of U^{233} have been measured. The fragment-yield vs. mass-number curves revealed a fine structure. It was found that the Cs^{136} yield was independent and an estimate is given of the independence of the Rb^{86} yield. As a result of the present measurements and data obtained earlier, an important part of the yield-mass curve for fission fragments has been plotted. From the curve, there has been determined the boundary for the transition from the emission of one neutron by light fragments to the emission of two neutrons. It is shown that the structure is associated with the moment of the act of fission.

As previously reported [1], an investigation of the yield-mass curve for heavy fragments from the fission induced by the irradiation of U^{233} with thermal neutrons revealed slight departures from smoothness in the curve at the region A = 141. For a further study of this phenomenon, the investigation of the corresponding part of the yield-mass curve for the light group of U^{233} fission products is of great importance. Unfortunately, the use of published data on the absolute yield of Sr^{89} [2] and five isotopes of zirconium [3] produced in the fission of U^{233} is impossible, since the yield-mass curves for zirconium were obtained under the assumption that there is no departure from smoothness in the yield-mass curve. In this sense, the results of [4], in which the yields of Sr^{88} and Sr^{90} were determined, are of greatest interest. Knowing the yield of Sr^{89} [2], one may plot an important segment of the curve. However, the low value of the expected effect falls within the limits of error of these measurements.

In the present work we have determined the yield-mass curve for U^{233} fission fragments with mass numbers from 88 to 96. We used the same sample of U^{233} [5] on which the earlier studies were made.

The relative yields of Y^{89}, Sr^{88}, and Sr^{90} were measured on a mass spectrograph by the integral mass-spectrograph method [6] with the use of a double-filament ion source from the ionization surface, i.e., without any preliminary chemical factionating of the initial solution of the irradiated U^{233} sample. In accordance with the

method, the relative coefficients of ionization of yttrium and strontium were measured: $\beta_Y = 1.0$; $\beta_{Sr} = 1.67 \pm 0.02$. The mass spectrograms were used to determine the ratio of the integral ion currents corresponding to the Sr^{88} and Y^{89} fragments: 1.35 ± 0.2. Consequently, the corresponding ratio of the yield of fragments with A equal to 89 to that with A equal to 88 is: $f_{89}/f_{88} = 1.24 \pm 0.03$. The relative yield of Sr^{90} was determined from the isotopic composition of strontium fragments. The fact that the Sr^{86} isotope is absent permitted an estimation to be made of the independent yield of Rb^{86} in U^{233} fission. Its value is smaller or equal to 0.8% of the absolute yield of Sr^{88}.

Some complications arose in the study of the yield of zirconium isotopes. It was established that the coefficient of ionization for zirconium was much smaller than for yttrium. Therefore, to increase the concentration the zirconium was separated from all the fragment masses. The separation was carried out by a thorium carrier with a double precipitation in the form of an iodate. The cerium produced in the process was separated by recovering $Ce^{\cdots\cdot} \rightarrow Ce^{\cdots}$. The final purification of zirconium from the carrier was done by the oxalate method.

After being converted into a nitrate, the purified zirconium was investigated for its isotopic composition (Table 1).

The separation of the zirconium was made necessary, unfortunately, by the impossibility of using the integral mass-spectrograph method for determining the

TABLE 1. Isotopic Composition of Zirconium Separated from the Solution of Irradiated U^{233}

Isotope mass	90	91	92	93	94	96
Amount in %	1,90±0,06	20,2±0,2	19,9±0,2	21,2±0,1	20,0±0,1	16,8±0,1

649

TABLE 2. Results of the Yield Measurements for Light Fragments From U^{233} Fission

| Isotope | Group of light fragments | | | | Group of heavy fragments | |
| | relative yield | | absolute yield % | | | |
	results of the present work	data from [3]			isotope	absolute yield, %
Sr^{88}	0,928±0,006	—	5,17±0,15		Nd^{143}	5,19±0,17
Y^{89}	1,148±0,030	—	6,36±0,28		Ce^{142}	6,06±0,24
Sr^{90}	1,0**	—	5,58±0,20		Pr^{141}	5,57±0,19
Zr^{90}	0,1092±0,0007***	—	—			
Zr^{91}	1,16±0,03	1,12	6,48±0,22		Ce^{140}	6,16±0,24
Zr^{92}	1,14±0,03	1,14	6,28±0,25		La^{139}	5,91±0,23
Zr^{93}	1,21±0,02	1,21****	6,75±0,17		Ba^{138}	—
Zr^{94}	1,15±0,02	1,16	6,43±0,25		Cs^{137}	6,16±0,14
Zr^{96}	0,98±0,04	0,96	5,47±0,29		Xe^{136}	—

* Included for comparison with the absolute yield of light fragments.
** Includes correction for β-decay.
*** The amount of Zr^{90} is determined from Sr^{90} for normalizing the yield of the zirconium isotopes.
**** Taken as reference.

TABLE 3. Results of the Measurement of the Barium Isotope Yield in U^{233} Fission (in %)

Isotope mass	Relative abundance	Yield in U^{233} fission (%)
136	0,146±0,003	0,08±0,02*
137	1,0	—
138	10,90±0,16	6,35±0,23

* Yield of Cs^{136} ($T_{\frac{1}{2}}$ = 13 days) produced in the fission.

relative yields of the zirconium isotopes. However, during the comparatively long period of time (5.1 years) which had elapsed since the irradiation of the U^{233} up to the time of the present measurements, a considerable amount of Zr^{90} produced as a result of the β decay of Sr^{90} * was accumulated in the sample. This permitted the normalization of the yields of the five zirconium isotopes with respect to the Sr^{90} yield (Table 2). The following value for the half life of Sr^{90} was used in the normalization: $T_{\frac{1}{2}}$ = 29.3 ± 1.6 years [4]. The absence of natural zirconium in the sample was confirmed by a number of "blind" experiments.

All relative yields were reduced to their absolute values based on the strontium by the method of isotopic dilution.

To compare the yield-mass curves for light and heavy fragments [1], the Ba^{138} yield had to be measured. The measurement was made by the integral mass-spectrograph method. The Ba^{138} and Pr^{141} lines corresponding to the integral ion currents of these masses were compared on the mass spectrograms. The results of the measurements are shown in Table 3. The presence of the

Ba^{137} isotope is explained by the β decay of the Cs^{137} ($T_{\frac{1}{2}}$ = 33 years). The presence of Ba^{136} among the fragments made it possible to determine the independent yield of Cs^{136} produced directly during the U^{233} fission (but not the entire chain of the decays of A = 136):

$$Cs^{136} \xrightarrow[\text{13 days}]{\bar{\beta}} Ba^{136} \text{ (stable)} .$$
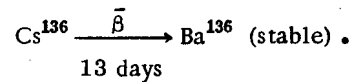
From the measurements, the yield-mass curve was plotted for the light fragments from the fission of U^{233} which, for the sake of clarity, was combined with the corresponding part of the yield-mass curve for the heavy fragments. Here, on the decreasing parts of the curves, where the errors of measurement of the yields do not essentially distort the shape of the curves, the data of other authors was utilized. It is seen from the figure that the sum of the mass numbers of the two fragments produced in each act of fission is 232, i.e., the light and heavy fragments seem to lose, on the average, one neutron. In the region A = 86-89 the emission curve for light fragments is displaced with respect to that for heavy fragments in the direction of smaller masses by one mass unit, since the light fragments in this region emit, on the average, not one but two neutrons each. This result is not unexpected. In [7-9], where the yield-mass curves were measured for U^{235} fission, a similar explanation for this phenomenon is given. This conclusion is in good agreement with the experiments of Fraser [10], from which it follows that the light fission fragments emit approximately 30% more secondary neutrons than the heavy ones.

------

* An estimate indicates that the possible independent yield of Zr^{90} does not exceed the error of measurement.

As may be seen from the figure, the relative yields of fragments with A equal to 91 and 92 agree within the limits of error of the measurements. But the lack of smoothness of the yield-mass curve in the region A = = 89-91 leaves no room for doubt.

In fact, the yield of fragments with A = 90 is far smaller than the yield of fragments with A equal to 91 and 89. It is also seen that the fragments with A = 93 have the maximum yield not only among the zirconium isotopes, which is in agreement with the data on the isotopic composition of zirconium [3] (see Table 1), but also among all light fragments. Thus, just as in the case of heavy fragments, a fine structure is observed on the part of the curve under investigation.

When the fine structures in the region of heavy and light fragments are compared a similarity is evident. The shape of the yield-mass curve for light fragments in the region A = 89-93 very closely follows that for the heavy fragments, but it is displaced by one mass unit in the direction of the light masses since the region of the light fragments emitting two neutrons is not bounded by the mass number 89, but extends further into the region of heavier masses. Here, there is evident not only a qualitative, but also a quantitative, agreement between both fine structures. It may be assumed that both fine
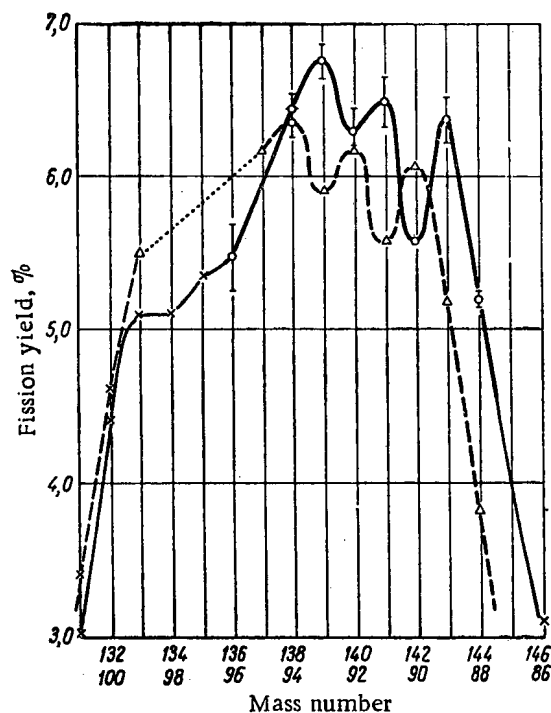
structures are produced simultaneously and that their relative displacement from one another by one mass unit is explained by the emission of not one, but two neutrons by the light fragments.

Both fine structures cannot be explained by the capture of the neutrons by the nuclear fragments, after the act of fission, owing to the small value of the capture cross sections.

The cause for the occurrence of the fine structures might be the emission of delayed neutrons by the fragments. It is difficult to explain in this way, for example, the above-mentioned qualitative and quantitative agreement of both fine structures.

Consequently, it is most probable that both fine structures are not only produced simultaneously, but are also directly associated with the instant of the act of fission. Therefore, the reason for their occurrence should be sought in the mechanism of the process of fission of the U^{233} nucleus.

The results obtained and the above discussion permit one to establish the boundary of the transition from the emission by light fragments of one neutron to the emission of two neutrons in U^{233} fission. As may be seen from the figure, it lies in the region A = 94-96. The same boundary for U^{235}, according to the data of papers cited above, is in the region A = 91-93. It is possible that this displacement of the boundary is explained by the slightly greater number of secondary neutrons produced in the fission of U^{233} in comparison with the number of neutrons produced in the fission of U^{235}. Moreover, our quantitative estimation of this effect is in good agreement with various known [11] values of the mean number of secondary neutrons ($\bar{v}$) for the act of fission of U^{233} and U^{235}.

The authors thank V. G. Zhuravlev for his photometric measurements of a large number of plates.

Yield-mass curve for fragments from U^{233} fission.

Ⓨ- data from the present work (errors of measurement

shown on the curve are errors in the relative yields; Δ-data from [1]; ✕-mass-spectroscopic and radiometric data of other authors; ——— light fragments; - - - heavy fragments; ...... part of curve not investigated.

LITERATURE CITED

1. V. K. Gorshkov, Collection: Physics and Heat Technology of Reactors, Supplement No. 1 to Atomnaya Énergiya [in Russian] (Atomizdat, 1958) p. 104.†
2. E. Steinberg, J. Seiler, A. Goldstein, and A. Dudey, USA AEC, report MDDC- 1632 (1948).
3. E. Steinberg, L. Glendenin, M. Inghram, and R. Hayden, Phys. Rev. 95, 867 (1954).
4. M. P. Anikina, R. N. Ivanov, G. M. Kukavadze, and B. V. Érshler, Atomnaya Énergiya 4, 198 (1958). †
5. G. M. Kukavadze, L. L. Gol'dnin, and M. P. Anikina, and B. V. Érshler, Materials of the International Conference on the Peaceful Uses of Atomic Energy.̇4 [in Russian] (Geneva, 1955) (Izd. An SSSR 1957) p. 275.
6. V. K. Gorshkov, Pribory i Tekh. Éksp. No. 2 53 (1957).
7. J. Petruska, H. Thode, and R. Tomlinson, Canad. J. Phys. 33, 693 (1955).

† Original Russian pagination. See C. B. translation.

651

8. J. Petruska, E. Melaika, and R. Tomlinson, Canad. J. Phys. 33, 640 (1955).

9. E. Melaika, M. Parker J. Petruska, and R. Tomlinson, Canad. J. Chem. 33, 830 (1955).

10. J. Fraser, Phys. Rev. 88, 536 (1952); 93, 818 (1954).

11. R. Leachman, Proc. Intern. Conference on the Peaceful Uses of Atomic Energy. 2 (Geneva, 1955) (United Nations, New York) p. 193.

120 cm CYCLOTRON

A. G. Alekseev, M. A. Gashev, D. L. Londysh, I. F. Malyshev,
I. M. Matora, E. S. Mironov, N. A. Monoszon, L. M. Nemenov,
V. V. Pirogovskii, N. A. Romanov, N. S. Strel'tsov, and N. D. Fedorov

The basic data on a cyclotron with a pole-piece diameter of 120 cm are given. The arrangement of the principal parts of the system, the design features of the individual units, the radio frequency (rf) installation, the method of measuring and correcting the magnetic field, the features of the deflection system, and the method of focusing the beam on a remote target are all described. Deuterons are accelerated to an energy of 13.7 Mev in this machine. The use of a deflection system with focusing properties makes it possible to use magnetic quadruple lenses with small apertures which bring practically the entire deflected beam to a remote target. The parameters of the machine are such, that it will be possible to increase significantly the energy of the accelerated ions in the future.

In 1955, the Scientific Research Institute for Electrophysical Apparatus and a group of colleagues of the Institute for Atomic Energy, Academy of Sciences, USSR, were presented with a problem: to develop a cyclotron which would provide intense beams of protons, molecular hydrogen ions, deuterons, α particles, and multiply charged ions. It was required that the cyclotron be reliable in operation, relatively simple to operate, and have adequate shielding against penetrating radiation. In order to carry out experiments with a minimum level of background radiation from the cyclotron, the ion beam is steered through the main shielding wall into an experimental area which has its own shielding. Conditions have been created for experiments with fast neutrons and for determining the neutron velocity spectrum by time-of-flight methods. The cyclotron can also be used for producing artificial radioactive isotopes. In the design of the cyclotron, a good deal of attention has been paid to radiological safety techniques; the basic operation of the machine is carried out by remote control.

The cyclotron laboratory is located in a two-story building with a sublevel. Figure 1 shows a plan of the first floor of the cyclotron laboratory and the arrangement of the apparatus. Part of the auxiliary equipment is located in the sublevel. The second story houses laboratories, a library, a construction department and other installations.

The constructional work for this cyclotrol laboratory was carried out by the Leningrad Construction Institute.

Electromagnet and Correction of the Magnetic Field

The cyclotron magnet is shown schematically in Fig. 2. The beams and uprights of the electromagnet are fabricated from three sections made up of St-3 sheets 40 mm thick. The weight of the heaviest section is less than 12.5 t, so that the magnet can be assembled and disassembled in the cyclotron room by means of a bridge crane with a loading capacity of 15 t.

The winding of the electromagnet consists of two series-connected coils 6.5 t in weight, which are made up of copper tubing with dimensions 20 × 5 mm. Each coil consists of seven sections which are cooled by distilled water. All fourteen sections of the windings are connected in parallel across the water manifold. The water flow in each parallel branch is monitored by means of a flow switch.

The diameter of the pole pieces of the magnet and the ceiling of the chamber is 1200 mm; the distance between the pole pieces is 345 mm; the ceiling thickness is 72.5 mm; the gap between the top and bottom is 170 mm. On the pole pieces of the magnet, there are two auxiliary uncooled windings of 500 turns each which are designed for a maximum current of 5 amp.

The power supply for the main windings of the electromagnet is a motor generator which provides dc power at 135 kw. The current in the windings is stabilized with an accuracy of 0.03% for a line-voltage change of ±10% and a line-frequency change of ±2%. The stabilization is realized by means of a standard BT-4 unit, which operates on a change of voltage in a shunt connected in the circuit of the magnet coil. The current is controlled by potentiometers, which are located at the central control panel.

The design of the magnet has been carried out by N. N. Indyukov, E. A. Bezgachev, and A. V. Klimov, under the direction of B. V. Rozhdestvenskii and B. E. Gristkov.

653
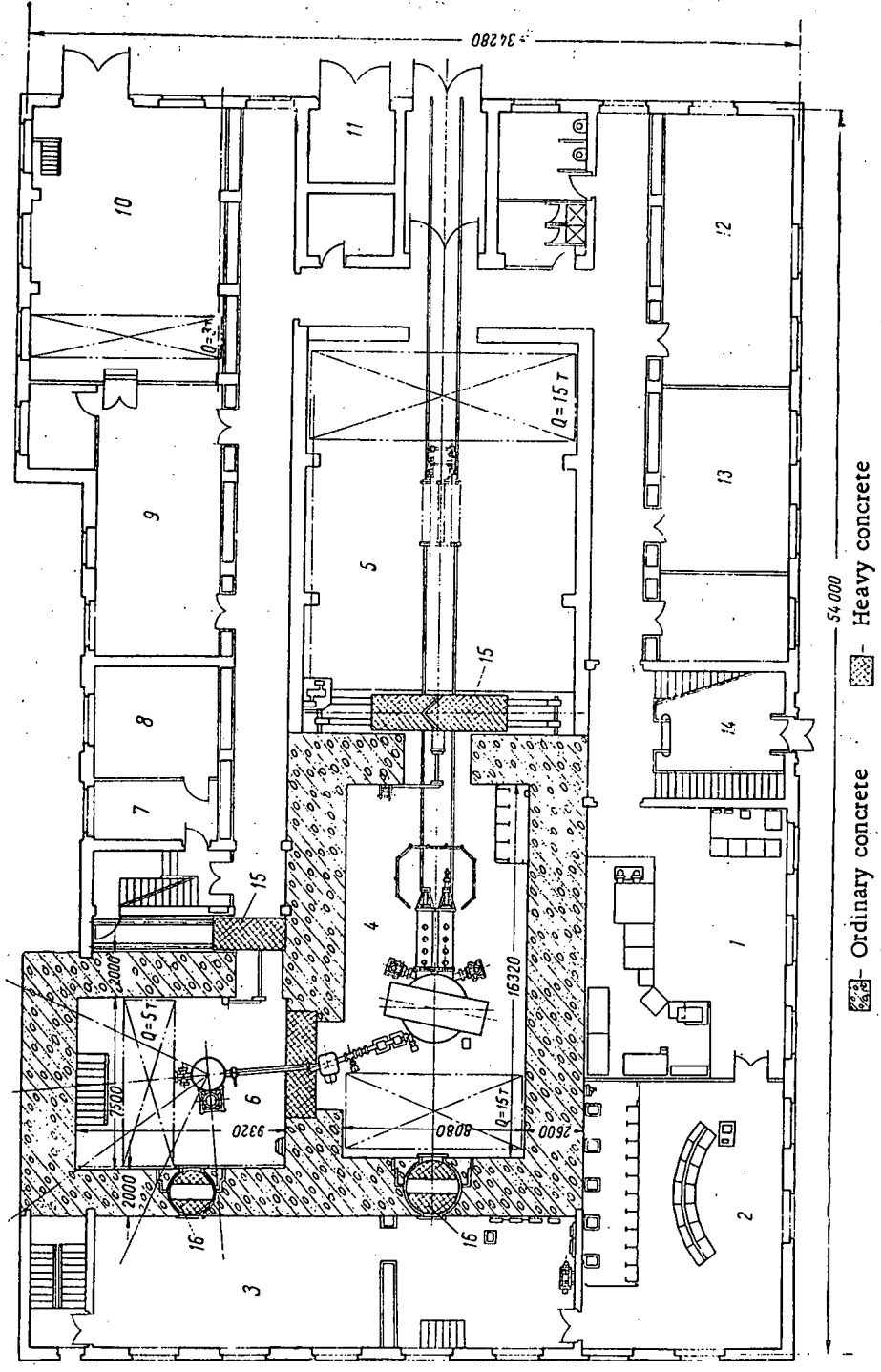
Fig. 1. Plan of the first floor. 1) Location of rf equipment; 2) central control panel; 3) installation for measuring apparatus for operation with neutron beams; 4) cyclotron rooms; 5) auxiliary room; 6) experimental room; 7) acid room; 8) storage-battery room; 9) shield room; 10) motor room; 11) transformer substation; 12) mechanical shop; 13) laboratory with physical equipment for which the foundation is required; 14) vestibule; 15) hoistable shielding gates; 16) entrance with rotatable shielding blocks.

654
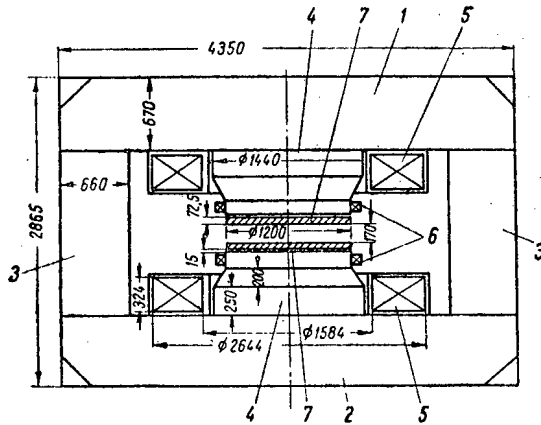
Fig. 2. Schematic diagram of the magnet. 1) upper cross piece; 2) lower cross piece; 3) vertical post 4) pole pieces; 5) main winding; 6) auxiliary winding; 7) roof of the acceleration chamber.

Fig. 3. The field intensity and field decay index of a function of radius: 1) curve showing the variation of magnetic field strength $\Delta H_z/H_{z\,cen}$ ($H_{z\,cen} = 14.7$ koe; 2) curve showing the change in the logarithmic magnetic field decay index n; 3) outer correction disc; 4) inner correction ring.

The magnetization curve is measured by an absolute method by means of a rotating cylindrical coil, which is placed at the center of the working gap in the acceleration chamber. The measurement of the radial decay of the magnetic field is carried out by use of a differential method. The radial coordinate of a movable coil is determined with an accuracy of ± 0.5 mm. The error in the measurements of the field intensity is less than 0.01% of the field strength at the center. The error in the measurements of the azimuthal nonuniformity is 0.007% of the field at the center. The position of the median magnetic surface is determined by the magnetic-weight technique, which has been developed by V.V. Pirogvoskii.

In order to investigate the effect of the position of the median plane of the magnetic field on the vertical displacement of the beam, we have used the auxiliary coils on the pole pieces of the magnet (cf. Fig. 2). The coils are connected in opposition so that the vertical field components produced by the coils cancel each other, while the radial components add. By means of these coils, it is possible to displace the beam of accelerated particles in the chamber, in the vertical direction without disturbing the resonance conditions.

The terminal radius of the cyclotron is 525 mm. The total field decay at this radius is 2%. In order to correct the magnetic field we use both internal rings and discs, which are located in the gap between the pole pieces of the magnet and the bottom and top of the chamber. Each gap is 15 mm high. In Fig. 3 we show the dependence of field strength and the field index on radius. The dimensions of the inner and outer correction elements are also shown.

The azimuthal correction of the magnetic field is accomplished by means of steel pieces ($5 \times 100 \times 250$ mm^3), which are moved in the radial direction in the gaps between the pole pieces and the top and bottom of the chamber. The motion is carried out by a control system which operates from the central control panel; this unit has indicators which indicate the position in the poles.
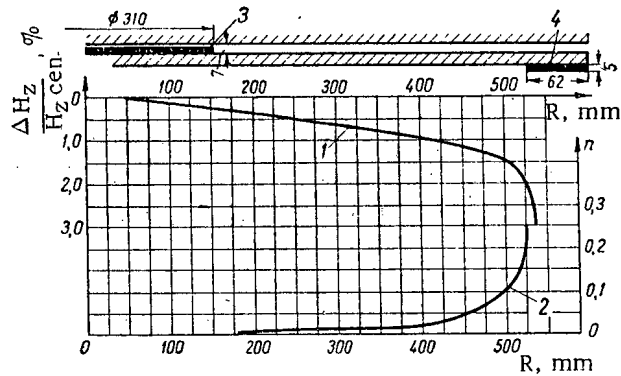
The amplitude of the first harmonic of the azimuthal nonuniformity of the magnetic field in the operating region is 6-10 oe before correction and 3 oe after correction.

The medium plane of the magnetic field is less than 5 mm from the median plane of the chamber.

Design of the Resonant-Line Chamber and Dees

The frame of the chamber is made from aluminum plates, which are connected by rubber gaskets. The ceiling of the chamber and the inner correction rings are made from St-3. The inner surfaces of a chamber ceiling and the correction rings are copper plated to a thickness of 0.05 mm, thus providing the required conductivity for high-frequency currents. The electrical connection between the top and bottom and the horizontal plates of the chamber is made by means of a system of spring contacts. The position of the top and bottom with respect to each other is determined by the regidity and accuracy with which the frame of the chamber is made; the departure from parallelism in the top and bottom inside the chamber is less than 0.05 mm. By means of four rollers, which are located on the frame, the chamber can be moved out of the magnet gap on rails which are provided for the purpose.

The resonance system of the cyclotron consists of two coaxial lines, a transition section (throat), the chamber, and the dees (Fig. 4). The tanks for the coaxial lines and the throat are made from steel and are rolled between copper sheets to which the water-cooling tubes are soldered. The design of the tank flanges, which connect the resonance line to the transition section and the transition section to chamber provides reliable electrical contact. The coupling sections of the resonance system, to which the dees are attached are duraluminum pieces rolled between copper cylinders, which are provided with water cooling. The dees can be moved in the vertical

655
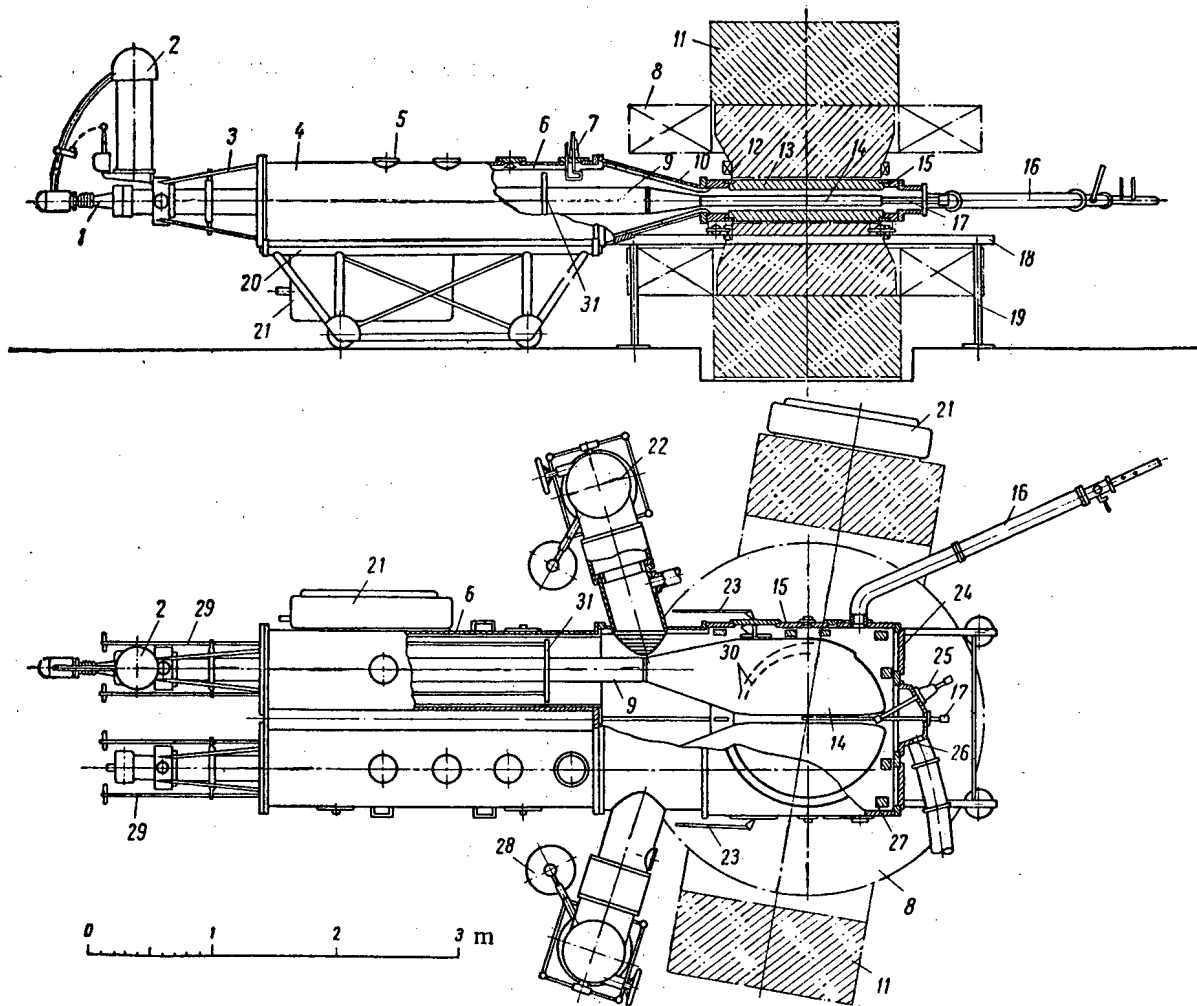
Fig. 4. Diagram showing the arrangement of the acceleration chamber and the resonance lines: 1) input feed-through insulator for the high voltage input of the deflection system; 2) vinyl plastic coil system used for cooling the high-voltage electrode in the deflection system; 3) adjustment device for the dee; 4) tank for the resonance lines; 5) ports for adjustment of the coupling loop; 6) copper sheet; 7) coupling loop; 8) coil for the magnet; 9) coupling section of the resonance line; 10) transition sections; 11) yoke of the magnet; 12) auxiliary windings; 13) roof of the acceleration chamber; 14) dees; 15) frame of the acceleration chamber; 16) line to vacuum gauge; 17) ion source; 18) rails for location of the acceleration chamber; 19) stand supports for the rails; 20) trolley; 21) water distribution manifold; 22) vacuum-pump installation; 23) trimmers; 24) observation window; 25) rotatable probe; 26) extraction window; 27) units for strengthening the acceleration chamber; 28) dewars with liquid nitrogen; 29) location rods for the contacts of the shorting plates; 30) deflection system; 31) shorting plates.

and horizontal planes and can be rotated about the axis of the coupling section without disturbing the vacuum by means of an adjustment device which is on the outside at the ends of the resonance lines.

The wavelength of the resonance system is varied from 18 to 34 m by motion of the shorting plates, which have spring contacts. The plates are provided with a mechanism which breaks the contact when the plates are in motion, and makes the contact when the plates are in a fixed position. The plates can be moved without disturbing the vacuum by means of a special mechanism which is located on the ends of the resonance lines. The fine tuning is carried out by remote control by varying the position of plates (trimmers) with respect to the dees.

The dees are made from rigid duraluminum stock, which is protected by copper sheets 1.5 mm thick. The cooling tubes, which are soldered to the sheets, are inside the cavity formed by the dees. In order to reduce the activation of the tubes by the accelerated particles the tubes are covered by graphite shields. The height of the dees is 86 mm (inside 70 mm).

In the central portion of the dees there are removable water cooled extension sections, which reduce the effective width of the accelerating gap. The deflection system is located in one of the dees.

For convenience in assembling and disassembling of the apparatus, the resonance lines with the dees can be removed from the chamber on a special trolley; the

656

system is separated outside the magnet windings at the point at which the tanks connect with the transition section. The vacuum connections to the transition section are left in place in this operation. The trolley moves along a track at the end of which there is a stop system, which is designed for assembly and disassembly of the coupling sections and adjustment of the resonance-line elements. A special trolley is used for assembly and disassembly of the accelerating chamber and the transition section, which is connected with it. On the trolley, there are rails which connect with the rails used for setting up the chamber. The acceleration chamber and the resonance line have been designed by A. I. Alyat'ev, I. F. Zhykov, and N. N. Rymyantsev under the direction of B. I. Produvnov.

Resonance System and rf Generator

The quality factor of the resonance system of the cyclotron has been measured with a standard signal generator with atmospheric pressure in the chamber and is found to be 5000.

The resonance system of the cyclotron is driven by a multistage generator through two coaxial feeders and a coupling loop which is located on the tanks. The rf generator operates in the wavelength range from 18 to 36 m at a power of 120 kw. The potential difference across the dees is 160-200 kv. If necessary, the generator can be driven by an external source.

A block diagram of the rf system is shown in Fig. 5. The generator consists of a four-stage exciter (continuously tuned) and a five-stage power amplifier. The last stage (fifth) is capacity coupled to the feeder.

The first stage of the power amplifier, which is a transition from the single-ended exciter to the following push-pull stage, is a single-ended circuit (GU-80 pentode) with a symmetric anode circuit. The second stage is a push-pull stage in which two GU-80's are used. The following stages of the power amplifier make use of disc-seal grid triodes (in the third a GU-10A, in the fourth a GU-22A, and in the fifth a GU-23). Tubes of this type are characterized by a minumum inductance in the grid lead and a small cathode-anode capacity.

The use of pentodes and a system of stages with a common grid makes it possible to operate the generator over the required wavelength range without neutralization.

The rf generator is characterized by a high-frequency stability (at least 10^{-4}) and features simple methods for changing the frequency and voltage applied to the dee.

During the proving-in operation, partial breakdowns in the chamber lead to glow discharges which can damage the dees. Hence, provision is made for self-excited operation of the power amplifier of the generator. In this case, the feedback voltage from the resonance circuit of the cyclotron is applied to the grid of the first stage of the power amplifier through a separate feeder with a special phase shifter. When a breakdown occurs,

the self-excitation becomes inadequate and the voltage to the dees is automatically reduced.

The generator circuit makes it possible to apply a pulsed supply to the dee circuit for examining new modes of operation under conditions of minumum activation and for carrying out special investigations. For this purpose, there is a modulator which generates pulses of variable width at repetition frequencies from 5 to 300 cps which is applied to the grids of stages I and II of the power amplifier. The modulator is also used in an automatic circuit for protecting the dees and the tubes in the generator from accidental breakdowns. The protection system also operates in the nonpulsed operation of the generator.

The thyratron rectifier of the rf generator is supplied from a motor-alternator unit which makes it possible to vary and stabilize the anode voltage of the generator tubes with an accuracy of 1%. The voltage to the dees is controlled from the central control panel by varying the anode voltage of stages IV and V of the power amplifier.

The design of the rf generator has been carried out in the G. M. Drabkin Laboratory by R. V. Vanatovskii, R. Yu. Protasovskii, and Yu. F. Tsibul'skii under the direction of A. S. Temkin.

Vacuum System

The acceleration chamber and the resonance lines are pumped by two oil vapor units (VA5-4) with a total capacity of 2500 liters/sec.

Two VAO5-1 vacuum units provide the required vacuum in the tube through which the ion beam passes to a remote target. The total capacity of these units is at least 250 liters/sec. The volume in which the target is located is pumped by a single VA2-3 unit with a capacity of 500 liters/sec.

The vacuum units are provided with nitrogen traps for condensation of the oil vapors. All units have valves with manual and remote control, which are closed automatically if there is a deterioration of the vacuum. The capacity of the pumps is indicated taking account of losses in the nitrogen traps and the valves at a pressure of $1 \cdot 10^{-5}$ mm Hg.

The preliminary pumping for operation of the diffusion pumps is carried out by two mechanical pumps (VN-7). The rough pumping is carried out through a separate line, which is directly connected with the cyclotron chamber and the other evacuated volumes. The remote control of the vacuum at specified points of the apparatus is provided by ionization gauges, magnetic discharge gauges, and thermocouple gauges. Special cutoff valves are used to make it possible to replace damaged gauges without disturbing the vacuum. The devices used for monitoring the vacuum and illuminated signals are located at the central control panel.

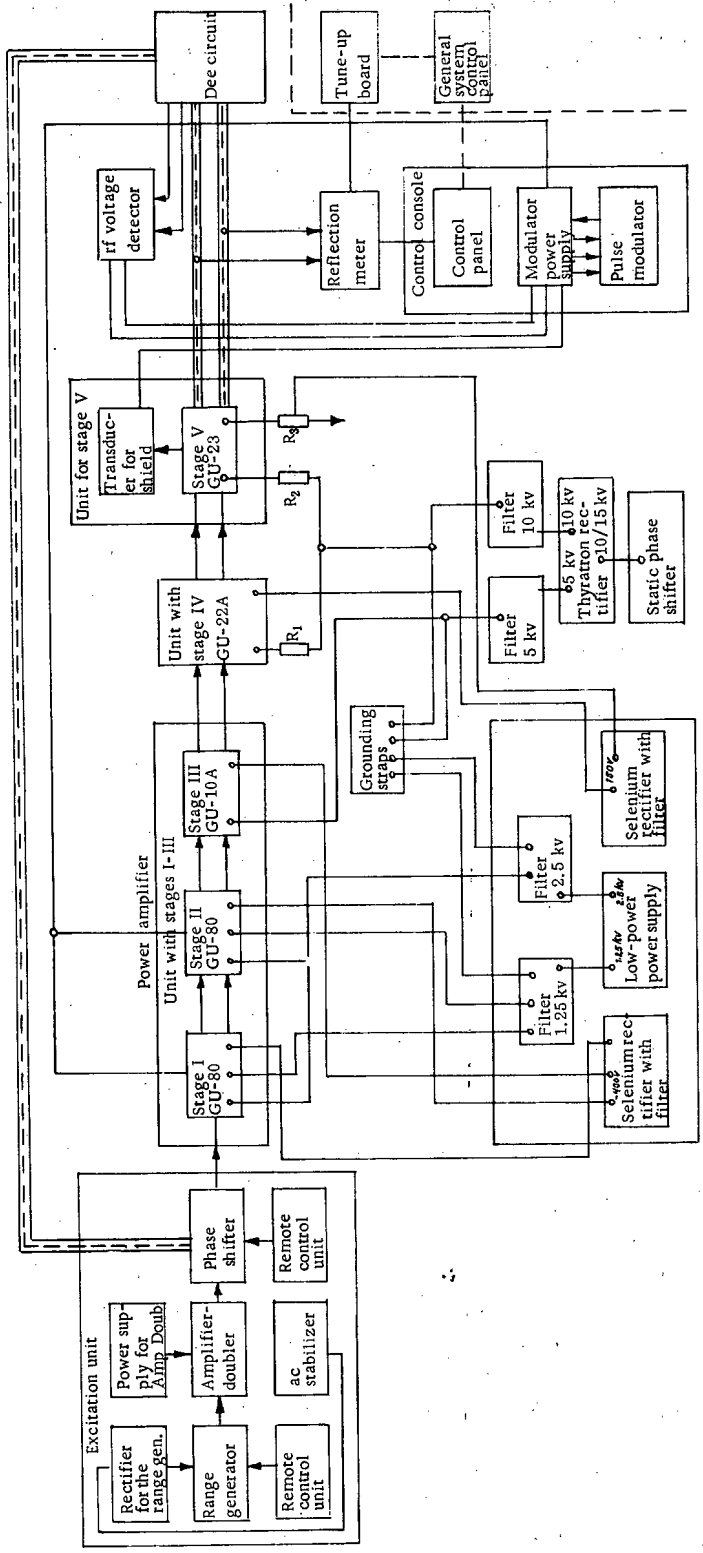The vacuum system has been designed by Ya. L. Mikhelis and N. M. Karpenko.

657

Fig. 5. Block diagram of the rf system.

658

Central Part of the Cyclotron and Ion Source

The initial motion of the ion is an important factor in the acceleration process [1, 2]. Calculations of the ion motion for the present machine have been carried out by I. M. Matora.

In order to reduce the energy spread in the external charged-particle beam, the ions from the source are extracted in one dee. In order to weaken the phase bunching of the ions, the distance between the breaks in the dees in the horizontal and vertical direction is reduced by means of special removable extruding sections (Fig. 6).
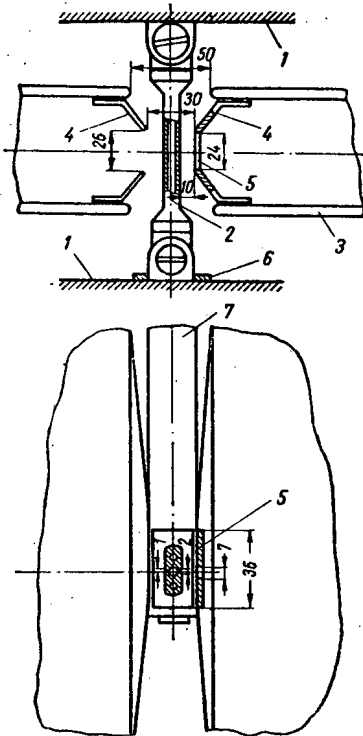

Fig. 6. Ion source and central part of the dees: 1) roof of acceleration chamber; 2) head of the ion source; 3) extraction dee; 4) extrusion section of the dees; 5) plane part of the extrusion with the slit; 6) location unit for locating the frame of the ion source; 7) ion source frame.

In the extraction dee, the extrusion is a plane electrode with a slit 7 × 25 mm, which essentially avoids any inhomogeneity in the electric field which would cause defocusing of the ion beam in the vertical direction. The geometry of the center is chosen on the basis of a calculation of the initial motion of the particles.

This cyclotron makes use of an ion source of the slit type with an incandescent cathode (tantalum filament 3 mm in diameter). The filament can be replaced in the source without disturbing the vacuum. Gas is admitted to the source by means of a special device [3]

When the source is supplied with deuterium or hydrogen, a current of 30-40 ma can be extracted from it. By changing the point at which hydrogen is applied in the gas discharge space, it is possible to favor the pro-

duction of atomic hydrogen ions or molecular hydrogen ions. The current of α particles extracted from the source, when helium is used is approximately 10-15 times smaller than the deuteron current.

Deflection System and Beam Focusing on a Remote Target

The cyclotron described here makes use of a deflection system with an inhomogeneous electric field [4, 5]. The design of the deflection system used in the present machine has been carried out by I. M. Matora. The advantage of this system, as compared with a convenient system (uniform field), lies in the fact that in addition to deflecting the beam of charged particles, this system compensates for the defocusing effect of the fringing field of the magnet.

The deflection system (Fig. 7) consists of two parts. The first part, which is essentially the same as that which is used conventionally, extends over an azimuthal angle of 40°. The distance between the electrodes varies from 6 mm (at the beginning) to 12 mm (at the end). The grounded electrode of this part of the system is made from tantalum or tungsten 0.2-0.8 mm in thickness.
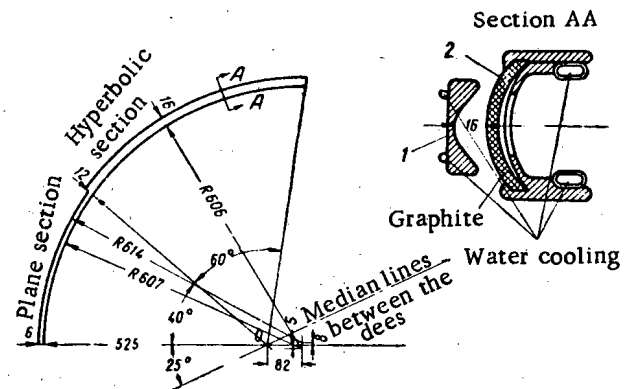
Fig. 7. Diagram of the deflection system. 1) potential electrode (profile equation $x^2-y^2 = 10.8$ mm^2); 2) grounded electrode (profile equation $x^2-y^2 = 26.8$ mm^2).

The electrodes of the second part of the deflection system constitute a section of a hyperbola. The azimuthal dimension of this part of the system is 60°. The distance between the electrodes is 16 mm. The grounded electrode of this part of the system is made from graphite. All the electrodes of the deflection system are water cooled. The electrical breakdown strength of the deflection system is such that voltages up to 70 kv can be used. The voltage comes from a 100 kv kenotron rectifier. The extraction coefficient of the deflection system is 40-50%.

The distance between the extraction port and the target located in the experimental room is 9 m. The diverging beam beyond the output port is focused by two magnetic quadrupole lenses (Fig. 8). As is well known, the use of magnetic lenses means that the focus can be va-

659

ried over wide distances along the optical axis. Because of the focusing effect of the deflection system, it has been found possible to use ML-5 quadrupole lenses, which have a relatively small aperture (139 mm). The optical design of the focusing system for the external beam has been carried out by Yu. G. Basargin.

The magnetic field gradient in the lenses is 350 oe/cm. The nominal excitation current is 60 amp. The current is stabilized within ± 1% by a stabilizer. The windings of the magnetic lenses are water cooled.

The magnetic lenses can be moved ± 20 mm in the vertical direction and ± 10 mm in the horizontal direction (along and transverse to the axis of the vacuum tube). The diameter of the vacuum tube along which the extracted beam of charged particles moves is 100 mm. The design and construction of the quadrupole lenses is due to N. A. Ostrovskii and N. I. Konovalov.

In order to reduce the level of the neutron background from the cyclotron in the experimental room, we make use of an electromagnet which steers the beam through an angle 13°. The pole piece of the magnet is trapezoidal (sides 366 and 434 mm, and height 300 mm). With a winding current of 21 amp (voltage of 110 v), a magnetic field of 4500 oe can be produced in the gap between the pole pieces (100 mm).

In order to make it possible to measure the beam current and the intensity distribution over the cross section of the beam, and to be able to obtain radioactive isotopes, the cyclotron is furnished with special probes. The arrangement of these probes is shown schematically in Fig. 8. Probe 5 is used for measuring the ion current at different radii inside the acceleration chamber (50 to 525 mm). This probe can also be used to measure the current in the deflected beam. The probe is moved by remote control by means of an electrical drive system. The position of the probe is indicated at the central control panel. Probe 4 is used for obtaining radioactive isotopes. By rotating the probe, the beam of ions can be distributed over a large surface so that the specific heat load can be reduced. The single-electrode probes 7-10 are used to measure the current distribution in the beam in both the horizontal and vertical directions. These probes are used primarily for adjustment of the focusing system in beam extraction and for monitoring the operation of the cyclotron.

Conclusion

With this cyclotron it is possible to accelerate deuterons to an energy of 13.7 Mev, in which case the current in the terminal radius is more than 1 ma. The extraction coefficient with the deflection system described here is 40-50%.

The focusing effect of the deflection system means that it is possible to use magnetic quadrupole lenses with a small aperture, and that practically all of the current in the deflected beam can be brought to a target located in the experimental room.

The design of the edge of the extraction electrode in the deflection system is such that it is impossible to withstand the extended heat load produced by the current of more than 1 ma which is obtained at the terminal radius.
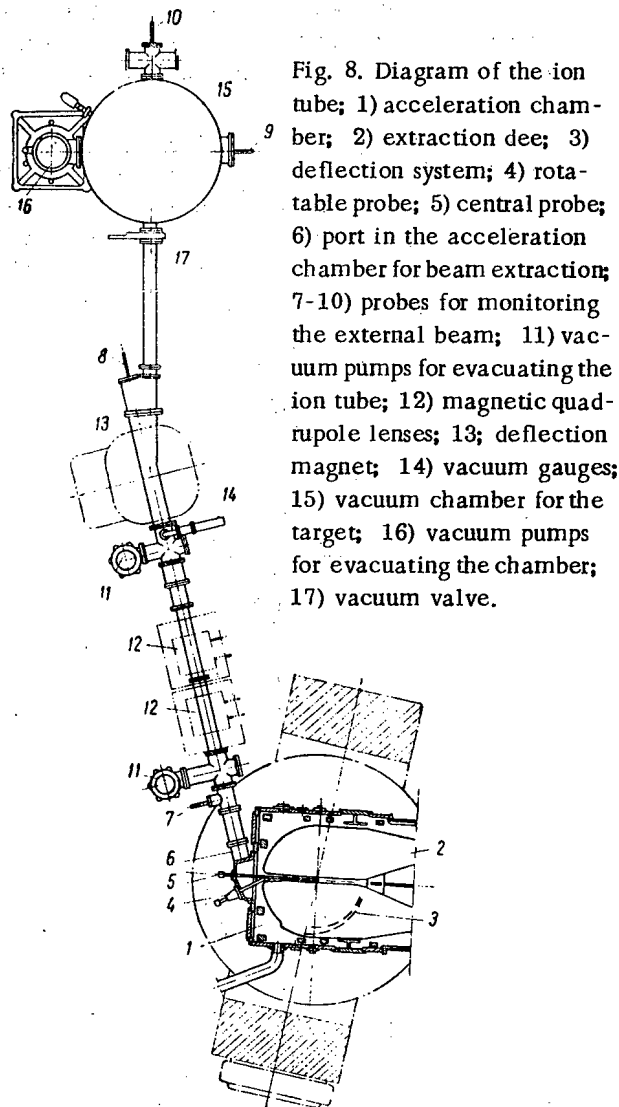
Fig. 8. Diagram of the ion tube; 1) acceleration chamber; 2) extraction dee; 3) deflection system; 4) rotatable probe; 5) central probe; 6) port in the acceleration chamber for beam extraction; 7-10) probes for monitoring the external beam; 11) vacuum pumps for evacuating the ion tube; 12) magnetic quadrupole lenses; 13; deflection magnet; 14) vacuum gauges; 15) vacuum chamber for the target; 16) vacuum pumps for evacuating the chamber; 17) vacuum valve.

Hence, in practice, the current in the deflected beam is limited to 100-200 μa. The cross section of the beam focused on the remote target is 15 × 20 mm; thus, the current density at the target is 40-80 μa /cm^2. Currents of this magnitude are more than adequate for carrying out most experiments and also make it possible to obtain radioactive isotopes outside the acceleration chamber.

There is good reason to believe that the deuteron energy in this machine can be increased to 15-16 Mev with a relatively small reduction in the ion current at the terminal radius. By accelerating ions of molecular hydrogen, without readjusting the resonance circuit of the cyclotron, it is possible to obtain protons with energies of 7.5-8 Mev. It is apparent that α particles can be accelerated to energies of 30-32 Mev; under these conditions, the beam current is approximately 10-15 times smaller than when deuterons or protons are accelerated. The wavelength used in the resonance circuit of the cyclotron and the potential difference between the dees (200 kv) means that in this machine it is possible

660

to accelerate protons directly to an energy of 11 Mev at approximately the same beam currents as with deuterons.

The machine described here has been found very reliable in operation. Special dosimetry measurements indicate that the concrete shield used for penetrating radiation provides absolutely safe operation for the operating personnel and experimenters. The monitor and shutdown system guarantee operation of the machine under operating conditions which satisfy all rules for radiological safety.

The systems used for control signaling and construction of the special electrical installations are due to V. S. Lyublin, N. B. Nevrov, P. S. Gornikel' who worked under the direction of G. S. Gordeichik.

An external view of the cyclotron is shown in Figs. 9 and 10. Similar systems constructed in the Soviet
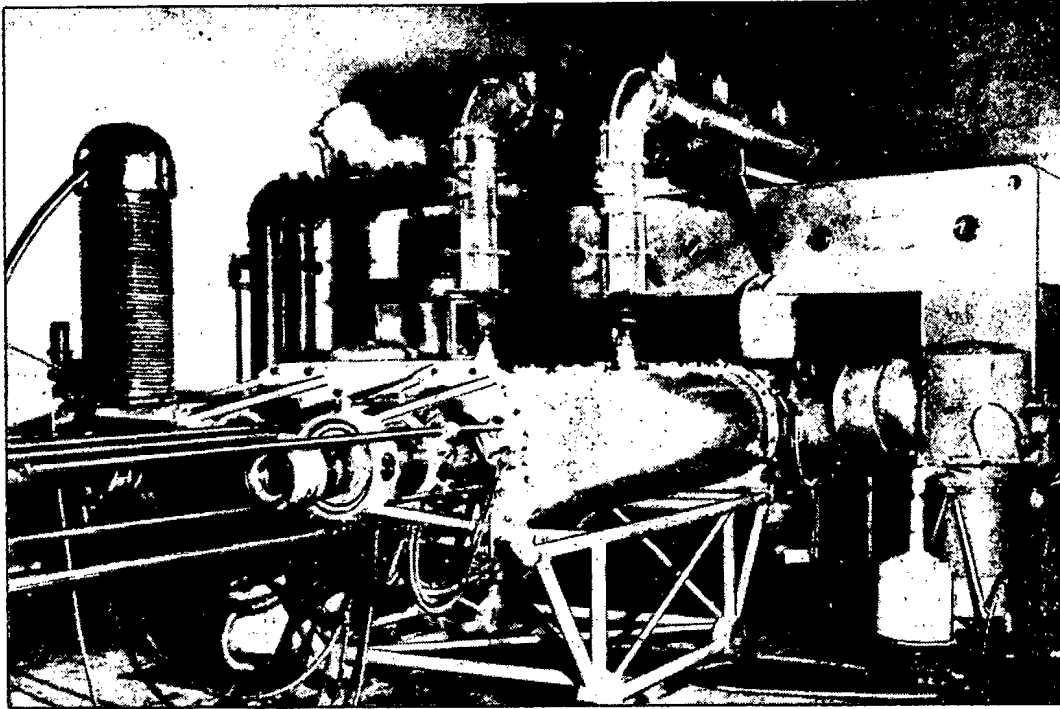
Fig. 9. General view of the cyclotron from the resonance-line side.
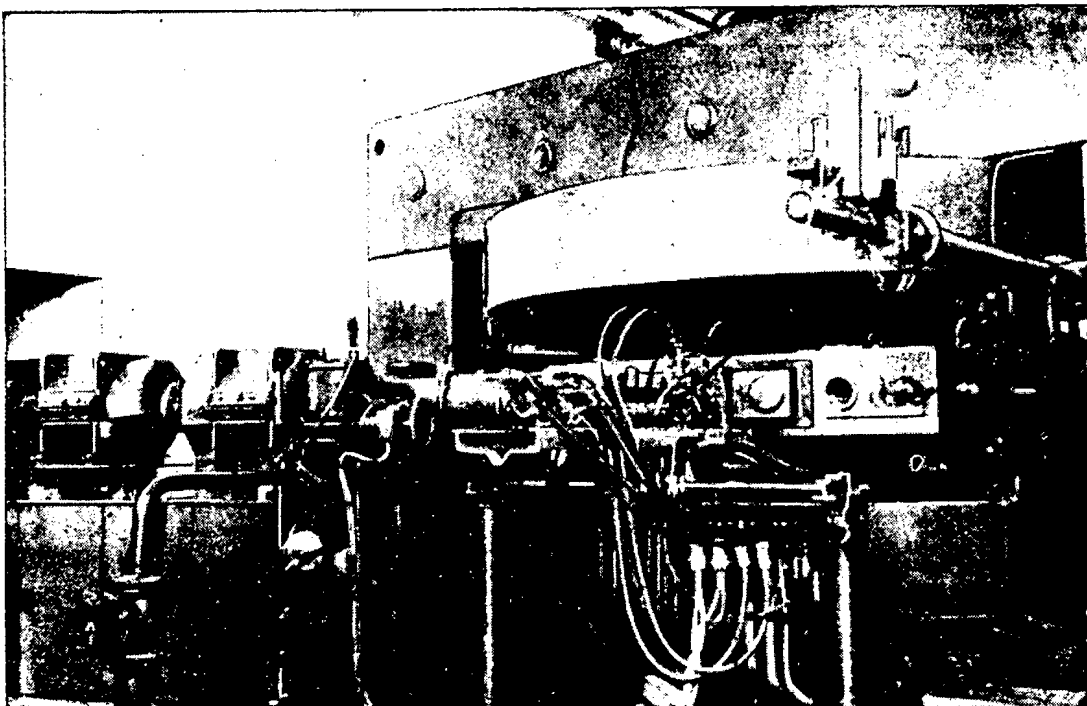
Fig. 10. General view of the cyclotron from the beam extraction side. The magnetic quadrupole lenses are shown at the left.

661

Union are now operating in the Rumanian National Republic, the German Democratic Republic, the Chinese National Republic,and the Polish National Republic. A machine of this kind is also being completed in the Czechoslovakian National Republic.

The tests of the first cyclotron of this kind were carried out in 1956 by workers of the Scientific Research Institute for Electrophysical Apparatus,including L. N. Baulin, R. N. Letunovskii, Yu. G. Basargin, A. V. Stepanov, G. A. Nalivaiko, M. D. Veselov, V. A. Suslov, and A. L Antonov. Work on these tests was shared by workers from the Institute for Atomic Energy, Academy of Sciences, USSR, including I. L Afanas'ev, A. A. Arzumanov, and R. A. Meshcherov. The deflection system and the magnetic quadrupole lenses were tested by workers at the Scientific Research Institute for Electrophysical Apparatus in 1956 with the cyclotron of the Institute of Physics of the Academy of Sciences, Ukr. SSR, including V. A. Kovtun. The cyclotron was constructed under the direction of A. A.

Mozalevskii, L. N. Fedulov, V. V. Romanov, and K. A. Asirev.

The authors wish to thank E. G. Komar for valuable advice, F. K. Arkhangel'skii for great help in tests of the first cyclotron and D. G. Alkhazov for discussion of a number of problems connected with the design of the cyclotron.

LITERATURE CITED

1. N. D. Fedorov. Atomnaya Énergiya 2, 385 (1957).*
2. V. S. Panasyuk, Atomnaya Énergiya 3, 341 (1957).*
3. Kondrashev, Nemenov et al., Pribory i Tekh Éksp. No. 3, 23 (1957).
4. Nemenov, Kalinin et al., Atomnaya Énergiya 2, 36 (1957).*
5. A. A. Arzumanov and E. S. Mironov, Atomnaya Énergiya 6, 202 (1959).*

*Original Russian pagination. See C. B. translation.

DISPERSION MECHANISM OF FLUIDS IN A BUBBLE-TRAY EXTRACTION TOWER, AND A METHOD FOR INTENSIFYING IT

N. P. Galkin, V. B. Tikhomirov, N. E. Goryainov, and V. D. Fedorov

Equipment involving the use of perforated (sieve) trays has met with great popularity in extraction operations, since perforated trays are simple in design, show little sensitivity to the presence of solid particulate matter in the process fluids, and are comparatively inexpensive.

The effectiveness of extraction in those equipments, as in other extraction gear, is dependent in the first instance on the amount of surface available for phase contact between the liquids. It is,therefore, very important to know the mechanism governing the formation of that contact surface in the process of relative fluid flow. This facilitates the study of the processes taking place in bubble-cap tray extraction towers, and of ways for intensifying the processes.

The amount of phase contact surface available depends largely on the degree of dispersion of the liquids, which is in turn determined by the relationship of the forces on a drop of liquid during its continuous advance through the column.

The dimensions of a liquid drop are determined by the equilibrium prevailing between inertia and surface forces. The inertia forces bring about atomization of the drops as they collide with one another and with the trays, while the surface forces, characterized by the value of surface tension, bring about coalescence of the drops. The size of the droplets is therefore dependent on the extent to which inertia forces are capable of overcoming the surface tension of the liquid phase.

The quality of the phase contact is characterized by the relationship of forces determining the frequency at which liquid is renewed in the tray orifices, since renewal of the contact surface occurs in the small layer of liquid immediately adjacent to the orifices.

The insufficient efficiency of conventional perforated-tray extraction towers owes to the fact that surface tension forces have a considerable edge over inertia forces, since the value of the latter is determined solely by the difference in the specific weights of the liquid constituents. At the same time, the use of similar equipment in application to gas (vapor)-liquid systems, e.g., in fractional distillation, yields good results. The high efficiency of fractional-distillation bubble-cap tray equipment is due to the fact that inertia forces in the latter are proportional to the difference in the specific weights of the vapor-liquid system, which is far in excess of the difference in the specific weights of two droplet-phase liquids.

A comparison of the operation of bubble-tray equipment in liquid-liquid systems and gas (vapor)-liquid

systems led to this concept: could not the energy of flow in an extraction column be increased by introducing a system of gas into a bubble-tray extraction tower through use of the forces acting in fractionating towers?
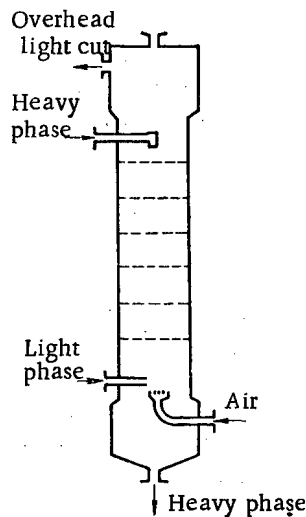
Fig. 1. Diagram of a tray tower with air mixing.

This approach to the problem of increasing extraction-efficiency merits attention further because, in the absence of other known methods for introducing additional energy from external sources (mechanical mixing devices, pulsed column, etc.) into a system of liquids, this approach does not result in more complicated design of the equipment, and involves no additional difficulties attendant upon actual use. Similar problems have not been posed by other researchers, and data on that question are not available in the literature.

The considerations mentioned above have been fully confirmed by experimental data and have led to the design of a bubble-tray column with air mixing, as shown in Fig. 1.

The column with air mixing differs from the conventional extraction tower incorporating sieve trays solely in that the lower portion of the column, where the light fraction is admitted, has air fed into it. Downcomers are omitted, and all of the streams pass through the same orifices of the downflow type trays. The stable mode of operation of the column is observed at air-flow speeds not in excess of 0.03 m/sec through a cross section of the column. When the flow rate of air is increased

663

beyond that point, bubbles appear between the liquid droplets, tending to diminish the effective surface available for phase contact between the liquids, and correspondingly reducing the separative capacity of the column. Furthermore, at air-flow rates in excess of 0.1 m/sec the normal operation of the extraction unit is impaired because of the appearance of a porous foam on the trays, since the air-flow rate through the total cross section of the column begins to exceed the rate at which bubbles of air entrained in the liquid freely escape.

The rate of air mixing assumed makes it possible to maintain a comparatively high value of the fluid dynamic loadings on the columns. It is interesting to note that the upper limit of the air-flow rate in an extraction unit embodying air mixing is the lower limit of the air-flow rate of bubble-cap tray equipment in gas–liquid systems, since the normal mode of operation of an extraction column is the bubble flow mode.

Investigations of bubble-cap tray towers with air mixing, carried out on a water–nitric acid–uranyl nitrate–tributylphosphate system in kerosene demonstrated that the separative capacity is almost three times as high as in conventional packed towers. The total liquid load amounted to ~ 300 cubic meters per sq. meter per hour at optimum air-mixing conditions. In studying the dependence of extraction efficiency on the rate of air mixture, it was revealed that the optimum conditions are arrived at at air-flow rates of 0.01–0.03 m/sec (Fig. 2). The losses in extractant discharging with the
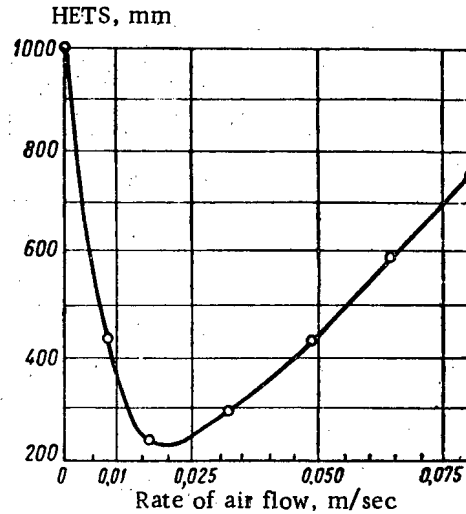
Fig. 2. Effect of rate of air flow on separative potential of extraction unit.
The height equivalent to a theoretical stage (HETS) for columns without air mixing, is arbitrarily assumed to be 1000 mm.

air from the column may be neglected, since they are quite small.

The investigations performed, showed that extraction towers incorporating air mixing are highly efficient and highly productive, so that further study in this field is of unquestionable interest.

SEPARATION OF MIXTURES OF ZIRCONIUM AND NIOBIUM BY REVERSED-PHASE PARTITION CHROMATOGRAPHY

S. Sekerski and B. Kotlinska

A method of partition chromatography using tributyl-phosphate adsorbed on silicone-coated silica gel has been developed; the method was successfully employed in the separation of zirconium from niobium.

An extraction technique which allows for separating substances having similar chemical properties is often used for separating mixtures of inorganic cations. But in the case where the distribution constants differ only slightly, however, the extraction process must be repeated through quite a few runs on the countercurrent principle using a series of separatory funnels, for example, or an extraction tower. These methods are not very convenient, so that the ion-exchange technique is most often resorted to under laboratory conditions. The merits of extraction and of the chromatographic technique are combined in partition chromatography, particularly in reversed-phase partition chromatography, where the organic solvent phase is the stationary phase. This technique has already been in use for some time in the separation of organic substances [1]. We attempted to use the reversed-phase partition chromatography technique to separate mixtures of inorganic cations, using tributyl-phosphate (TBP) adsorbed on siliconated silica gel as the stationary phase. To check the efficiency of this method, we chose the separation of mixtures of zirconium and niobium. The eluting agent used was nitric acid.

Carrier-free radioisotopes Zr^{95} and Nb^{95} were used in the work. In experiments involving pure zirconium, it was separated from niobium by the technique described in [2]. TBP was purified by sublimation at reduced pressure and heating with a 0.5% solution of NaOH, followed by a repeated flushing with water. "Hyflo Super Cel" silica gel with grains of ~ 0.08 mm diameter was siliconated with the aid of dimethyldichlorosilane, and was then dried at 100°C. The silica gel thus obtained exhibited excellent adsorption behavior with respect to various organic fluids (1 gram of silica gel adsorbed ~ 0.6 ml TBP).

The columns were prepared via two techniques:

1. After loading the column with silica gel, a specified amount of TBP saturated with HNO_3 was introduced into the column and TBP-saturated HNO_3 was used to flush the column till all air was removed.

2. The silica gel was shaken up with a suspension of TBP in HNO_3, and the TBP was then adsorbed on silica
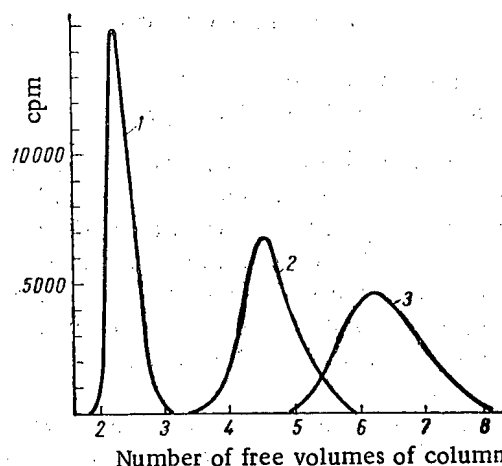
Fig. 1. Elution curve for elution of zirconium by nitric acid at different concentrations of latter: 1) 4.0 M HNO_3; 2) 4.6 M HNO_3; 3) 5.1 M HNO_3.
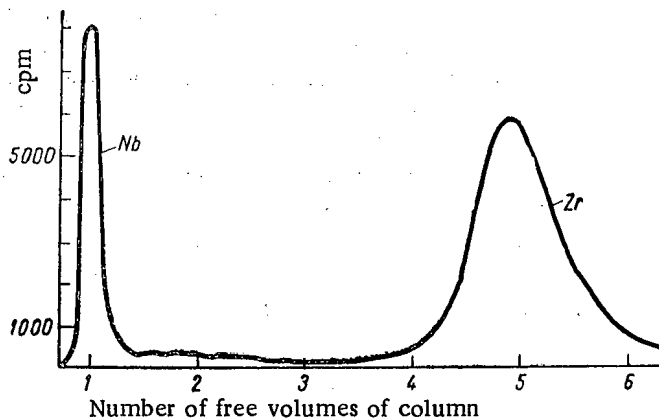
Fig. 2. Separation of niobium from zirconium using 4.6 M HNO_3.

gel. After removal of air bubbles the mixture was introduced into the column.

Columns prepared by any of the methods described above showed no appreciable change in their properties, at least in the course of one month.

Columns 0.5 cm in diameter containing 0.5 g of silica gel and 0.3 ml TBP were usually employed; the height of the adsorbent layer was 5 cm.

665
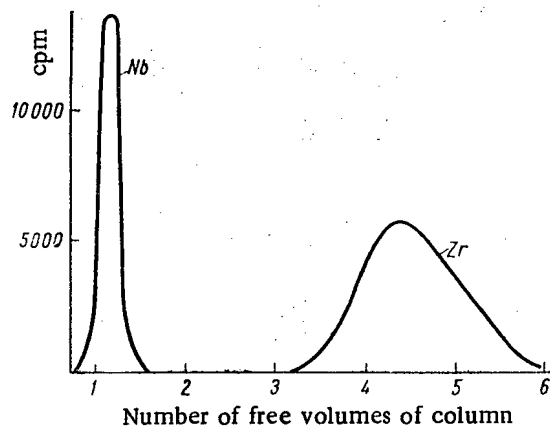
Fig. 3. Separation of niobium from zirconium using 4.6 M HNO_3 + 0.3% H_2O_2.

In carrying out the experiment, a small amount (0.05-0.1 ml) of solution containing active isotopes was introduced into the top of the column, which was then washed with TBP-saturated HNO_3. The rate of discharge of the solution was ~ 0.12 ml/min·cm^{-2}. Drops of eluate were collected and evaporated on rosettes of technical grade paper. The activity was measured by means of an end-window counter.

The free volume of a column was determined by using Cs^{134}. All measurements were carried out at a temperature of 21 ± 3°C.

Figure 1 shows elution curves for the elution of zirconium by nitric acid at different acid concentrations. As is evident, typical chromatographic curves are obtained for zirconium in the TBP (stationary phase)—nitric acid (mobile phase) system. These curves do not appear exactly symmetrical, but do not have very long tails. The position of the peak is strongly dependent on the concentration of HNO_3, and is independent of the rate of flow of the solution over the range flowrates 0.04-0.42 ml/min·cm^{-2}.

Separation of zirconium and niobium was carried out with the aid of 4.6 M HNO_3. At that concentration, the ratio of the partition coefficients of zirconium and niobium was already large enough, and the curve of zirconium was not very smeared. As seen in Fig. 2, the

peaks belonging to the elements are sharply separated since niobium is detected right after the first free volume is passed, but the niobium curve has a long tail to it. It is possible to obtain niobium of high purity on separating by this technique, but the radiochemical purity of zirconium will never exceed 98%. The use of more highly concentrated HNO_3 impairs the quality of the separation, since the niobium curve has a larger tail under those conditions. The reason is probably the fact that niobium forms complexes with H_2O_2 was used to good advantage. It was found that, the best results were obtained on using 0.1-0.3 % H_2O_2 and 4.6 M HNO_3. At that concentration of H_2O_2, the niobium curve from the effluent peaks sharply in a narrow band, and the activity between the curves drops to a few counts per minutes. The zirconium curve exhibits almost no displacement, but is more smeared out and asymmetric in shape (Fig. 3). This complication may be removed with ease by washing the column down with dilute nitric acid immediately after the niobium appears.

After running a few chromatograms it was discovered that the elution curve of zirconium, left standing for a few days, became more and more smeared out and diffuse, but that it again became narrow and symmetric in its geometry after heating of the zirconium in 10 M HNO_3. This fact indicates that zirconium can probably be found in different forms even in 5 M HNO_3, the equilibrium between the variants becoming established slowly.

Separation of a mixture of cations having similar chemical properties by means of partition chromatography using TBP as the stationary phase is thus entirely within the realm of possibility. Since many cations in the form of different salts (nitrates, chlorides, bromides) are extracted with the aid of TBP, it may be anticipated that the technique described above will prove to be of more extended value. At the present time, studies are in progress in our laboratory on the application of this technique to the separation of rare earths.

LITERATURE CITED

1. G. Howard and A. Martin, Biochem. J. 46, 532 (1950).
2. E. Huffman and L. Beaufait. J. Amer. Chem. Soc. 71, 3179 (1949).

666

COMPOSITION AND DISSOCIATION CONSTANTS OF Pu (V) AND Pu (III) COMPLEXES WITH ETHYLENEDIAMINETETRAACETIC ACID

A. D. Gel'man, A. I. Moskvin, and P. I. Artyukhin

Up to the present, there have been no data available in the literature on the formation of complexes by Pu (V) with anions of acids. It is assumed that Pu (V) possesses the least affinity to complex formation, compared to plutonium compounds of any degree of oxidation.

The authors carried out a study of complex formation by Pu (V) with one of the most powerful chelating agents, ethylenediaminetetraacetic acid (EDTA) [1], using the ion-exchange method. As preliminary experiments carried out with macroscopic quantities of Pu (V) indicated, the latter is fully stable for several days. The original solution of Pu (V) was obtained by reducing Pu (VI) with hydrogen peroxide at pH = 3-4.

The study of the distribution of trace amounts of Pu (V) between solutions and KU-2 resin in ammonia form was carried out both in the presence of the chelating agent and, in its absence, over the pH range from 3.3 to 5.1, at an ionic strength $\mu = 0.05$ (for 0.05 M NH$_4$Cl solution), and at a temperature of $20 \pm 1°$C. Adsorption of PuO$_2^+$ is very limited at higher concentrations of salt in the solutions ($\mu > 0.05$). The equilibrium between the solutions and adsorbent on shaking was attained in less than 3 hr. The content of plutonium in the solutions was ascertained by radiometric means.

It was found that the complex ion PuO$_2$Y^{3-} (Y^{4-} being the EDTA ligand) formed in the pH interval studied. Its dissociation constant with respect to concentration, calculated on the basis of the equation

$$K = \frac{[\text{PuO}_2^+][\text{Y}^{4-}]}{C_c}$$

(where C$_c$ is the concentration of the complex) was

$6.8 \cdot 10^{-11}$. It is interesting to note that Np (V) also forms an EDTA-complex of similar composition with

$$K = 4.4 \cdot 10^{-11} \text{ [2]}.$$

The composition and stability of the EDTA complexes of Pu (III), Pu (IV), and Pu (VI) were determined earlier [3] by means of various physicochemical methods. It was found, that plutonium, at pH = 3.3 and in the valence states mentioned, forms complex ions of the type MY^{z-4} (where z is the charge on the cation), while Pu (III) and Pu (IV), also form the complex M$_2$Y^{2z-4} in the presence of a large excess of plutonium ions.

We used the ion-exchange method to study complex formation by Pu (III) in EDTA solutions as the pH was varied from 1.2 to 3.4, when hydrogen-containing EDTA anions participated with the Y^{4-} ions in forming the complexes. A study of the distribution of Pu (III) between the solution and adsorbent was carried out, following the procedure outlined above, in a nitrogen atmosphere and at an ionic strength $\mu = 1$ (in 1 M NH$_4$Cl).

The composition and the dissociation constant K$_n$ of the EDTA complexes with Pu (III) were determined by solving the system of equations

$$\frac{C-[\text{Pu}^{3+}]}{[\text{Pu}^{3+}]} = \sum_{n=1}^{n} \frac{[\text{Y}^{4-}]^n}{K_{1_n}} + \sum_{n=1}^{n} \frac{[\text{HY}^{3-}]^n}{K_{2_n}} + \sum_{n=1}^{n} \frac{[\text{H}_2\text{Y}^{2-}]}{K_{3_n}} + \sum_{n=1}^{n} \frac{[\text{H}_3\text{Y}^-]^n}{K_{4_n}} \qquad (1)$$

by the method of least squares. In this equation, C is the total concentration of all possible forms of plutonium in the solution at equilibrium; [Y^{4-}], [HY^{3-}], [H$_2$Y^{2-}], and [H$_3$Y$^-$] are the equilibrium concentrations of the EDTA anions, which are calculated on the basis of the equations cited in [4]. The concentration of free Pu^{3+} ions was derived from the equation [Pu^{3+}] = $\alpha \cdot$ q, where α is the distribution constant of Pu^{3+} between the solution and the adsorbent in the absence of chelating agent; q is the amount of Pu^{3+} adsorbed by the resin in the absence of the ligand. The calculations showed that the complex ions PuY$^-$ and PuHY$^-$, whose dissociation constants are $4.4 \cdot 10^{-18}$ and $6.2 \cdot 10^{-10}$, respectively, form under the conditions indicated.

It is interesting to correlate the pK values of the MY$^-$ complex ions for trivalent transuranium elements in the Pu $\rightarrow$ Cf series (see table below).

It is clear from the Table, that as the atomic order number Z of an element increases, the stability of complexes of the MY$^-$ type increases in correspondence with the reduced ionic radius r of the cation (i.e., with increase in the ionic potential $\varphi = Z/r$).

Calculations demonstrated that the pK value of trivalent transuranium elements is related to their atomic number Z by the following equation:

$$pK = 0.0645 \cdot Z^{1.24}. \qquad (2)$$

667

Dissociation Constants of EDTA Complexes of Trivalent Transuranium Elements (at $\mu = 0.1$)

Element	pK based on (2)	pK based on experimental data	Literature references
Neptunium	17,8	—	—
Plutonium	18,0	18,1; 18,3*	[3—4]
Americium	18,3	18,16	[6]
Curium	18,5	18,45	[6]
Berkelium	18,8	—	—
Californium	19,0	19,09	[6]

*The pK value of a PuY⁻ complex was converted, on the basis of Davis' equation [5], for ionic strength $\mu = 0.1$.

The pK values computed by means of this equation for the complexes of interest here show satisfactory agreement with the values of the constants found experimentally. By means of (2), we evaluated the pK values cited in the Table for EDTA complexes of Np (III) and Bk(III), of the MY⁻ type. In the future it would be interesting to determine these values experimentally.

The available data on the stability of EDTA-complex ions of plutonium [1, 3, 4] provide the possibility of carrying out a comparison of the relative affinity of Pu (III), Pu (IV), Pu (V), and Pu (VI) to form complexes. It is a familiar fact that the complexing power is enhanced as the formal charge on the ion increases and as the ionic radius decreases, and is also a function of the structure of the cation itself. A comparison of the dissociation constants of EDTA complexes of plutonium shows that the affinity for complex formation in the different plutonium ions falls off in the following sequence:

$$Pu^{4+} > Pu^{3+} > PuO_2^{2+} > PuO_2^{+},$$
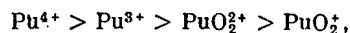
i.e., in the order of decrease in the ionic potential φ.

LITERATURE CITED

1. A. D. Gel'man, P. I. Artyukhin, and A. I. Moskvin, Zhur. Neorg. Khim. 4, 1332 (1959).
2. A. D. Gel'man and M. P. Mefod'eva, Doklady Akad. Nauk SSSR 124, 815 (1959).
3. J. Foreman and T. Smith, J. Chem. Soc. 1957, 1752.
4. A. I. Moskvin and P. I. Artyukhin, Zhur. Neorg. Khim. 4, 591 (1959).
5. C. Davies, J. Chem. Soc. 1938, 2093.
6. Atomnaya Énergiya 4, 602 (1958).*

*Original Russian pagination. See C. B. translation.

EXPERIMENTAL DETERMINATION OF THE TRUE SPECIFIC HEATS OF URANIUM, THORIUM, AND OTHER METALS

E. A. Mit'kina

The true specific heats of uranium, thorium, beryllium sodium, and a bismuth-lead alloy, were determined by a relative heating and cooling method [1] and an absolute method involving the use of an electron-radiation calorimeter [2].

The cooling and heating method was modified somewhat. Specimens (or control blanks) of cylindrical form ($\phi = 15 \times 15$ mm) were selected, since the cooling conditions for such specimens were characterized by low values of the Biot modulus (below 0.05), so that the variation of temperature with time for any point on the cylinder might be assumed to be uniform.

Applying the appropriate mathematical reduction of the cooling curves [3], the following formula was obtained for determining the specific heat of a specimen:

$$c(t) = c_1(t) \frac{G_1}{G} \frac{\tau_1}{\tau}, \qquad (1)$$

where $c_1(t)$ is the specific heat of the reference standard; G_1 is the weight of the reference; τ_1 is the cooling time of the reference; G is the weight of the specimen; τ is the cooling time of the specimen.

In order to avert oxidation of the specimen and reference standard, experiments were carried out in an inert-gas atmosphere and in a vacuum.

The specific heat in the electron-radiation calorimeter was determined on the basis of equation

$$c = \frac{Q}{G \Delta t}, \qquad (2)$$

where Q is the amount of heat introduced into the sample by electron flow, during a time τ, equal to 0.239 Ivτ (where I is the amount of current; v is the voltage between the heating filament and the specimen, which acts as the anode); G is the weight of the specimen; Δt is the change in the temperature of the specimen.

The electron-radiation calorimeter was operated in the following fashion: at a distance of 4-5 mm from the test sample, i.e., the anode, is placed a tungsten heater filament 0.05 mm in diameter, supplied by storage batteries at a voltage of 4-5. A potential difference of the order of 200 v is supplied for a time τ across the heater filament and the specimen. Any temperature increase in the specimen is sensed by a thermocouple. The primary temperature of the specimen is determined by balancing the heat produced by the electric furnace 4, the heater filament, and the cooling by water of the quartz envelope of the calorimeter.
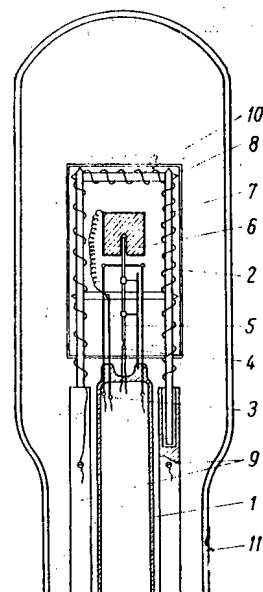
Electron-radiation calorimeter.

The vacuum system assures a vacuum of the order of $5 \cdot 10^{-5}$ mm Hg in the calorimeter. The design details of the calorimeter may be seen in the accompanying diagram. The calorimeter is assembled on a support consisting of a bellows covered by a flange using lead packing. The support has a water cooling jacket, and is equipped with a duct connected to a diffusion pump. A specimen holder 1 consisting of a glass tube with a system of crossbars soldered to it bearing on picein lubricant is passed through the flange, the crossbars serving to hold the cathode filament 2 in tension, to provide a lead-in for the anode conductor 3, the thermoelectrodes 4, and for mounting of a thin dual-channel tube for the thermocouple 5, while at the same time, serving as a support for the test sample 6. A quartz frame 7, needed to fasten the winding of the electric heating unit, supports a radiation screen 8, the latter made of tantalum foil. The quartz frame is fastened to the flange by two long brass pins 9, which conduct current to the heating unit 10. The entire apparatus is enclosed in a quartz envelope 11, mounted on the flange with picein lubricant.

The sample was weighed on analytical balances mounted on a chromel-constantan thermocouple and placed inside the calorimeter. In determining the specific heat of the melt, the latter was placed inside a

669

TABLE 1. Characteristics of Materials Tested

Material	Degree of purity, in %	Thermal conductivity, kcal/m·hr·°C	Specific heat, cal/g°C
Uranium	99,72	19 at 20° C	0,03 at 20° C
Thorium	99,81	36 at 20° C	0,03 at 20° C
Beryllium	99,80	100 at 20° C	0,4 at 20° C
Sodium	Technical grade	50 at 100° C	0,3 at 100° C
Alloy (Pb 43.5%, Be 56.5%). . . .		10 at 150° C	0,03 at 150° C

TABLE 2. Results of Measurements of the True Specific Heats of the Materials Tested

°C	Specific heat, cal/g°C				
	Uranium	Thorium	Beryllium	Sodium	Alloy (Pb 43.5%, Bi 56.5%)
50	0,0268*	0,0250*	0,465*	—	0,0298*
100	0,0284*	0,0268*	0,490*	0,320*	0,0332*
150	—	—	—	0,320*	0,0350*
200	—	—	—	0,320*	0,0353*
250	—	0,0315⁺	—	0,320*	0,0355*⁺
300	0,0345⁺	0,0330⁺	—	0,320⁺	0,0355*⁺
350	0,0362⁺	0,0340⁺	0,615⁺	0,320⁺	0,0355*⁺
400	0,0378⁺	0,0350⁺	0,635⁺	0,320⁺	0,0355*⁺
450	0,0394⁺	0,0360⁺	0,655⁺	—	0,0355*⁺
500	0,0410⁺	0,0365⁺	0,672⁺	—	0,0355*⁺
550	0,0425⁺	0,0374⁺	—	—	—
600	0,0440⁺	0,0380⁺	—	—	—
650	—	0,0388⁺	—	—	—
700	—	0,0390⁺	—	—	—

Note. Asterisks denote specific heat data obtained by the relative method, while crosses denote data obtained in the electron-radiation calorimeter.

hermetically sealed thin-walled metal crucible of known specific heat. The setup required a vacuum and controlled heat conditions for satisfactory operation. The anode voltage, the anode current, and the time during which the current flowed were measured; changes in the temperature of the specimen were recorded on a PPTN-1 potentiometer.

Table 1 gives the characteristics of the materials tested, based on data from several papers, while the results of measurements of the specific heats of those materials are entered in Table 2.

The relative error in the determination of specific heat by the cooling and heating method may be represented as the sum of the relative errors incurred in finding the values entering into (1), and were evaluated at 1.5-2%.

The fact that the cathode filament was positioned in close proximity to the specimen inside the electron-radiation calorimeter brought about radiation heating, which restricted the lower temperature limit of the measurements to 200-250°C.

The experimental error associated with electronic heating of the specimen (work function of the electrons, thermal energy introduced by electrons in the sample) amounted to approximately ± 2%. The relative error incurred in the specific heat determinations was ± 1.5-1.8%.

LITERATURE CITED

1. G. M. Bartenev and Ya. L. Turovskii, Zhur. Tekh. Fiz. 10, 514 (1940); 10, 1074 (1950); 17, No. 11 (1957).
2. H. Klinkhardt, Ann. phys. 84, 167 (1927).
3. E. V. Kudryavtsev, The Use of Thermal Transients in Studies of Heat Release in Aviation Engines [in Russian] (Oborongiz, 1948).

670

MEASUREMENT OF ELECTRICAL RESISTIVITY OF
PILE-IRRADIATED BOILING NITROGEN

Yu. K. Gus'kov and A. V. Zvonarev

In studying radiation-induced dislocations in solids, experiments on the irradiation of such solids over a broad range of temperatures, starting with the lowest temperatures, are called for. Low-temperature conditions may be attained by cooling the samples to be irradiated using liquefied gases. Liquid nitrogen (boiling point −196°C) is the most readily available of these. In addition, nitrogen has a low activation cross section, which facilitates handling of the liquefied gas.

We carried out measurements of the electrical resistivity of liquid nitrogen after irradiating it in a reactor. The diagram shows the Dewar vessel in which the measurements were carried out.

The electrodes used were two copper plates each 2.4 cm^2 in area, which were soldered to the cores of a 0.75 mm diam BPTE cable, which was fixed in place inside copper leads. The metal braiding of the cable was stripped from a length 10 mm around the spot where the electrodes were soldered on. The spacing between elelctrodes was 5 mm. The Dewar vessel had a capacity of 118 g liquid nitrogen. The resistivity was measured by a TO-1 instrument (over a range of measurements of 10^6 - 10^{12} ohm).

The electrical resistivity of liquid nitrogen subjected to an in-pile bombardment in a nuetron and gamma flux of 10^{11} particles per cm^2 per sec was reduced to 10^{12} ohm/cm^3, and dropped to 4 · 10^9 ohm/cm^3 in a flux of 1.5 · 10^{13} particles per cm^2 per sec.

This resistivity was retained until the liquid nitrogen was evaporated down to the level of the electrodes. The resistivity in the interval between the electrodes began to fall afterwards. When the liquid nitrogen had been completely driven off, the resistivity of the interelectrode spacing dropped to 7 · 10^7 ohm/cm^3.

When irradiated in a reactor, liquid nitrogen boiled vigorously and the time required for its evaporation was reduced by the order of one magnitude. The values cited for the electrical resistivity (10^{12} and 4 · 10^9 ohm/ / cm^3) are therefore with reference to what actually takes place within an environment of liquid nitrogen.

The relation between the changes in the resistivity of boiling nitrogen and the level of the irradiation flux is close to a linear function. The nonlinearity may be explained by an increase in the vapor content in the boiling nitrogen owing to increased evolution of energy within the walls of the Dewar flask, in the electrodes, and in the nitrogen itself, as the flux is increased.

It is to be noted that not only the average vapor content in the medium in question, but also the distribution of vapor content relative to the test sample, which is a factor dependent on the concrete experimental conditions, must be taken into account in evaluating in-pile experiments involving irradiation of materials in a liquid-nitrogen atmosphere.

In conclusion, the authors would like to take this opportunity to express their gratitude to A. K. Krasin, Doctor of Physical and Mathematical Sciences, for his kind interest in the work, and to A. G. Vishnyak, for his kind assistance in the execution of the experiment.
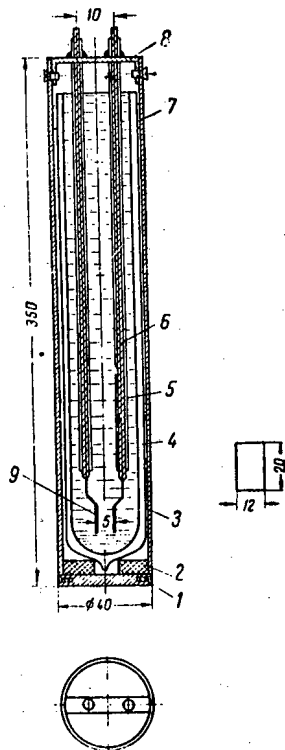
Dewar vessel:
1) aluminum bottom;
2) rubber spacer disk;
3) aluminum tubing, $\phi = 40 \times 1$ mm; 4) glass Dewar; 5) copper tubing, $\phi = 3 \times 0.5$ mm; 6) cable; 7) rubber packing; 8) copper plate; 9) copper electrode.

USE OF THE REACTION O^{18} (α, n) Ne^{21} TO DETERMINE THE CONCENTRATION OF ALPHA-ACTIVE SUBSTANCES IN AQUEOUS SOLUTIONS

V. V. Ivanova, A. I. Nazarov, E. V. Polunskaya,

A. G. Khabakhpashev, and É. M. Tsenter

The amount of alpha-active substances present in aqueous solutions is usually determined either by sample analysis or else by using an alpha counter place above the surface of the solution. Neither method is suitable for highly alpha-active solutions, since sample analysis contaminates the working area and use of an alpha counter placed above the solution complicates the situation greatly, because the background rises rapidly during rinsing or replacement of the counter.

In certain cases, the amount of alpha-active substances present in an aqueous solution can be determined by measuring the neutron yield * of the reaction O^{18} (α, n)Ne^{21}. Notwithstanding the fact that a natural mixture of oxygen isotopes containly only 0.204% of the isotope O^{18}, the neutron yield is sufficient for the determination of the amount of alpha-active substances, owing to the large cross section of the (α, n) reaction for the isotope O^{18} [1]. Such a method permits standard measurements to be carried out remotely and without disturbing the airtightness of the system.

In the present work, we determined the sensitivity of the method, dependence of sensitivity on the volume of active solution, effect of composition of the solution on neutron yield, and the permissible limit of gamma background.

For the case where the neutron counter was placed in a special sleeve in the center of a cylindrical tank of the active solution, the sensitivity of the method was approximately determined (number of counts recorded by the counter for an alpha-active substance concentration of 1 C/liter):

$$N = A \sum_{i=1}^{n} N_i, \qquad (1)$$

where A is the number of neutrons per second per cubic centimeter of solution for an alpha-active-substance concentration of 1 C/liter; N_i is the number of counts recorded by the counter from the ith region of the tank (Fig. 1) for a neutron-source density of 1 neutron/cc·sec.

For a nitric acid solution of polonium, the quantity A was experimentally found to be equal to 1.6. The quantity N_i was measured with a Po-α-Be neutron source in a tank of 84 liters volume (43 cm high, 50 cm in diameter). An SNM-9† counter served as a neutron detector.
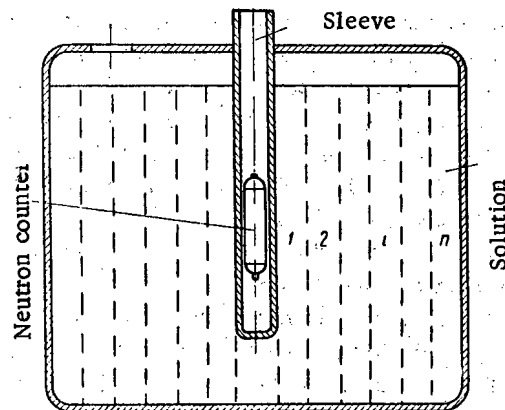
Fig. 1. Experimental arrangement for measurement of the concentration of alpha-active substances in solution by means of neutron yield.

The sensitivity in this case was found to be equal to 330 counts/min.

Taking a summation in (1) up to the kth region (k < n) gives the sensitivity for the volume $\sum_{i=1}^{k} V_i$, surrounded by a layer of water of volume $\sum_{i=k}^{n} V_i$ (where V_i is the volume of the ith region of the tank). The dependence of the sensitivity on volume was determined in this manner (Fig. 2).

The effect of composition of the solution on neutron yield can be found by the following method. If the composition of the solution is determined by using element weight concentrations α_0, α_1, α_2, ...,(α_0 is the concentration of the element on which the (α, n) reaction operates), then the atomic concentration of the ith element (number of atoms per cubic centimeter)will be $\alpha_i \rho N_0 / A_i$ where ρ is the density of the solution, N_0 is Avogadro's number, and A_i is the atomic weight. If the relative

---

* Determination of the concentration of α-active substances by neutron yield was proposed by E. V. Polunskaya and A. I. Nazarov.

† The counter operates in the corona discharge cycle. The counter cathode is covered with amorphous natural boron [2].

672
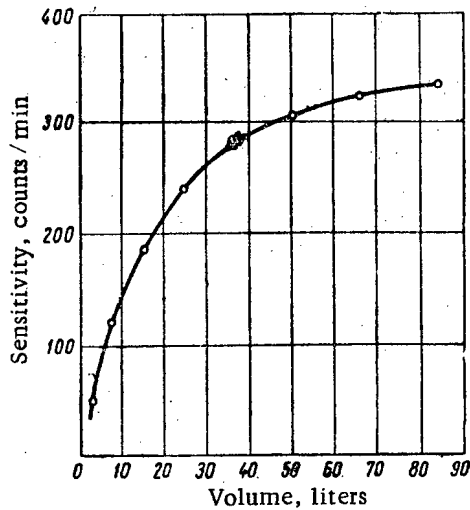
Fig. 2. Dependence of sensitivity on volume of the alpha-active solution for a concentration of 1 C/liter.

stopping power is denoted by $\underline{S}_i$, then the stopping power of the ith element on conversion to cubic centimeter is

$$\beta_i = \frac{N_0 \alpha_i \rho S_i}{A_i} . \qquad (2)$$

The range of alpha particles in the element on which the (α, n) reaction operates is

$$m = \frac{\beta_0}{\beta_0 + \sum_1^m \beta_i} = \frac{1}{1 + \frac{\sum \alpha_i S_i / A_i}{\alpha_0 S_0 / A_0}} , \qquad (3)$$

which is numerically equal to the ratio of the neutron yield from a solution composed of n + 1 elements to the yield from a pure-element target, provided that the identical alpha activity exists.

Knowing the stopping powers and weight concentrations of the elements making up the solution, one can determine the dependence of the relative neutron yield on the composition of the solution. These determinations showed that neutron yield is little affected by variation of the solution acidity within wide limits or by the admixture content. Thus, for example, using a nitric acid concentration change from 1N to 8N, the neutron yield decreases only by 2%. This results was verified experimentally.

If the solution contains uranium or plutonium, the neutron yield will be increased because of fission of U^{235} and Pu^{239} nuclei, and will be decreased because of the stopping power of alpha particles by the atoms of these elements. Evaluation of these effects showed that for a uranium concentration in the solution of 100 g/liter (natural mixture of uranium isotopes), the neutron yield increases 2.6% because of fission neutrons and decreases 3% because of alpha stopping. Thus, the addition

of uranium to the solution has practically no effect on the neutron yield, provided one can neglect the alpha activity of the uranium itself. For a plutonium concentration of 1 g/liter in the solution, the neutron yield increases 10% because of fission neutrons, and this change in the neutron yield must be taken into account during calibration.

The addition of several light elements having high (α,n) reaction cross sections can increase the neutron yield and introduce error into the measurements. The permissible concentration of light elements can be determined by simple computation. Thus, the neutron yield increases by 1% for a concentration of 8mg/liter of beryllium, 1.4 g/liter of aluminum, or 0.42 g/liter of sodium.

The method described above was verified experimentally with polonium solutions. A KN-14 ionization chamber was placed in the sleeve of the tank (see Fig. 1) containing the solution. The recording apparatus was located 30 meters from the tank. The equipment registered 720 counts/min for a solution concentration of 1 C/liter; hence, it was possible to determine polonium content as low as 10-12 mC/liter. Measurements of the polonium concentration by means of the neutron yield were checked by a calorimetric method. In all cases the deviation did not exceed 4%. The first calorimetric measurement was used as a calibration.

The neutron yield from a solution of 0.5 liter volume was measured with a fast-neutron scintillation
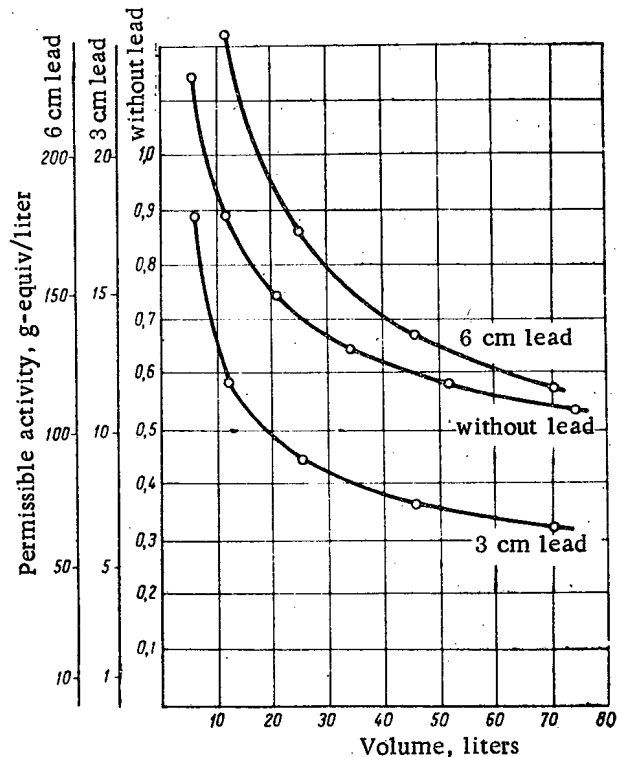
Fig. 3. Dependence of limiting permissible concentrations of gamma-active substances on volume of the solution for various thicknesses of lead shielding.

673

counter. The scintillator was made of paraffin and zinc sulfide. For a polonium content of 1 C in the solution, 10 counts/min were recorded. These measurements were also calibrated by the calorimetric method; the deviations did not exceed 10%.

If it is absolutely necessary to determine the concentration of an alpha-active substance in a solution which also contains a significant amount of gamma-emitting elements, then it is convenient to use SNM-9 counters, which can operate in gamma fields of 1000 r/hr. The sensitivity can be increased 20- to 30-fold by connecting several enriched-boron counters in parallel. Moreover, it is possible to measure the plutonium concentration in the solution, beginning at 20-30 mg/liter with a permissible gamma-active substance concentration equal to 0.6 g-equiv/liter. With the use of lead shielding, the limiting permissible concentration of gamma-active substances can be increased significantly. Figure 3 shows the dependence of the limiting permissible concentration of gamma-active substances on volume of the solution for various thicknesses of lead shielding.

Thus, the method described above permits remote determination of the amount of alpha-active substances in a solution without disruption of airtightness. By this method, one can measure concentration beginning at 1-2 mC/liter, while various admixtures to the solution have only a small effect on the measured results.

The use of lead shielding permits measurements with gamma-active substance concentrations in the solution of approximately 150 g-equiv/liter.

LITERATURE CITED

1. I. A. Sordyukova, A. G. Khabakhpashev, and E. M. Tsenter, Izvest. Akad. Nauk SSSR Ser. Fiz. 21, 1017 (1957).
2. A. B. Dmitriev, Pribory i Tekh. Eksp. No. 2,3 (1957).

674

GAMMA-RADIATION OF THE FISSION FRAGMENTS
OF U ^{235} AND Pu^{239}

Yu. I. Petrov

With the aid of air-equivalent ionization chambers and a Geiger counter, the γ radiation of fragments of U^{235} and Pu^{239} was investigated over a wide range of times (0.6 sec - 11 hr) after the targets were subjected to pulsed irradiation in the thermal neutron flux of the heavy-water nuclear reactor of the Academy of Sciences, USSR [1]. The short-duration irradiation of the targets (1 sec) was accomplished by a pneumatic arrangement. Ionization measurements were performed at various distances from the targets in air and in water. Flat thin-walled (1-2 cm) hermetic plexiglas chambers with aluminum foil electrodes 13μ thick were used. The ionization currents, after having been amplified by a constant-current balanced amplifier, were recorded by a loop oscillograph. By the use of over-all negative feedback [2, 3] in the amplifier, the real effective-input time constant of the amplifier RC = 1.5 sec was decreased to the value $(RC)_{eff} = 0.01$ sec. The number of fissions in the targets was determined by the β activity of copper indicators, irradiated together with the target, which were calibrated with the aid of a fission chamber containing known weights of U^{235} or Pu^{239} (the method was developed in 1952 by O. I. Leipunskii, P. A. Yampol'skii, and V. N. Sakharov). The weight of U^{235} and Pu^{239} in the targets was determined by comparison with the γ activities of the simultaneously irradiated targets and standard samples of natural uranium or Pu^{239}. The comparison was made under standard conditions with the aid of a Geiger counter. It was shown that within the limits of experimental error (10%), the γ radiations of the U^{235} and Pu^{239} fragments have the same decay kinetics, the same mean energies of the γ quanta, and the same total γ-ray energy-yield per fission. Because of this, the results are for the most part given below for U^{235}.

After corrections were introduced for the decay of the fission products during the time of exposure of the targets in the reactor, our results were extrapolated to the time t = 0.05 sec after fission by the method of joining with the data of I. I. Levintov and V. N. Shamskev. In 1952, these authors used a Geiger counter to measure the kinetics of the γ radiation of fragments of U^{235} and Pu^{239} in time intervals of 0.05-3 sec and 0.05-0.7 sec, respectively, after irradiation (a 10^{-2} sec pulse) of the samples by slow neutrons, and did not find any significant

difference between the data for U^{235} and Pu^{239}. The results of the measurement of ionization currents in water are well approximated by the formula

$$i(r, t) = 1.16 \times$$
$$\times 10^{-23} [10.73 \exp(-0.238 r) + \exp(-0.0775 r)] [1.78 \times$$
$$\times \exp(-3.14 t) + 1.825 \exp(-0.545 t) + \exp(-0.091 t)]$$
$$\text{amp/cm}^3\text{-fission,} \qquad (1)$$

where $0.05 \le t \le 14$ sec; $8.2 \le r \le 70$ cm and the currents are referred to 1 cm^3 of the volume of the chamber and to one fission of the U^{235}.

The data from several sources for the kinetics of the short-lived γ radiation of the fragments are shown in Fig. 1. The curves combine at t = 2 sec. It is interesting to note the coincidence of the data for U^{235} fission by thermal neutrons and the fission of natural uranium by 14 Mev neutrons (the experiments by O. I. Leipunskii and co-workers in 1952).

Figure 2 shows the kinetics of γ radiation of U^{235} fragments according to the data of ionization measurements in air. The initial portion of the curve is described by (1) to within the limits of accuracy of the measurements (10%). A much sharper drop-off ($t^{-0.8}$) in the γ activity of the fragments was obtained in measurements made with a Geiger counter [5] (for a time interval of 1.25-17 sec) than what follows from our data. Measurements of the γ activity of the fragments in the time interval 24 sec-11 hr were carried out jointly by us and G. G. Petrov in 1953, using a lead-walled Geiger counter (wall thickness 1 mm) and an aluminum-walled Geiger counter (wall thickness 4 mm). The decay curves for both counters are described by a common formula in overlapping sections (5-10 hr). The results of the measurements taken with the aluminum-walled counter are shown in Fig. 3.

The separate components of the total γ radiation of the fission products are differently attenuated in passing through the scattering medium; as a result, the decay curves measured at various distances from the targets can be distinguished from each other. The correctness of (1) for the distance interval 8.2-70 cm, and the coincidence of the decay curves for measurements in water and air indicate a rough similarity in the compo-

675
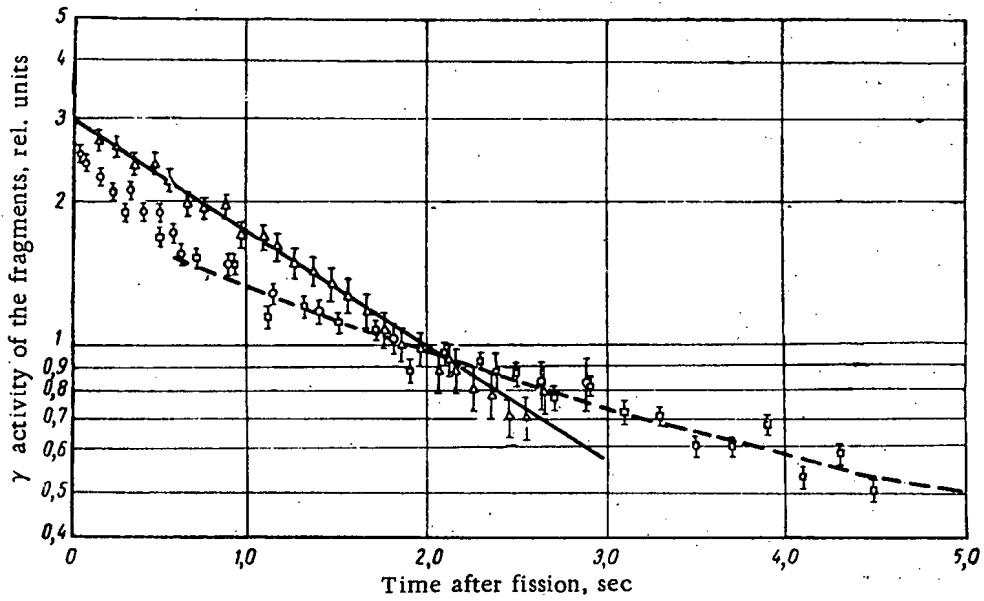
Fig. 1. Kinetics of the short-lived γ radiation of the U^{235} fission fragments: ---- data of the present study; $\ominus$- data of I. I. Levintov and V. N. Shamskev; $\triangle$- data of [4]; $\ominus$- data of O. I. Leipunskii and co-workers for the fission of natural uranium by 14 Mev neutrons.
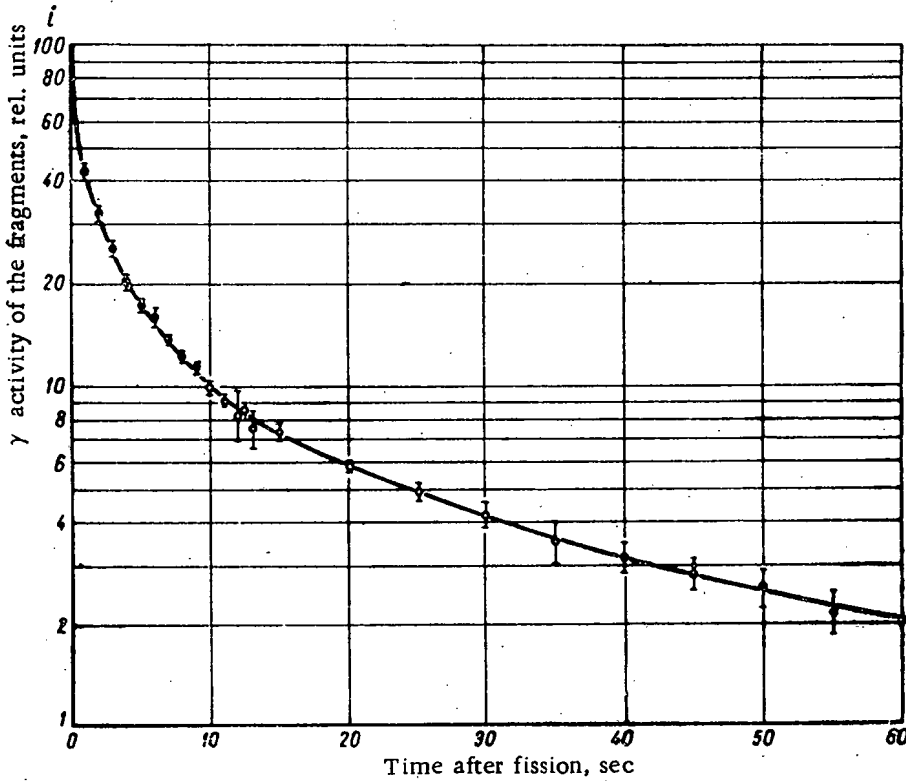
Fig. 2. Kinetics of the γ radiation of the U^{235} fragments according to data from ionization measurements in air.

676
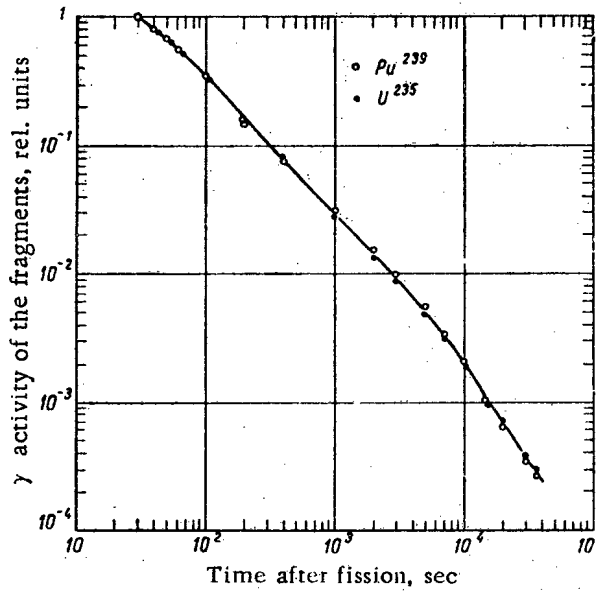
Fig. 3. Kinetics of the γ radiation of the fission fragments of U^{235} and Pu^{239} according to data from an aluminum-walled Geiger counter.

Fig. 5. Energy yield of γ radiation of fragments per U^{235} or Pu^{239} fission:
1) data of the present study; 2) total energy of β, γ radiation, and neutrino [8]; 3) data of Fermi and King [8]; 4) data of Moon and Hoffman [8]; 5) data of [6]; 6) data of [9].
Approximation of the curve E_γ (t)

Fig. 4. Spatial distribution of γ radiation: ———data from [7] for γ radiation in water; —✕—data for γ radiation of the fragments in water according to (1) for t = 1 sec; — — — data for γ radiation of the fragments in air for t = 1 sec.

nents and an approximate constancy in the average energies of the γ quanta of the fragments during the first few seconds of decay. The constancy of the average energy of the γ radiation of the fragments of U^{235} during a 5 minute period after fission has been experimentally established [6].

Figure 4 gives the spatial distribution of γ radiation in water for γ quanta with energies of 0.41, 1.25, and 2.8 Mev [7]. Crosses and a dotted line are used to plot the data for radiation of fragments according to measurements in water (1) and air, for t = 1 sec. The difference $\Delta \ln ir^2$ as a function of γ-quantum energy for r = 70 cm is shown above. It is evident that the average of the γ radiation of the fragments $h\nu_{av} = 1.5$ Mev. This estimate of the energy of the γ radiation of the fragments is sufficiently accurate, since it automatically takes into account the effect of multiple scattering of γ quanta in a dense medium. Experiments with the absorption of a collimated beam by copper and aluminum filters gave a value of $h\nu_{av} = 1.6 \pm 0.3$ Mev for the first few seconds of decay [5].

We determined the total energy yield of the γ radiation in 1 sec per fission E_γ (t) by three independent methods: 1) by integration of the spatial distribution of the dosage in water; 2) by the data from the ionization measurements in air, under the assumption that $h\nu_{av} = 1.5$ Mev; 3) by comparison of the γ activities of targets made of U^{235}, Pu^{239}, and standard Na^{23} samples, all exposed together to thermal neutrons. The comparison was made with the aid of a thin-aluminum-walled Geiger counter for which the dependence on the quantum energy of the recording efficiency in the energy range 0.2-3 Mev was nearly [10] linear, consequently making the counting rate proportional to the energy flux of the γ radiation. The results of the measurements made by the first and second methods are the same, to within an accuracy of 5%. The results of measurements made by the third method coincide with the data from the ionization

677

Interval of time after fission	$E_\gamma(t), \quad \dfrac{\text{Mev}}{\text{sec}\cdot\text{fission}}$
0,05—14 sec 10—60 sec 60—7200 sec 1,5—14 hr	$0,18\ [1,78\ \exp(-3,14\,t)+1,825\ \exp(-0,545\,t)+\exp(-0,091\,t)]$ $6,26\cdot10^{-2}\ [2,18\ \exp(-0,159\,t)+\exp(-0,0239\,t)]$ $1,145\ t^{-1,05}$ $2,97\cdot10^{-4}\ t^{-1,45}$

measurements in water within the limits of experimental error ($\sim$ 10%), in the overlapping portions of the decay curves (25-60 sec).

An approximation of the curve $E_\gamma(t)$ for various intervals of decay time is listed in the table.

A summary of the results for $E_\gamma(t)$ is shown in Fig. 5. Curve 2 gives the theoretical values of the total energy of the radiation (β, γ radiation, and neutrino) obtained by considering the totality of the fission products as a single statistical collection [8]. Unpublished results of Fermi and King, and also Moon and Hoffman, were taken from [8].

The results of [6] are evidently lower by a factor of more than 1.5 as a result of inaccurate calibration of the apparatus. The reason for the discrepancy between our data and those of [9] is unclear.

The author thanks Prof. O. I. Leipunskii for proposing this subject and for his scientific assistance.

LITERATURE CITED

1. Yu. I. Petrov, Dissertation [in Russian] (Institute of Chemical Physics, AN SSSR, 1953).

2. G. S. Tsykin, Negative Feedback and Its Application [in Russian] (Svyaz'tekhizdat, 1940).

3. H. Thomas, Electronics 19, 130 (1946).

4. J. Brolley and D. Cooper et al., Phys. Rev. 83, 990 (1951).

5. O. I. Leipunskii, V. N. Sakharov, and V. I. Tereshchenko, Atomnaya Énergiya 2, 278 (1957).*

6. N. Sugarman and S. Katcoff et al., Radiochemical Studies: The Fission Products, N.Y., (McGraw-Hill, N. Y., 1951) p. 371, Book I.

7. V. N. Sakharov, Atomnaya Énergiya 3, 334 (1957).*

8. K. Way and E. Wigner, Phys. Rev. 73, 1318 (1948).

9. V. N. Sakharov and A. I. Malofeev, Atomnaya Énergiya 3, 334 (1957).*

10. H. Bradt, P. Gugelot et al., Helv. phys. acta 19, 77 (1946).

* Original Russian pagination. See C. B. translation.

A NEUTRON DETECTOR WITH CONSTANT SENSITIVITY
TO NEUTRONS WITH ENERGIES FROM 0.025 to 14 Mev

P. I. Vatset, S. G. Tonapetyan, and G. A. Dorofeev

A neutron detector consisting of a boron counter and a cylindrical paraffin block in which the counter was placed is described in [1, 2]. This detector possesses a constant sensitivity to neutrons in the energy interval from a few hundred kev up to 5 Mev and a drop in sensitivity outside this interval. It is impossible to measure neutron flux sufficiently accurately using such a detector even if the neutron energy is within the limits of the range of constant sensitivity of the detector, since the calibration of the detector is usually made using standard sources (Ra-α-Be, Po-α-Be) which have a complex neutron spectrum, which ranges to energies above 11 Mev.

The sensitivity of a similar detector depends not only on the configuration and dimensions of the paraffin block, the role of which was explained in [1], but also on the dimensions of the boron counter and its position in the paraffin block. We somewhat modified the construction of the detector and investigated its sensitivity to neutrons of various energies for different modes of placement of the boron counter in the paraffin block. A

drawing of the neutron detector is shown in Fig. 1. The configuration and dimensions of the paraffin block were taken from [1]. The diameter of the boron counter was increased to 30 cm.

The counter was filled to a pressure of 140 mm Hg with enriched BF_3 (70% B^{10}), with a plateau 300 wide at a working voltage of 1700v.

The increase in the diameter of the boron counter led to a relative increase in its sensitivity to fast neutrons. One can explain this qualitatively in the following manner. On encountering the paraffin block, the neutrons are slowed to thermal energies. At the front part of the paraffin block, where the apertures are located, thermal neutrons are formed mainly at the expense of slow neutrons, while at a greater depth, they are formed at the expense of fast neutrons. The diffusion length of thermal neutrons in paraffin is of the order of 2-3 cm. The "effective diameter" of the paraffin cylinder, from which the thermal neutrons are likely to strike the boron counter because of the presence of the apertures, is greater at

Fig. 1. Diagram of the neutron detector.

679

Fig. 3. Sensitivity of the boron counter as a function of neutron energy for various positions of the counter in the paraffin block.
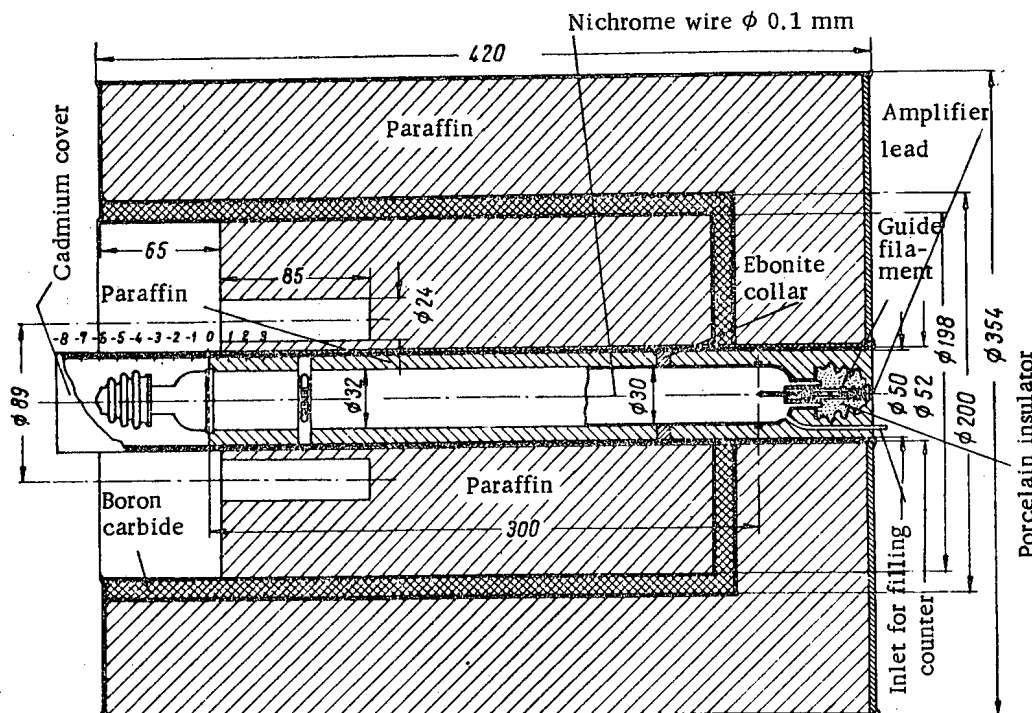

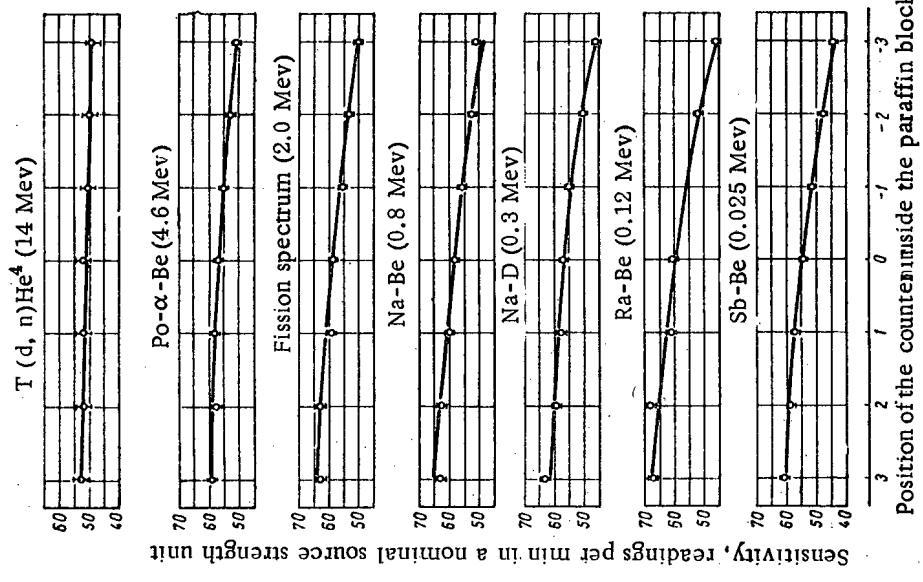Fig. 2. Sensitivity of the boron counter as a function of its placement inside the paraffin block, for various neutron energies.

the front part of the block than at the rear part.

The relative increase in the "effective diameter" due to an increase in the diameter of the boron counter is greater for that portion of the detector where this diameter is smaller; i.e., for fast neutrons, which also increases the detector's relative sensitivity to fast neutrons.

The study of the sensitivity of the detector to neutrons of various energies, was carried out under conditions of good geometry. The background from scattered neutrons was at most 6%. A 1 Curie Sb^{124} gamma source located at a distance of 20 cm along the axis of the detector did not bring about any significant change in its sensitivity to neutrons. The strength of the standard source of neutrons was known to within an accuracy of ±3%. Relative measurements of the strength of Sb-Be, Ra-Be, Na-D, Na-Be, Po-α-Be neutron sources, and of a source whose spectrum approximated that of fission neutrons, were made in accordance with a method described in [3] with an error of at most ± 1.5%.

The flux of 14 Mev neutrons from the $T(d,n) He^4$ reaction was determined by using the α-particle yield.

The position of the boron counter relative to the front face of the paraffin block was checked by the use of marks made every 10 mm on an aluminum tube 50 mm in diameter in which the boron counter was placed. The space between the counter and the aluminum tube (see Fig. 1) was filled with paraffin to the 0 mark, coinciding with the origin of the sensitive region of the counter.

It is clear from Fig. 2 that the sensitivity of the detector falls when the boron counter is shifted inside the paraffin block. This is explained by the fact that when the beginning of the counting volume of the counter approaches the front face of the paraffin block, the portion of the thermal neutrons escaping from the block which are intercepted by the counter decreases; upon further shifting, the start of the counting volume of the counter is buried in the paraffin and moves away from the neutron field, determined by the distribution of thermal neutrons in the front layers of the paraffin block. It is clear that the lower the energy of the incident neutrons, the stronger this effect is manifested. The absolute drop in detector sensitivity is 14 Mev neutrons is explained by the small diameter of the working portion of the paraffin block.

The dependence of neutron energy on the sensitivity of the boron counter is depicted in Fig. 3 for various positions in the paraffin block. The results of the measurements show that in position 3 the detector possesses practically constant sensitivity for neutrons with energies from 0.8 to 14 Mev. For the interval from 0.025 to 14 Mev the best approximation to a constant sensitivity was obtained in position 1. In this case, the sensitivity of the neutron detector in the 0.025-5 Mev interval was constant within the experimental error of the measurement (± 3%) and drops by 11% for neutron energies of 14 Mev.

In conclusion, the authors consider it their duty to express their gratitude to K. D. Sinel'nikov, A. K. Val'ter, I. V. Kurchatov, and I. N. Golovin for their interest in the present study and their assistance rendered during the progress of the work. The authors also thank T. I. Lyashenko and L. Ya. Kolesnikov for taking part in various phases of the work.

LITERATURE CITED

1. A. Hanson and J. McKibben, Phys. Rev. 72, 673 (1947).
2. R. Nobles, R. Day et al., Rev. Sci. Instr. 25, 334 (1954).
3. B. G. Erozolimskii and P. E. Spivak, Atomnaya Energiya 2, 327 (1927).*

* Original Russian pagination. See C. B. translation.

ALL-UNION SYMPOSIUM ON RADIOCHEMISTRY

V. N. Shchebetovskii

A symposium devoted to the study of the state of trace amounts of radioelements in solution met in Leningrad, March 3-5, 1959. Over two hundred representatives from various scientific research institutions of Moscow, Leningrad, Kiev, Novosibirsk, Tbilisi, Gor'kii were in attendance; 28 reports and papers, which elicited considerable interest and a lively discussion, were heard.

The symposium reviewed the research carried out by Soviet radiochemists on the state of radioelements in solution, and outlined the pathways pointing to the ultimate solution of that problem. In a report by I. E. Starik entitled, "Contribution to the problem of the molecular state of trace quantities of radioelements in solution," it was noted that most of the attention in studies on the state of radioelements in solution has been centered on the ion-dispersed colloid and pseudocolloid forms, while the molecular form has hardly been studied at all. The method of adsorption on hydrophobic non-ion-exchange surfaces (ftoroplast-4 [Kel-F], paraffin)in combination with studies of the effect of different salts on adsorption behavior, aided in the successful discovery of the existence of a molecular form of zirconium, polonium, americium, promethium found in trace concentrations in solutions of different composition.

Several reports (I. E. Starik, N. I. Ampelogova, F. L. Ginzburg, L. I. Il'menkova, I. A. Skul'skii, L. D. Sheidina) dealt with the study of the state of ultralow concentrations of radioelements in solutions. By employing a variety of techniques (adsorption and desorption, ultrafiltration, centrifugation, electrophoresis, deposition on metals) the authors determined the pH regions in which the radioelements are found in ionic, colloidal, or pseudocolloidal forms. It was found that zirconium exists in the ion-dispersed state up to pH = 1.5, americum up to pH = 5, protactinum up to pH = 3. Zirconium passes over into the form of a true colloid at pH = 4, americium at pH = 9, protactinium at pH = 5. The state of polonium over a wide range of pH values (1-14) was also determined.

M. N. Yakovleva and M. A. Shurshalina suggested the use of the dialysis technique in studying the state of the uranium carrier in natural waters. A positive feature of this method is its simplicity, and the possibility and feasibility of employing it under field conditions.

Several reports dealt with research into the state of radioelements in solution, where ion exchange techniques were applied. The method of relative absorption curves was used by V. I. Paramonova and E. F. Latyshev in their studies of complexing of tetravalent ruthenium with chlorine ions. The existence of four forms of ruthenium:

$$[Ru(OH)_2]^{2+}, [Ru(OH)_2Cl_2]^0, [Ru(OH)_2Cl_4]^{2-}, [RuCl_6]^{2-}$$
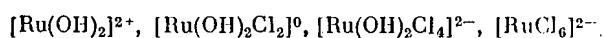
was detected in the 1 N HCl-1 N HClO$_4$ system, depending on the concentration of hydrochloric acid. A report delivered by K. B. Zaborenko, A. V. Zaval'skaya, and V. V. Fomin, touched on the question of ion-exchange determinations of the composition and of the instability constants of complex cerium oxalates. The existence of the $[CeC_2O_4]^+$ ion, whose formation constant is $1.1 \cdot 10^4$ at an ionic strength of 1, was detected. By using the ion-exchange method combined with solubility determinations, A. I. Moskvin discovered that complex formation of plutonium and americium with anions of oxalic, phosphoric, and ethylenediaminetetraacetic acids proceeds stepwise with the relationship between the discrete forms of the complex ions behaving as a function of the concentration of the chelating ligand. It was found that the complexing power of several plutonium ions falls off in the order of increase in their ionic potential.

A. M. Trofimov and L. N. Stepanova proposed a new method for determining the amount of charge on ions of radioelements in solution, using ion exchange resins having different swelling properties. The method was used for investigating the dependence of the amount of charge of zirconium in nitric acid solution on the acidity of the latter; it was demonstrated that use of the proposed method also aided in monitoring the progress of the polymerization process of ions of the radioelement in solution. N. V. Vysokoostrovskaya, A. M. Trofimov, and B. N. Nikol'skii, with the aid of the ion-exchange and potentiometric techniques, proved the absence of any appreciable chelation between potassium and ethylenediaminetetraacetic acid.

Determinations of the state of the compound to be extracted, in the organic phase, had notable value in investigations of the extraction process. It was shown that the degree of hydration of $UO_2(NO_3)^-$ in several ethers and esters falls off in the transition from the first members of a given homologic series to the later members; addition of benzene and chloroform involves lowering of the degree of hydration (V. M. Vdovenko, E. A. Smirnova). The degree of hydration of nitric acid in dibutyl diethylene glycol ether proved to be 1.72 (V. M. Vdovenko, N. F. Alekseeva, and the degree of solvation, found by the dilution technique, was 1 (V. M. Vdovenko, A. S. Krivokhatskii).

A. K. Lavrukhina reported that determinations of the dependence of the partition coefficient between the organic and aqueous phases on the concentration of the elements made it possible to establish the state of a substance in solution and to find the range of concentrations over which complexing, polymerization, or dis-

sociation of the compounds to be extracted occurs. In investigating the aniline extraction of sexavalent tungsten from hydrochloride media, V. I. Kuznetsov and P. D. Titov discovered a sharp increase in the partition coefficient when molybdenum or vanadium was added to the solution. The observed coextraction phenomenon is explained by the authors as the formation of mixed isopolyanions and may serve usefully in studies of the state of the substance in dilute solutions.

A separate panel session was devoted to the study of the state of hot atoms, and to several related questions in radiation chemistry. A. N. Nesmeyanov reported on the displacement of hydrogen in benzene by recoil atoms P^{32}, As^{76}, Sb^{124}, demonstrating the fact that the formation of phenyl-derivatives may proceed along the line of "epithermal" reactions. B. G. Dzantiev reported on reactions between recoil atoms, which were products of the nuclear reactions $Li^6(n, \alpha)$ T and $N^{14}(n, p)$ C^{14}, in a medium of cyclanes. It was established in the experiments that together with a trace of the original compound, tagged reaction products originating in destruction and condensation reactions were also obtained. The chemical utilization factor of the hot atoms reached 30-40% for tritium, 60-80% for carbon. P. I. Artyukhin, who studied the effect of NO_3^- and H^+ ions on the rate of re-

duction of sexavalent plutonium in response to spontaneous α emission, voiced the proposition that the reduction occurs on account of the hydrogen peroxide and nitrous acid forming as a result of the radiation effects.

The first-ranking importance of research on the state of radioelements in solution for modern theory and practice was acknowledged in the course of a broad discussion. All of the methods used at the present time in research on this problem were subjected to critical evaluation. The participants taking the floor addressed themselves to the need for a more rigorously grounded thermodynamic approach, and the simultaneous utilization of several methods for an unambiguous resolution of the problem of the state in which each element exists. Note was taken of the importance of further study on the molecular form of radioelements in solutions, and on the need to search out new techniques for detecting them. The desirability of correlating the results obtained with trace quantities and bulk quantities of a substance by the use of the same method was underscored. The need for more intense development of research work on the study of the forms in which hot atoms are found in solution, was noted. Hopes were also expressed for closer cooperation in research in the fields of the chemistry of hot atoms and of radiation chemistry.

SCIENTIFIC CONFERENCE OF THE MOSCOW ENGINEERING AND PHYSICS INSTITUTE (MIFI)

G. A. Tyagunov

The annual scientific conference of the Moscow Engineering and Physics Institute (MIFI) was convened from April 17 to May 15, 1959. In addition to the staff and workers at MIFI, over 600 persons from more than 100 different institute and research institutions and bodies were in attendance; 148 reports were heard at the two plenary sessions and in the panels of the eighteenth section.

At the plenary sessions, primary attention was centered on the reports delivered by M. K. Romanovskii, N. G. Basov, and A. I. Leipunskii. Romanovskii reported on the development of thermonuclear research and gave a general review of the methods and results obtained on various thermonuclear-fusion experimental devices. Basov told of the physical fundamentals of masers (molecular oscillators) and maser amplifiers; of several engineering principles and design details of these devices; and of the feasibility of employing them under conditions where the signal-to-noise ratio must be increased hundreds of times during amplification, where frequencies must be generated at constant values, and where narrow bandwidth requirements are stringent. Leipunskii presented a report on the development of fast reactors. Experiments performed under his guidance showed the full technical

feasibility of building a fast neutron reactor using natural uranium as fuel, and functioning as a breeder for nuclear fuel. At the present time, a prototype nuclear reactor of that type is being planned.

Of the eleven reports read out at panel sessions of the section on theoretical physics, particular interest was focused on three reports. I. Ya. Pomeranchuk reported on the theory of peripheral collisions between mesons and nucleons. Low-energy nucleon scattering (at energies down to 30-40 Mev) takes place by interactions associated with meson exchange. The reporter demonstrated that by using Green's function it is possible to describe the interaction of the nucleons by the exchange of a single meson and to study the dependence of the interaction cross sections on the energy of the nucleons and their orbital moments. In a report entitled "Superfluidity and the moments of inertia of nuclei," A. B. Migdal, made an attempt to shed light on several nuclear effects observed, in particular, the moments of inertia of nuclei, for which purpose the basic tenets of the new theory of superfluidity were applied to nuclear matter. A. S. Kompaneets, in a report bearing the title "A strong electromagnetic-gravitational wave," considered electromag-

683

netic and gravitational fields in a vacuum jointly, and demonstrated that the appearance of discontinuous solutions is possible.

At the panels of the section on experimental physics, over 19 reports were delivered, among which there were, worthy of special note, one by V. I. Gol'danskii, "On the levels of intrashell excitation of nuclei and ways of achieving it," a paper by O. L. Rozental' and L. A. Prokhorova, "Analysis of possible experiments on measuring the 'dimensions' of μ mesons," two papers by V. I. Dianov-'Jokov, "The spectrum of liquid and crystalline oxygen under pressure," and "A facility for measuring absorption curves" (the first of these deals with investigations of the behavior of oxygen in the liquid and crystalline states at pressures of 8-10 thousand atmos), and a report by V. K. Lyapidevskii and O. V. Glamazdina, "On new applications for the diffusion chamber."

In the panel session on electrophysical facilities, the interest of those attending was stimulated by reports delivered by A. V. Shal'nov (on the variational characteristics of the linear accelerator, the wide-bandwidth properties of iris-loaded waveguide, parametric curves for attenuation calculations) in which a method for the design of traveling-wave linear electron accelerators, conferring excellent engineering performance characteristics on the associated planned equipment, is considered. Two new theories on electron capture in the betatron mode of acceleration were propounded in reports by P. A. Ryzin and A. B. Minervin, and another by A. I. Zaboev.

A report by E. G. Pyatnov showed the possibility of neglecting insignificant nonlinear dependencies of the accelerator parameters on the wavelength of the rf oscillator, when switching the accelerator to other wavelengths (over the 9 to 11 cm wavelength region). The output beam constants then vary by 3-4% over the bandwidth in question. A report by S. P. Lomnev and G. A. Tyagunov provided a detailed analysis of magnetic focusing conditions in a linear electron accelerator, and proposed a beam focusing method where the beam is directed along the axis of a scalloped magnetic field.

Other reports of interest were one on the 3 Mev lineac in use at MIFI (O. A. Val'dner, P. A. Dmitrovskii, D. M. Zorin, and Yu. V. Mizin), and one on research into electron flow in the magnetic system of the elutron, a gamma spectroscope using recoil electrons with the scattering fields taken into account (V. V. Kuznetskii, O. A. Val'dner, V. V. Kotov, and V. N. Chesnokov).

Seven reports devoted to scintillation counters and gamma dosimeters, as well as gamma spectrometers, and a report on delayed-coincidence circuits for measuring time intervals of the order of $10^{-8} - 10^{-9}$ sec, were heard at the panel session of the section on the physics of shielding.

Reports on studies made on liquid heat-transfer agents were given at the panel sessions of the power engineering and physics section. A report delivered by O. A.

Kraev outlined a new pulse technique for measuring the thermal conductivity of liquids. Experiments performed by the author displayed good agreement with the theory which the author proposed earlier as the basis for the technique. In a report entitled "Heat rejection to the Na-K eutectic flowing in an annular clearance," (authors: E. M. Khabakhpashev, Yu. M. Il'in, and D. A. Chirov) provided information on the development of a fuel element made from a bundle of thin rods, with simultaneous temperature sensing. The experiments conducted by the authors provided confirmation for the theoretically predicted rules governing this case. A similar paper by V. I. Petrovichev describing work with mercury provided the same results over a wide range of Peclet numbers.

Reports heard at the panel session of the electronics section were devoted to the study of transistorized circuitry and properties thereof. The greatest impact was made by N. M. Roizin's paper: "Features of the junction transistor operation in pulsed circuits ("pulse dissipation," "recombination effect" , parameter variation) in which the author successfully provided a theoretical explanation of all of the observed effects.

In the section on computers, papers on digital computers excited particular interest in the audience. Among the reports meriting special mention were "The methods for design and calculation of pulse transformers in circuits with semiconductor components," by O. S. Poturaev, and "A method for evaluating the characteristics of magnetic recording of pulses," by Ya. A. Khetagurov, and "A system of components for a general-purpose digital computer," by B. I. Kal'nin.

In the section on automation and remote control, attention was focused on a report by V. S. Malov, "Multiple-channel monitoring of process control data," another by P. I. Popov, "Analysis of several automatic startup systems for power and power supply facilities," and one by Yu. I. Topchiev, "Methods of analysis of the control parameters of nuclear reactors in stepwise and linear patterns of variation in reactivity."

The remaining reports were devoted to a study of automatic control components and subassemblies, while one of the papers dealt with an investigation of the possibility of enhancing the sensitivity of the microwave spectroscope.

At the panel sessions of the section on metallurgy and metallography, a considerable portion of the papers presented, dealt with questions of obtaining pure and alloyed metals, and the study of their properties. In addition, some of the reports considered the use of autoradiography techniques in the study of metals. Of particular note are the papers submitted by G. A. Leont'ev and A. I. Evstyukhin, "Study of the iodide method of niobium refining, and the properties of the metal obtained thereby," one by P. L. Gruzin and G. G. Ryabova, "Study of microdistribution of elements (carbon, tungsten, iron, etc.) in zirconium and its alloys, using the autoradiography technique," by G. B. Fedorov, "Deter-

684

mination of the heats of sublimation of zirconium and nickel, using the radioactive tracer technique;" and by G. B. Fedorov and A. N. Semenikhin, "Determination

of the diffusion coefficients of chromium, nickel, and iron in nickelchrome steels."

The proceedings of the conference will be published in symposia under the auspices of the MIFL

ATOMS FOR PEACE
V. F. Kalinin
(From the Exposition of the Achievements of the Soviet Union
in the Fields of Science, Engineering, and Culture)

The "Atoms For Peace" section of the Soviet exposition at New York occupied one of the most prominent spots in the exhibit. The section showed (by means of operating models, mock-ups, lighted panels)how the Soviet Union is employing atomic energy to peaceful ends.

The exposition opens on a huge panel lettered "ATOMS FOR PEACE." The first section is devoted to the techniques used in accelerating elementary particles, and to the work of the Joint Institute for Nuclear Studies. From the very opening days of the exposition, a large mock-up of the 10 Bev accelerator (Fig. 1) attracted the attention of visitors. Many of them were curious as to whether the machine was actually in operation, and were very surprised to find out that it is one of the most powerful accelerators in operation in the entire world, and that it surpasses the American cosmotron accelerators.

The work of the Joint Institute for Nuclear Studies is shown on the exhibit stand. A large variety of photographs are on display, and a newsreel is shown continuously. Visitors display interest in the scale models of the 680 Mev accelerator and the mass-produced cyclotrons and electrostatic generators, which have been delivered by the Soviet Union to other countries in keeping with its policy of collaboration and aid enabling them to set up their own atomic science research centers.

The following section of the exhibit is devoted to thermonuclear-controlled fusion research in which, as acknowledged by the Americans, Soviet scientists occupy one of the leading places. There is a scale model ($\frac{1}{2}$ natural size) of the "Alpha" facility, a large toroidal chamber. A text read off continuously by a mechanical stand attendant assists visitors to the exhibit in orienting themselves as to the function of the devices whose mo-

dels are on display, including the "OGRA" facility, the giant magnet trap.

In the section dealing with nuclear power, scale models are on display and information is given (by the mechanical speaker) of a large-scale industrial experiment now being carried out in the USSR for selecting the most economically competitive nuclear electric power station type. This section has on view models of several power stations and reactors (Figs. 2, 3). The scale models are made in such a way that the operation of the nuclear-power generating stations will become clear to everyone, even the observer with little pertinent knowledge: miniature master-slave manipulators simulating the charging and discharging of fuel elements are operated by remote control, and water circulates through the coolant pipes. A large display panel reminds the visitor that the first line (100 Mw) of a large nuclear electric power station of 600 Mw full rating was started up in September 1958, in the USSR.

The section on isotopes occupies a large area. Dozens of instruments and arrangements, show how Soviet engineers are using isotopes in industry.

The "ATOMS FOR PEACE" section ends with an exhibit of the atomic-powered icebreaker "Lenin," modeled to scale (Fig. 4), and a mock-up in natural size of the reactor installed in the vessel (see Fig. 3). The details of the icebreaker are explained by light bulb panels and an automatic speaker.

On the whole, the exhibits on display in the "ATOMS FOR PEACE" section, provide a striking and convincing picture of the broad scope of applications of nuclear power in the Soviet Union.

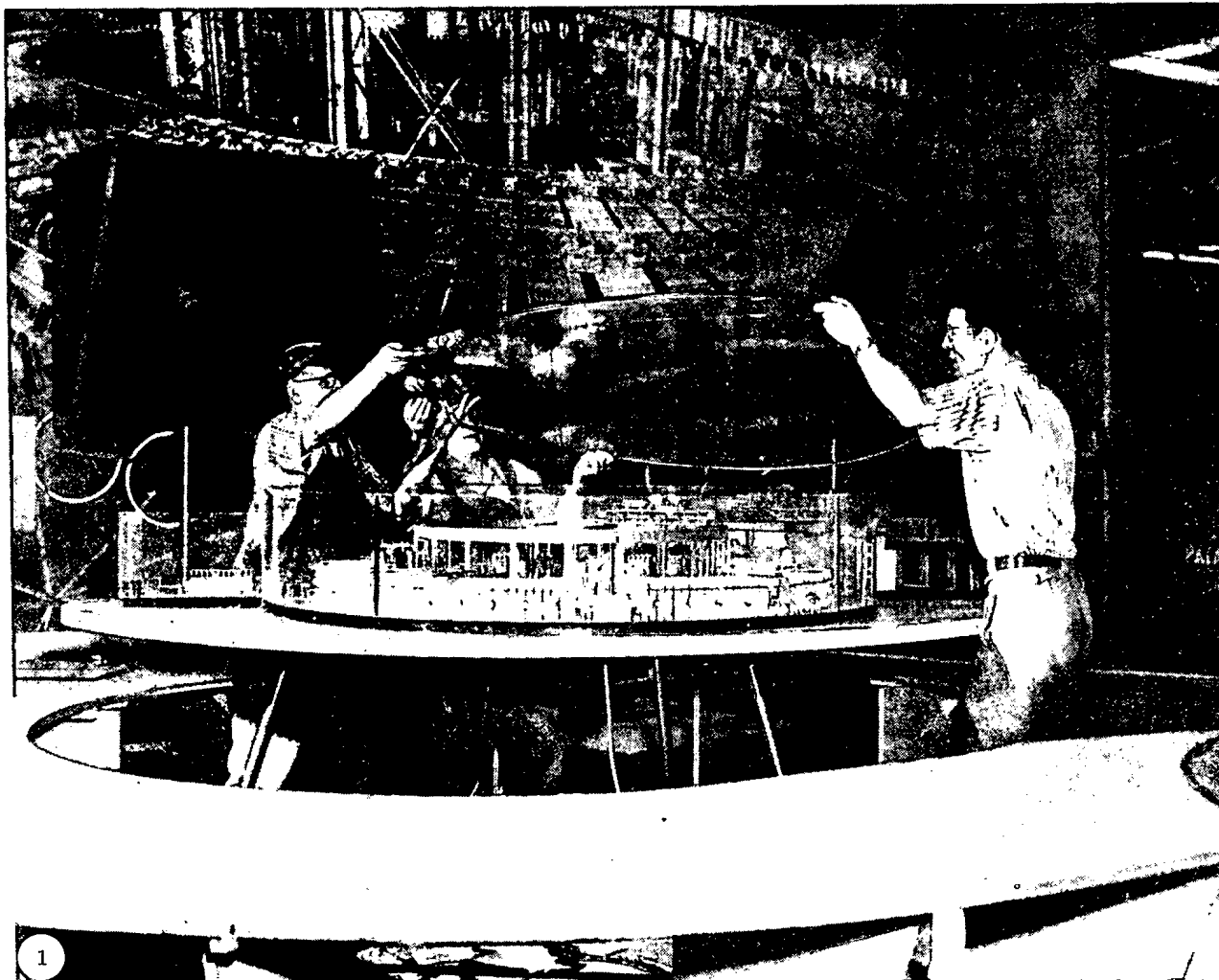Fig. 1. Installation of scale model of the 10 Bev proton synchrotron.

Fig. 2. Installation of a model of a nuclear electric power generating station.

Fig. 3. At the scale models of the turbine hall of the nuclear electric power station (on the right), and the reactor of the a- tomic icebreaker "Lenin" (background).

Fig. 4. The first visitors see the installed scale model of the atomic icebreaker "Lenin."

686

687

MAGNETIC MOMENT OF THE μ MESON

Detection of the anisotropy in electron emission in the decay of μ mesons made possible the exact measurement of the magnetic moment of μ mesons. The simplest elementary particle, the μ meson is the only one of the unstable particles which does not experience strong interactions with other particles. Dirac's equation predicts a value of 2 for the g factor of a μ meson of spin $\frac{1}{2}$. When account is taken of corrections for radiation, we arrive at a value

$$g = 2\left(1 + \frac{\alpha}{2\pi} + 0.75\frac{\alpha^2}{\pi^2} + \ldots\right) = 2 \cdot 1.00116,$$

where α is the fine-structure constant [1]. The deviation of the experimental value of the spectroscopic g factor of the μ meson from the predicted value would indicate the incorrect introduction of radiation correctives and, as a consequence, the inadequacy of quantum electrodynamics when applied to the μ meson. The first measurements recorded [2-4] lacked the necessary precision to support such a comparison.

The so-called "stroboscopic" method for determining the μ meson [5] was developed recently. In this method, a μ meson polarized along its direction of motion is brought to rest in a target to which is applied a magnetic field H, perpendicular to the direction of spin of the μ meson. This magnetic field causes the spin of the μ meson to precess. The number of decay electrons emitted in a given direction is determined from the formula

$$\exp\left(-t/\tau\right)\left(1 + a\cos\omega_H t\right),$$

where α is the asymmetry factor of the decay electrons, τ is the mean life of a μ meson; ω_H is the frequency of precession of the spin of a μ meson.

To determine the precessional frequency of the spin of a μ meson, we use the formula

$$\omega_H = geH/2m_\mu c,$$

where e is the charge of an electron; m_μ is the mass of a μ meson; c is the speed of light.

In an experiment completed recently at Columbia University (USA) [6], the stroboscopic method was employed, yielding a value of the g factor of the μ meson which exceeded the predicted theoretical value. The experimental arrangement may be seen in the diagram above. A beam of μ^+ mesons is passed through a series of counters, graphite and copper filters, and a fast counter, and is stopped in a target placed inside the gap between the magnet pieces. The entering μ meson is identified by the coincidences $123\overline{4}$, which open the gate for $2 \cdot 10^{-7}$ sec for a μ-meson pulse, and $6 \cdot 10^{-6}$ sec for a decay-electron pulse. The decay electron when forward scat-

tered is determined by the coincidences $\overline{1}345$, and when back-scattered, by the coincidence $23\overline{1}4$ (the bar above the number of the counter denotes an anticoincidence).
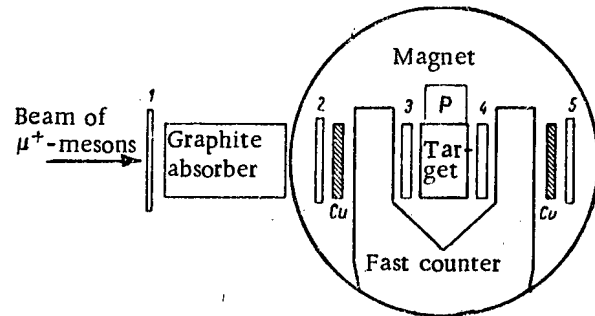
Diagram of experimental arrangement for determining the g-factor of a μ-meson (numerical figures denote scintillation counter units), with P as the specimen for measuring nuclear magnetic resonance effects.

The precessional frequency ω_H is measured by means of a reference oscillator having a frequency ω equal to 86.2 Mc, close to the frequency ω_H. To achieve this, the phase difference Φ between the moment of arrival of a μ meson and the moment of escape of a decay electron is measured. When ω_H is equal to ω, the phase distribution $n(\Phi)$ of the electrons is time-independent. When ω_H is not equal to ω, on the other hand, the phase distribution of electrons acquires the form $n(\Phi + \alpha)$, where $\alpha = (\omega_n - \omega)T$ (T being the time elapsed since the measurements were begun). Pulse generators operated at 85 Mc, and triggered by the fast counter, are used to record the phases of the pulses of the μ meson and decay electron. The phase of the pulses is found by observing the beats of the pulse generators with the reference oscillator. The precision achieved in the time determinations is $\pm 5 \cdot 10^{-10}$ sec. The phase difference is converted into amplitude and recorded by a kicksorter. The gate system yields pulses corresponding to a specified direction for the decay electron (forward or back emission) and a specified time T.

Measurements were performed at different values of ω close to ω_H, using three targets of aluminum, copper, and bromoform, respectively. The resonant frequency of precession of protons in the water molecule was measured on this arrangement. The result was computed in the form of the ratio of precessional frequencies of μ meson and protons. After introducing corrective terms for diamagnetism in the case of copper and aluminum, values of the ratios which showed agreement within the limits of experimental error ($\pm 0.007\%$) were found for all three targets.

688

The value of the mass of the μ meson, equal to (206.86 $\pm$ 0.11) m_e [7], where m_e is the mass of an electron, was used to compute the g factor for the μ meson. A value of 2 (1.0020 $\pm$ 0.0005), which is higher than the theoretically predicted value, was thereby derived.

Even when using the lower limit for the mass of a μ meson, based on the energy of the γ rays emitted when a μ meson jumps from one Bohr orbit to another in a mesoatom (m $_\mu \geq$ 206.78 $\pm$ 0.01), the value of the g factor so obtained is equal to or larger than 2· ·(1.00158$\pm$ 0.00005), which is at variance with the theoretical value [8].

The difference may quite possibly be a reliable indication of the fact that the μ meson has somewhat different properties from those of an electron with the mass of a μ meson.
P.K.

LITERATURE CITED

1. C. Sommerfield, Phys. Rev. 107, 328 (1957);
   A. Petermann, Helv. phys. acta 30, 407 (1957);
   H. Suura and E. Wichmann, Phys. Rev. 105, 1930 (1957).
2. R. Garwin et al., Phys. Rev. 105, 1415 (1957);
   J. Friedman and V. Telegdi, Phys. Rev. 105, 1681 (1957).
3. J. Cassels et al., Proc. Phys. Soc. 70A, 543 (1957).
4. T. Coffin et al., Phys. Rev. 109, 973 (1958).
5. R. Lundy et al., Phys. Rev. Letters 1, 38 (1958).
6. R. Garwin et al., Phys. Rev. Letters 2, 213 (1959).
7. K. Crowe, Nuovo Cimento 5, 541 (1957).
8. A. Petermann and Y. Yamaguchi, Phys. Rev. Letter 2, 359 (1959).

THE PRESENT STATE OF THE ART IN PROTON SYNCHROTRONS

At the present conjuncture, the proton synchroton is the only type of accelerator which is capable of accelerating particles to the highest energies. Facilities of this species are designed to accelerate heavy particles, i.e., protons. The advantage of the proton synchroton when compared to the synchroton is in the absence of the difficulties associated with energy losses by radiation. Radiation losses set the limit to the practically attainable energies (around 10 Bev) of electrons accelerated in electron synchrotrons. Radiation losses in proton synchrotrons would come to play a crucial role only at energies of the order of 10^4 -10^5 Bev, which is far out in front of the engineering and economical possibilities facing us at the present time in accelerator design.

Proton synchrotrons were planned from the very beginning as very-high energy facilities. It suffices to remember that the first proton synchrotrons build included the 1 Bev machine at Birmingham (England), commissioned in 1953, the 3 Bev Cosmotron and the 6.2 Bev Bevatron (USA), commissioned in 1952 and 1954, respectively, and finally the most powerful accelerator of all those presently in operation, the 10 Bev proton synchrotron [synchrophasotron] of the Joint Institute for Nuclear Studies (USSR), put into service during 1957. The building of machines of this species was the fruit of the urgent need for an intense source of high-energy particles, arising in connection with research in the domain of the physics of elementary particles, which entered into a particularly vigorous phase of development during the mid-Forties, when the discovery of the charged π meson (1947),which interacts strongly with nuclei,was made in cosmic rays.

The theoretical prerequisite underlying the feasibility of building a particle accelerator capable of bringing particles to energies of the order of the mean energy of cosmic rays (10 Bev) was the discovery, in 1944, of the principal of phase stability, by the Soviet scientist V. I. Veksler [1]. The use of this self-focusing principle, which has undergone much further development at the hands of Soviet and foreign scientists, forms the basis of the operation of proton synchrotrons, as well as, generally speaking, all resonant cyclic accelerators, no matter what the type of magnetic system used in them.

A powerful stimulus for the planning and designing of large proton synchrotrons was also furnished by the discovery in 1953, by E. Courant, M. Livingston, and H. Snyder, of the strong-focusing principle [2], which provided the possibility of reducing the cross section of the magnetic pole gap used. This made possible a great reduction in the power supplies to the magnetic system, a reduction in cross sectional dimensions and weight, and,as a consequence a reduction in the relative costs of the machines. There thus appeared the practical possibility of increasing the maximum attainable energy of accelerated protons in proton synchrotrons by a factor of about 5 to 10. This increase in the maximum energy of protons accelerated was, it is true, attained at the expense of much tighter tolerances on the configuration of the guide field and on the geometry of the magnetic system. For example, the precision specified in the mounting of the magnets in a 50-60 Bev proton synchrotron amounts to ~ 1 mm at the perimeter of an orbit of about 1.5 km.

At the present time, about 15 proton synchrotrons using weak or strong focusing arrangements are being designed or under construction in various countries around the world. The pertinent data on the largest of the proton synchrotrons in operation or under construction are given in the accompanying table [3-6].

689

The Largest Proton Synchrotons

Country	Energy, Bev	Year Commissioned	Focusing	Radius of curvature of orbit	Number of sectors	Max. value of magnetic field, kgauss	Input power, Mva	Wt. of magnet iron, 10³ t	Reserve magnet power supply system	Duration of cycle, sec	Frequency of revolution	Particle output, pulses	Size of chamber, cm²	Type of injector	Guide field frequency, Mc
In Operation															
USSR (Joint Institute for Nuclear Studies)	10	1957	weak	28	4	13	140	36	flywheels	3.3	5 per min	10^9-10^{10}	200×40	Lineac	0.19-1.45
USA (Radiation Laboratory Univ. of California)	6.2	1954	weak	15.2	4	13.8	100	9.7	flywheel	1.85	11 per min	-	112×25	9.8 Mev lineac	0.36-2.46
USA (Brookhaven National Lab.)	3	1952	weak	9.15	4	13.8	26	2	flywheel	1	12 per min	10^{10}-10^{11}	71×15	Van de Graaff accelerator	0.33-4.18
Planned and under construction															
USSR	50	-	strong	167	105+15 compensated	12	96	22	flywheels	3.8	6 per min	-	20×12	100 Mev lineac	2.6-6.1
USA (Brookhaven National Laboratory)	30	1960	strong	85.4	240	13	-	4	-	1	3 per min	-	15×6.5	50 Mev lineac	1.5-4.5
Switzerland (CERN)	25-28	1960	strong	70	100	12-14	27-32	3.4	flywheels	1	1 per 3.5 sec	$5 \cdot 10^9$	16×8	50 Mev lineac	3-10
USA (Argonne National Lab.)	12.5	1962	edge, weak	22.3	8	20	40	1.5	flywheel	1	15 per min	10^{12}	38×11	50 Mev lineac	4.2-13.3
USA (Oak Ridge National Lab.)	12	model tested '57	strong	43	32	10	0.7	1.2	Condenser	1/120	60 per sec	20 μa aver. current	13×6	cyclotron with azim. field varia.	98-115
Australia (Australian National Univ.)	10.6	research project since '53	weak	4.8	4	80	500	iron-free	homopolar generator	0.8	1 per 10 min	-	22×22	8 Mev cyclotron	1-7.5
USSR	7	-	strong	27.8	98+14 compensated	9.5	-	2.7	flywheels	1.5	12 per min	-	11×8	4 Mev lineac	0.65-8.5
Brit. (Retherford High-Ener.Lab.)	7	1961	weak	18.8	8	14	100	7	flywheels	0.7	25-30 per min	10^{12}	91×23	Mev lineac	1.4-8.02
USA (Princeton University)	3	1960	weak	9.15	16	13.8	3	0.35	Condenser	0.025	20 per sec	0.08 μa aver. current	25.4×5.7	3 Mev Van de Graaff accelerator	2.5-30

The largest of the projects in this group of accelerators is the Soviet 50-60 Bev proton synchroton project. A particular striking feature of the plan for this machine is the absence of the so-called "critical" energy characteristic of all conventional strong-focusing accelerators. In accelerator practice, this term is taken to mean that value of the energy of the accelerated particles at which the self-focusing operation breaks down: the stable phase becomes unstable, and conversely. The transition through the critical energy is fraught with large losses in particle energy, and imposes additional and prohibitively stringent specification on the rf system of the strong-focusing proton synchrotron. This unpleasant bug was circumvented in the 50-60 Bev accelerator project by introducing 15 compensating magnets with fields of reversed sign into the magnetic system.

A project for a 7 Bev proton synchrotron, which will serve as a model for the 50-60 Bev machine, also envisages compensation of the "critical" energy.

It should be noted that some weak-focusing proton synchrotrons, such as the 12 Bev Argonne machine and the 3 Bev Princeton machine, for example, were entered well into the planning stage even after the appearance and elaboration of the strong-focusing principle. The reason for this "reversion" to weak-focusing practice was the existence of appreciable defects inherent in strong-focusing accelerators. Those bugs included, primarily, difficulties encountered in injecting protons into the vacuum chamber of the strong-focusing accelerator, since the injection must be completed in less than a single revolution. This results in a reduction in the intensity of the accelerated beam of particles, since it imposes requirements which are difficult to fulfill on the proton beam to be injected, added to the requirements for rather high energies (from one to several tens of mega-electron-volts) and requirements for monoenergetic particles (ranging from several tenths to several hundredths of a percent). In those cases where a high order of intensity took priority in the specifications, the weak-focusing proton synchrotron was therefore the preferred type. Several flaws remained, nevertheless, in the magnetic system of weak-focusing machines.

Now, e.g., the Argonne proton synchrotron is an accelerator with a zero-gradient guide magnetic field. Particles are focused in this field by skewing the edges of the eight sectors by approximately 11° with respect to the orbit. The functioning of the sectors with edges skewed is similar to the behavior of magnetic lenses with fringe focusing, such as used in mass spectrometers. The use of fringe focusing makes it possible to avert the saturation effects which tend to narrow the effective region of the magnetic pole gap. This provides those responsible for carrying out the project with the possibility of employing very powerful magnetic fields (of the order of 20 kilogauss) and of greatly reducing the weight of the magnet assembly. The effective frequency of the betatron oscillations (0.75-0.875 oscillations per revolution) in the Argonne 12.5 Bev proton synchrotron is roughly the same as in conventional weak-focusing systems. Another peculiarity of this accelerator is the use of extremely high injection energies (of the order of 50 Mev), which makes it possible to reduce the size of the equipment, to reduce the power supplies to the magnetic system, and to narrow down the interval over which the frequency of the accelerating field varies. All of those improvements, in the opinion of the authors of the project, provide an opportunity for obtaining an accelerated beam intensity of $\sim 10^{12}$ protons per pulse.

The same problem in increasing the intensity of the proton beam (up to 0.1 μa) was resolved in the Princeton project for a weak-focusing 3 Bev proton synchrotron by a choice of more rigid tolerances on various injection parameters, by guiding magnetic-field parameters, and by increasing the pulse repetition rate.

Projects for proton synchrotrons now in the planning stage were iniated for the most part in the period from 1948 to 1955. New projects are not forthcoming, as best as can be judged from a survey of the literature on the subject. This allows us to infer that there will be a slowing up in the tempo of development of proton synchrotrons, apparently due to the large capital expenditures involved in building them as well as to the beginnings of research in the last two years on new types of accelerators incorporating fixed magnetic fields enabling sharp increases in intensity, and the development of new energy storage systems for performing experiments involving colliding beams of particles. Owing to the fact, that the energy of colliding beams coincides with the energies of the beams in the center of mass system, the use of such systems is equivalent to the use of a conventional accelerator with a fixed target having particle energies $2(E/E_0)$ times larger than the energy of either of the colliding beams (E_0 here denotes the rest energy of the particle). For example, the collision of two beams at 10 Bev energy would make it possible to observe the same reactions as would be obtained in using a conventional accelerator capable of reaching 200 Bev.

Further progress in the field of the development of proton synchrotrons, will, therefore, apparently proceed along the line of improving the design and increasing the mean intensity of the accelerated particles, with a certain slowing down of the tempos of growth in peak energies.

LITERATURE CITED

1. V. I. Veksler, Doklady Akad. Nauk SSSR 43, 346 (1944); 44, 393 (1944).
2. E. Courant, M. Livingston, and H. Snyder, Phys. Rev. 88, 1190 (1952).
3. V. V. Vladimirskii, E. G. Komar et al., Atomnaya Energiya No. 4, 31 (1956).*
4. Phys. Today 7, 23 (1954).
5. Proceedings of the CERN Symposium 1, 323, 529 (1956).
6. P. Bowler, Nuclear Eng. 4, 157 (1959).

*Original Russian pagination. See C. B. translation.

BRIEF COMMUNICATIONS

USSR. A 24-liter propane bubble chamber with $55 \times 28 \times 14$ cm^3 of the volume accessible to photo-graphic recording, designed for work in a fixed time-invariant magnetic field, has been developed at the Joint Institute for Nuclear Studies. Water, separated from the propane by means of bellows, is used as pressure transmission agent. The illumination used in the bubble chamber is placed at right angles to the axis of photographs. The bottom of the chamber is covered with dark glass to secure a dark background.

USSR. In the Nuclear Physics Research Institute attached to the Moscow State University, work has been completed on devising a dual-crystal Compton-type gamma spectrometer with no collimation of the bundle of gammas, which makes it possible to sharply increase the aperture (by 100-1000 times) without loss of resolution. Both of the crystals (the analyzing and the control crystals) in the arrangement are brought together as close as possible, and the gamma source to be investigated is positioned between them. To eliminate any background due to cascading gamma quanta or annihilation gammas, measurement of the spectrum is repeated a second time (the repeat run using a lead plate positioned between the source and the control cyrstal). The resolution of the Compton peaks is slightly less sharp (by 15-20%) than the resolution achieved for photopeaks of the same energies.

The instrument was designed for the analysis of low-intensity gamma-emitting preparations, and for searching out and studying weak gamma lines in radioactive isotopes at gamma-quanta energies in excess of 0.5 Mev.

USSR. A simple-design pulse-height integrator, capable of summing the amplitudes of a train of pulses arriving sequentially and of determining the mean value of the amplitudes when the duty factor of the recording channel is not too large, has been developed at the Nuclear Physics Research Institute of Moscow State University. The instrument is based on the transformation of the signal to be recorded into a packet of pulses, such that the number of pulses N in the train is uniquely and completely specified by the amplitude of the input signal V_a. Summing over the number of pulses in the pulse trains at the output of the pulse-height converter circuit is executed by a scaling circuit having a scaling factor of 10^3 and a resolving time of $5 \cdot 10^{-5}$ sec. With a rather simple 10-channel time analyzer performing the function of discriminating with respect to pulse train duration (with the aid of delay lines in the form of 10 one-shot multivibrator flipflops excited in series), and parallel photorecording of each pulse of the neon scale indicating lamps, the instrument is capable of simultan-

eously recording the pulse-height distribution and of determining the mean amplitude of the pulses recorded. The instrument was employed to make a record of the mean magnitude of infrequent pulses (~ 10 min^{-1}) arriving from an ionization chamber, in measurements of the mean ionizing power of cosmic radiation.

USSR. V. G. Chaikov has studied the possibility of devising thermostable halide counters. He demonstrated that the variation in the characteristics of halide counters in response to a temperature rise comes about as a result of evaporation of products of the interaction of the halide with the structural materials of the counter, within the working volume of the counter. Careful preliminary removal of those reaction products, succeeds in increasing the thermostability of the counters to the level of 170-200°C.

IAEA. The regularly scheduled session of the Council of directors of the Agency met in Vienna, April 7-18, 1959. The Council approved plans for contracts with the Soviet Union, the USA, and Great Britain on the delivery of nuclear materials to the Agency. The contracts stipulate the basic conditions, under which nuclear materials will be transferred to the Agency, or to member nations of the Agency, when so indicated. It is stated in the contracts with the Soviet Union, USA, and Great Britain that nuclear materials turned over to the Agency by the said nations will remain within the borders of the nations contracted to deliver them until the delivery order is received from the Agency.

The Soviet Union agreed, as a first step towards the realization of the IAEA statutes in life, to place at the disposal of the Agency 50 kg of U^{235} of any desired concentration (up to 20% U^{235} content) in the form of metallic uranium, chemical compounds, or in the form of manufactured fuel elements. The price of the uranium, will be set at the level of the minimum prices on the world market effective at the time of delivery. The draft of the contract stipulates that the government of the USSR expresses its readiness to produce, now or in the future, fissile and other special materials needed by the Agency for its activity on behalf of the peaceful utilization of atomic energy.

The Council of directors of IAEA adopted a resolution on other important questions relating to the activity of the Agency in rendering technical assistance to underdeveloped countries in the area of the peaceful uses of atomic energy. In particular, it was decided to study the question of setting up one or several isotope centers for the training of specialists, for the Arab countries, the other countries of Africa, and for countries in the Middle East.

The Council of directors adopted a decision to send two missions to the Latin American countries for the purpose of rendering technical assistance to several countries in that region in developing their national programs on the utilization of atomic energy for peaceful purposes.

IAEA. A conference of experts from several nations, devoted to the elaboration of a set of international rules governing the transportation of radioactive isotopes, met in April, 1959. The rules drawn up will be sent out to member nations of the Agency for discussion and corrections.

Hungary. The country's first research reactor, 2 Mw (th), was loaded to criticality on March 25, 1959, in Budapest. The reactor is a water-cooled water-moderated (VVR-S) type operating on oxide enriched to 10% uranium. The reactor was built with the aid of the Soviet Union.

Rumania. The Institute of Nuclear Physics of the Rumanian Academy of Sciences (Bucharest) now has at its disposal an atomic reactor and a cyclotron. The Institute is engaged in the training of specialist personnel for work in the field of the utilization of atomic energy for peaceful purposes. Radioactive isotopes produced by the Institute are meeting with application on a broad scale in the petroleum industry (in radioactive logging of oil wells), in medicine, biology, chemistry, metallurgy, and other branches of the economy.

Yugoslavia. An agreement was signed between Yugoslavia and Poland, covering 1959 and 1960, on collaboration in the cause of the use of atomic energy for peaceful purposes.

USSR. On July 21, 1959, the BR-5 fast nuclear reactor was brought up to design power rating (5000 kw).

The successful startup of the reactor marked the completion of a great stage in the work of Soviet scientists and engineers aimed at the development of the problem of nuclear power reactors based on fast neutrons.

While only the uranium isotope U^{235}, 1/140 being natural uranium, may be used as nuclear fuel in thermal power reactors, fast power reactors are capable of also using uranium-238, and thorium, to produce electric power. This is of the most far-reaching significance for the national economy, since the raw materials base of the nuclear power industry will then be expanded without bound, and the basis will be laid for the economically competitive operation of nuclear-fueled electric power generating stations.

The erection of the BR-5 was preceded by the building of several physical fast-neutron reactors ranging from 10 w to 200 kw power output, which provided the opportunity for a broad variety of physics experiments.

The BR-5 reactor, which is the most powerful fast reactor in operation at the present time, is designed to provide the solution to a number of engineering and technological problems associated with the building of industrial-scale nuclear electric power stations.

The BR-5 reactor has a core of plutonium cooled by fused sodium at an exit temperature of 450°C. The reactor is equipped with a large number of ancillary experimental devices installed for the performance of the necessary research experiments in chemical processes and nuclear physics.

NEW LITERATURE

Books, Symposia, Periodicals Recently

Published

Proceedings of the Second International Conference on the Peaceful Uses of Atomic Energy. Reports by Soviet Scientists. Vol. 3. Nuclear Fuel and Reactor Metals. Edit. by Academician A. A. Bochvar, Academician A. P. Vinogradov, Corresponding Member of the Academy of Sciences of the USSR, V. S. Emel'yanov, Doctor in Engineering Sciences A. P. Zefirov. Moscow. Atomizdat, 1959. 670 pages, 30 rubles, 30 kopeks.

The book comprises a collection of the reports dealing with problems of the geology and mineralogy of uranium deposits, methods of exploration of those occurrences, and some questions in the primary processing of uranium ores and of the raw materials for reactor materials, and, finally, problems in the metallurgy of nuclear fuel.

The results of the study of the geological structure of uraniferous provinces, the patterns discernible in the arrangement of ore-bearing beds within those provinces, zones of oxidation of uranium occurrences, paragenetic associations of uranium minerals, new data on uranium minerals, structural conditions of the formation of uranium occurrences, and other related topics are reported on in these papers.

A description is provided of the different methods resorted to in the beneficiation of uranium ores, and examples of ore processing are given. Several papers describe the properties of uranium, plutonium, and the alloys they form with other elements. Problems in the stability of uranium and relating to structural materials subjected to irradiation are discussed.

Papers are presented on the technology and processing of zirconium and beryllium, and on the manufacture of chemically pure calcium, strontium, and other metals.

Proceedings of the Second International Conference on the Peaceful Uses of Atomic Energy. Reports by Soviet Scientists. Vol. 4. The Chemistry of Radioelements and Radiative Transmutations. Edited by Academician A. P. Vinogradov. Moscow, Atomizdat, 1959. 336 pages, 15 rubles, 70 kopeks.

The reports, collected in a book, are devoted to various aspects of chemical problems and problems arising in connection with the use of atomic energy for peaceful purposes.

Methods used in the purification and extraction of plutonium and uranium from spent reactor fuel, the separation of fission-fragment and rare-earth elements; the chemistry of complex compounds formed with thorium, uranium, americium, and modern techniques in the study of the state of radioactive substances in solution are dis-

cussed in the papers; the laws governing sorption of radioelements by soils and minerals, which is of major importance for the solution of problems concerning the burial of radioactive wastes, are also discussed.

Problems involved in the effects of radiations on matter are dealt with in reports on the radiation chemistry of aqueous solutions, on the effect of ionizing radiations on raw rubber, vulcanized rubber, etc.

Proceedings of the Second International Conference on the Peaceful Uses of Atomic Energy. Reports by Soviet Scientists. Vol. 5. Radiation Biology and Radiation Medicine. Edited by Corresponding Member of the Academy of Medical Sciences A. V. Lebedinskii. Moscow, Atomizdat, 1959, 430 pages, 21 rubles, 80 kopeks.

This volume contains reports devoted to problems concerning the effects of ionizing radiations on the human organism and on animal organisms, and questions involving the use of radioactive isotopes in biological research, medicine, and agriculture. A. V. Kozlova, in her report, presents a review of the applications of radioactive isotopes and ionizing radiations in the USSR in the therapy and diagnostics of various diseases.

The volume presents a broad choice of original materials reflecting the latest research efforts, particularly materials on the use of the tritium isotope in radiobiological research, on the mechanism of the action of radiations on the nervous system, on primary processes occurring in tissues when bombarded by radiation emissions; also materials on radiation genetics and on the effect of small, local radiation doses.

Proceedings of the Second International Conference on the Peaceful Uses of Atomic Energy. Reports by Soviet Scientists. Vol. 6. The Production and Use of Isotopes. Edited by Academician G. V. Kudryumov and Corresponding Member of the Academy of Sciences of the USSR I. I. Novikov. Moscow, Atomizdat, 1959, 388 pages, 18 rubles, 90 kopeks.

This volume presents a collection of reports illuminating several up-to-date techniques employed in the separation of light isotopes and isotopes in the middle section of the periodic table (the method of low-temperature distillation in the separation of hydrogen isotopes, the electromagnetic separation method, the thermal diffusion method).

The bulk of the papers included in this volume serve to illustrate the varied range of approaches in the use of isotopes for the solution of concrete technical problems and problems arising in the operation of the national economy. In particular, a review article by A. V. Topchiev and collaborators describes various methods of isotope applications (such as tagged atoms or radiation sources) in chemistry, metallurgy, instrument de-

sign, agriculture, and in other branches of science and technology.

The book also includes papers devoted to problems of dosimetry, radiometry, and health physics in handling radioactive isotopes.

A. K. Lavrukhina, Successes in Nuclear Chemistry. Moscow, published by Academy of Sciences of the USSR, 1959, 144 pages, 2 rubles, 20 kopeks.

This book, one of the popular science series put out by the Academy of Sciences Press, sheds light on the fundamental historic moments of nuclear chemistry: the general characteristics of nuclear processes are described and an account is given of radiometric techniques, of the methods of α β and γ spectroscopy, scintillation methods, the technique of thick-layered photoemulsions, etc.; nuclear reactions taking place under the effects of particles of various energies, as well as reactions occurring in the interior of the sun, the stars, and interstellar space are considered; a short description is provided of the most important fields of application for the various nuclear reactions, and a number of questions involving the systematics of radioactive and stable isotopes are discussed.

A. A. Zhukhovitskii, Labeled Atoms. Moscow, Voenizdat, 1959. 114 pages, 1 ruble, 75 kopeks.

This book, part of the "Popular Science Library" series, describes succinctly some examples of the utilization of radioactive isotopes—"labeled atoms"—in biology, medicine, chemistry, physics, military science, metallurgy, geology, etc. The examples cited serve to illustrate the exceptional variety and fertility of the labeled-atom technique. The book is written for a broad audience of readers acquainted with chemistry, physics, and mathematics at the secondary-school level.

Max Planck—Festschrift—1958. (Max Planck 1958 Jubilee edition). Published (in German) by B. Kockel, Leipzig, W. Macke, Dresden, and A. Papapetrou, Berlin. 413 pages.

This book, published on the hundredth anniversary of the birth of the renowned German physicist Max Planck, contains the following articles solicited from well-known Soviet and foreign scientists: G. Falkenhagen: Max Planck's works on electrolysis and the further development of the topic; H. Honl and K. Westphal: The further development of Kirchhoff's diffraction theory into a rigorous theory; V. Rubinovich: A graphic conceptual picture of electric quadrupole and magnetic dipole radiations; H. Alfvén: The pulse spectrum of cosmic radiation; V. A. Ambartsumyan: On the stellar association Perseis-1; S. Chandrasekhar: The thermodynamics of thermal instability in fluids; L. Infeld: Variational principles in relativistic dynamics; M. Sasaki: Relativistic gases; S. Moller: On the energy of an open system in the general theory of relativity; J. Weissenhoff: The classical-relativistic treatment of the problem of spin; N. Bohr: Philosophical problems in quantum

mechanics; V. Fok: On the interpretation of quantum mechanics; L. Broil'*: Max Planck's great discovery, the mysterious constant h; L. Rosenfeld: Max Planck and the foundation of the statistical nature of entropy; K. Nowobatcki: Statistics of gas and radiation; P. Caldirola and A. Loinger: The development of the ergodic approximation in statistical mechanics; P. Gombás: On the theory of matter subjected to high pressures; P. Zwicky: Destruction of matter of nuclear density and nuclear "building blocks;" J. Supek: Differential equations of the electrical conductivity of metal at low temperatures; H. Fröhlich: Phenomenological theory of energy losses of fast particles in solids; O. Scherzer: Interference of incoherently scattered electrons; D. Blokhinstev: On the structure of elementary particles; E. Caianiello: Some remarks on the ultraviolet catastrophe; A. Sokolov: The longitudinal polarization of Dirac particles and the conservation of parity; O. Heber: Some physical and mathematical properties of nonlocalized fields; P. Dirac: Equation of electron waves in a Riemann space; N. Schönberg: Quantum theory and geometry; D. Ivanenko: A note on a nonlinear theory of matter; J. Destuches: On the quantizing concept; L. Pauling: Quantum theory and chemistry; L. Janósi: Planck's philosophical views on physics.

E. Funfer and H. Neuert, Zahlrohre und Szintillationszähler [Gas-discharge Tubes and Scintillation Counters], Karlsruhe, Verlag C. Braun, 1959, 356 pages.

Second, fully-revised edition. The monograph deals with an analysis of the mechanism involved in the operation of proportional counters, G-M counters, scintillation counters, crystal counters, and their applications in measuring and detecting ionizing radiations.

Bulletin of the International Atomic Energy Agency, Vol. 1, No. 1 (1959). The first issue of the Bulletin of the International Atomic Energy Agency has appeared in print. The bulletin is schedule for quarterly printing in Russian, English, French, and Spanish. It will contain materials treating of the activities of IAEA. The first issue contains the following articles and correspondence: "Aid rendered to Brazil, Pakistan, and Thailand;" "The use of radioisotopes in medical diagnostics;" "The reactor construction schedule in Japan;" "Contracts for scientific research work on radiation;" "Research work / at the University of Vienna for the benefit of IAEA;" "Distribution of fallout products and decay products in the biosphere;" "Safe handling of radioisotopes;" "Production of heavy water at Aswan;" "Legal protection against radiation hazards;" "Extraction of uranium from phosphates in the United Arab Republic;" "Program of the International Atomic Energy Agency on the exchange and training of nuclear specialists;" "Centers for training specialists in Latin America;" a list of conferences, exhibits, and courses on the training of specialists in atomic energy applications.

* Transliteration of Russian — Publisher's note.

695

Nukleonika (Poland) vol. IV, No. 2 (1959). This issue contains the following articles: B. Buras and J. O'Connor,"Interaction of neutrons and phonons in solids;" T Adamski,"Chemical engineering problems in uranium processing in the light of the Second Geneva Conference;" S. Minc,"Some chemical problems discussed at the Second Geneva Conference;" E. Minczewski,"Problems in analytical chemistry in the light of the Second Geneva Conference;" S. Andrzejewski,"Perspectives of the development of nuclear power in the light of the Second Geneva Conference;" W. Ostrowski,"The major problems in the biological sciences and medicine as seen at the Second Geneva Conference;" J. Hurwic,"Health physics problems in personnel clothing in the light of the Second Geneva Conference;" Z. Jaworowski,"Measurements of radioactive fallout in the Hornsund fjord (Spitsbergen);" A. Kazimirski,"Design, manufacturing technology, and features of BF_3 -loaded proportional counters."

Correspondence: A 144-channel neutron time-of-flight analyzer, designed for operation with a mechanical chopper. Reviews. Chronicle. Bibliography.

ARTICLES FROM THE JAPANESE PERIODICALS

GENSHIRYOKU HATSUDEN

(ATOMIC POWER ENGINEERING)

AND

GENSHIRYOKU KŌGYŌ*

(ATOMIC INDUSTRY)

Genshiryoku Hatsuden, vol. 2 (1958)

No. 1.

Okada, Makoto: Thermonuclear fusion research. Review article (6-13); Suzuki, Eiji: Control system of a nuclear reactor and studies of the dynamic behavior of the control system in a pilot plant.

No. 2.

Aochi, Tetsuo: Regeneration of nuclear fuel by solvent extraction (9-16); Goto, Niki et al.: Fuel burnup calculation in uranium-graphite reactors, using digital computer facilities (39-54); Kanbara, Toyoji et al.: Brief description of the Japanese research reactor (JRR-1) and its performance characteristics (55-63); Aoki, Tomo: Maximum permissible radiation dosage for humans and problems in shielding against radioactive radiations (66-69).

No. 3.

Aochi, Tetsuo: Regeneration of nuclear fuel by solvent extraction IL (5-12); Hasegawa, M.: Iron and steel parts used in nuclear reactors (13-25). Homoto, Shoji: Nuclear reactor calculations in fast power excursions (26-32).

Genshiryoku Kōgyō, vol. 4 (1958).

No. 1.

Sato, Kagasei: Large-size pressurized-water reactor for ships displacing 80,000 tons with 40,000 hp propulsion engines (6-12); Makimura, Ryutaro: Small pressurized-water reactor for vessels displacing 40,000 tons with 20,000 hp propulsion engines; Shigemitsu, Tomomichi: Radioactive radiations and plastics. IL (36-37); Mada, Junpei: Experimental research on nuclear chain reactors in Japan (41-44); Takeyoshi, In: A high-efficiency reactor burning liquid-metal fuel. Its design features, examples of reactor calculations, and operation. II. (51-55); Somiya, Naoyuki: Characteristics and applications of isotopes. (62-65).

No. 3.

Taroyoshi, Seki: Uranium production by magnesium reduction (9-13); Fukai, Yuzo: One-group calculations of the neutron flux distribution in a boiling-water reactor (22-27); Kozeki, Koji: Deposits of radioactive minerals in Japan, and perspectives of exploitation (28-32); Sata, Toshi: Use of Radioisotopes in Studies of the mechanism in metal wear (47-51).

No. 5.

Sugimoto, Asao: Construction of Japan's first experimental nuclear reactor, the JRR-3 (4-6); Asaoka, Takumi: Core design in the nuclear reactor JRR-3 (7-13); Sasakura, Hiroshi: Shielding design in the nuclear reactor JRR-3 (14-20); Ishikawa, Hiroshi: Control-rod design in the nuclear reactor JRR-3 (21-24); Shimai, Sumu: The basic planning of the nuclear reactor JRR-3 (31-36); Shimai, Sumu: Instrumentation and equipment planning for the experimental nuclear reactor. Idemura, Hideo: Design of the water and gas flow systems in the nuclear reactor JRR-3 (39-42); Haraswa, Susumu: Control system design in the nuclear reactor JRR-3 (43-49); Henmi Fumihiko: Design of fuel charge-discharge equipment in the nuclear reactor JRR-3 (54-58); Kawasaki, Masayuki: Nuclear fuel for the JRR-3 reactor, and pertinent reactor data (65-71).

No. 6.

Uchida, Taijiro and Goto, Tetsuo: Structure of the pinch effect in nuclear fusion reactions (18-21); Kitao, Kazuo: Relaxation time and deceleration of charged particles in ionized gases (22-26); Yamamoto, Takamitsu: Facility for achieving a controlled fusion reaction by means of annular currents, and its use. (27-31).

No. 8.

Sakai, Toshinouji: Economic performance of atomic-powered ships, and perspectives in their use. L (8-13);

*Translator's note: genshiryoku = atomic energy; hatsuden = electric power generation; kōgyō = industry

Ono, Kazuro: Studies on special nuclear reactions at the Institute of Physics of Tokyo University (21-25); Yamamoto, K.: Safety practices in handling radioactive isotopes (26-32); Kaide, Takeshiro: Radioactivity and crude rubber. I. (36-37).

No. 9.

Shiga, Shiro: Means for atomic radiation shielding, and their uses (23-29); Completion of the building project of the nuclear reactor JRR-3 (38-40).

No. 10.

Yokota, Yoshisuke: Experimental production and use of glass for gamma-ray shielding (14-19); Ishihara, Toyohiko et al.: Automatic monitoring stations for the detection of radioactivity (26-29); Shielding glasses (67).

No. 12.

Imai, Munemaru and Oshima Hironosuke: The Hitachi Central Scientific Research Institute, named after the founder of nuclear technology in Japan (52-58).

Articles from the Periodical Literature

Yu. K. Akimov, "Recording of counting errors and omissions in scaling circuits" Pribory i Tekh. Éksp. No. 2, 113-114 (1959).

Yu. D. Arsen'ev and E. K. Averin, "On the approximate determination of the optimum cycle in dual-circuit atomic power stations," Teploénergetika No. 5, 29-33 (1959).

M. A. Baranovskii, "Use of superheated steam in nuclear electric-power stations," Izvest vyssh. ucheb. zaved. Énergetika No. 1, 33 (1959).

I. V. Batenin et al., "The effects of neutron bombardment on the fine crystalline structure of metals and alloys," Fiz. Metal i Metalloved. 7, 243-246 (1959).

N. A. Burgov et al., "Resonant scattering of gamma rays from Ni^{60}," Zhur. Éksp. i Teor. Fiz. 36, 1612-13 (1959).

A. I. Burnazyan et al., "Health and hygienic measures observed on board the atomic icebreaker 'Lenin' ", Med. radiologiya 4, 70-72 (1959).

A. A. Vorob'ev et al., "Choice of optimum transmission band in an amplifier operating in unison with an ionization chamber," Pribory i Tekh. Éksp. No. 2, 95-102 (1959).

N. N. Gratsianskii and N. A. Bogacheva, "Studies on the corrosion behavior of solid solutions of metals, using radioactive isotopes. The In—Pb system," Zhur. Fiz. Khim. 33, 677-682 (1959).

A. I. Grimm and A. L. Kartuzhanskii, "Effects of irradiation of potatoes and onions, using a radioactive cobalt source [vegetables in storage]," Symp. of scientific papers of the Leningrad inst. of commerce No. 13, 14-29 (1959).

P. L. Gruzin et al., "Investigation and monitoring of the blast-furnace process, using radioactive isotopes and radiations," Stal' No. 4, 291-297 (1959).

R. A. Demirkhanov et al., "Mass of the Pu^{239} nuclide," Zhur. Éksp. i Teor. Fiz. 36, 1595-6 (1959).

A. A. Zaitsev et al., "On the possibility of determining the potential of a plasma space by the characteristics of the noise excited in the gaseous discharge," Zhur. Éksp. i Teor. Fiz. 36, 1590-1 (1959).

D. I. Zakutinskii and O. S. Andreeva, "Toxicology of uranium compounds (survey article)," Med. radiologiya 4, 81-5 (1959).

A. M. Ivanchenko, "Enchancing the stability of operation of scintillation counters," Pribory i Tekh. Éksp. No. 2, 150-1 (1959).

V. A. Kirillin and S. A. Ulybin, "Experimental determination of specific volumes of heavy water," Teploénergetika No. 4, 67-72 (1959).

Yu. L. Klimontovich, "Energy losses of charged particles by excitation of plasma oscillations," Zhur. Éksp. i Teor. Fiz. 36, 1405-18 (1959).

B. Ya. Kogan et al., "On the simulation of nuclear power systems," Avtomatika i Telemekhanika 20, 349-54 (1959).

F. G. Krotkov, "Health problems at the Second Geneva Conference on the peaceful uses of atomic energy (September 1958)," Vestnik Akad. Med. Nauk SSSR No. 3, 55-64 (1959).

A. S. Kuz'minskii and E. V. Zhuravskaya, "Stability of vulcanized rubbers to the action of ionizing radiations," Khim. nauka i promyshlennost' 4, 69-73 (1959).

G. Ya. Lyubarskii and R. V. Polovin, "On the disintegration of unstable shock waves in magnetohydrodynamics," Zhur. Éksp. i Teor. Fiz. 36, 1272-78 (1959).

M. A. Mazing and S. L. Mandel'shtam, "On the broadening of spectral lines in a strongly ionized plasma," Zhur. Éksp. i Teor. Fiz. 36, 1329-31 (1959).

O. M. Mdivani and T. G. Gachechiladze, "On the angular distribution of neutrons in the $C^{13} (\alpha, n) O^{16}$ reaction," Zhur. Éksp. i Teor. Fiz. 36, 1591-2 (1959).

V. E. Mitsuk and M. D. Koz'minykh, "The electric field in a micorwave plasma as a function of time," Zhur. Éksp. i Teor. Fiz. 36, 1603-4 (1959).

B. Moiseev, "Automation of the processing of charged-particle track photographs in bubble chambers," Priroda No. 5, 82-84 (1959).

697

A. N. Protopopov et al., "Angular anistropy and energy data of the fission process," Zhur. Éksp. i Teor. Fiz. 36, 1608-9 (1959).

A. N. Protopopov and V. P. Éismont, "On the dependence of the degree of angular anisotropy of the fission process on the structure of the nucleus," Zhur. Éksp. i Teor. Fiz. 36, 1573-74 (1959).

D. I. Ryabchikov and E. K. Gol'braikh, "Thorium and thorium compounds, Uspekhi Khim. 28, 408-435 (1959).

B. N. Samoilov et al., "Polarization of cobalt and iron nuclei in ferrites," Zhur. Éksp. i Teor. Fiz. 36, 1366-67 (1959).

I. K. Sokolova, "Investigation of chemical systems for dosimetry (review article)," Med. radiologiya 4, 78-80 (1959).

K. N. Stepanov, "On the penetration of an electromagnetic field into a plasma," Zhur. Éksp. i Teor. Fiz. 36, 1457-60 (1959).

A. A. Titlyanova and N. A. Timofeeva, "On the mobility of cobalt, strontium, and cesium compounds in soil," Pochvovedenie No. 3, 86-91 (1959).

A. F. Fedorov, "Natural radioactivity of marine organisms," Priroda No. 4, 86-88 (1959).

Yu. A. Tsirlin, "Disperse-phase fast-neutron detectors," Zhur. Tekh. Fiz. 29, 530-538 (1959).

P. I. Chalov, "Isotope ratio of U^{234}/U^{238} in certain secondary minerals," Geokhimiya No. 2, 165-170 (1959).

L. I. Shmonin et al., "Neutron flux of the earth's crust," Geokhimiya No. 2, 105-109 (1959).

D. Aliaga-Kelly, Nuclear Power 4, 111-112 (1959).

W. Arnold, Nuclear Sci. and Eng. 5, 105-119 (1959).

L. Barbieri et al., Nuclear Sci. and Eng. 5, 105-119 (1959).

R. Bartholomew et al., Canad. J. Chem. 37, 660-663 (1959)

G. Bell, Nuclear Sci. and Eng. 4, 138-139 (1959).

E. Bernshon et al., Nucleonics 17, 112-115 (1959).

M. Bleiberg, Nuclear Sci. and Eng. 5, 78-87 (1959).

F. Boeschoten and K. Groenewolt, Physica 25, 398 (1959).

K. Boyer et al., Phys. Rev. Letters 2, 279-280 (1959).

F. Brooks, Nuclear Instr. and Methods 4, 151-163 (1959)

R. Carter, "Compatibility problems in the use of graphite in nuclear reactors," Atompraxis 5, 142-47 (1959).

W. Clarke, Nuclear Power 4, 109 (1959).

C. Clayton, Research 12, 148-154 (1959).

C. Clayton, Reasearch 12, 172-178 (1959).

L. Cohen and W. Stephens, Phys. Rev. Letters 2, 263-264 (1959).

H. Corben, Nuclear Sci. and Eng. 5, 127-131 (1959).

V. De Sabbata, Suppl. Nuovo Cimento 11, Ser. X, 225-314 (1959).

R. Enstrom, "Manufacture of tubular type fuel elements for the CP-5 reactor," Atompraxis 5, 147-54 (1959).

B. Fabre and F. Rossillon, "Melusine, the first reactor of the Grenoble nuclear research center," Industries Atomiques 3, 42-49 (1959).

R. Garvin et al., Phys. Rev. Letters 2, 213-215 (1959).

H. Gebauer, "Dependence of optimal cathode thickness of G-M counter on the atomic number of the material and on the energies of the gammas intercepted," Atomkerneregie 4, 135-38 (1959).

C. Gerard, Nuclear Power 4, 86-91 (1959).

W. Gerlach and K. Stierstadt, "Investigations of radioactive fallout and of radioactivity of the air," Atomkernenergie 4, 143-147 (1959).

E. Graul and H. Hundeshagen, "Methods and technology of analysis and synthesis of tritium-labeled substances," Atompraxis 5, 154-160 (1959).

A. L. Gray, Nuclear Power 4, 103-105 (1959).

G. Greenough, Nuclear Power 4, 92-96 (1959).

H. Griem et al., Phys. Rev. Letters 2, 281-282 (1959).

G. Keepin, Nuclear Sci. and Eng. 5, 132-136 (1959).

M. Kostin, Nuclear Instr. and Methods 4, 99-102 (1959).

W. Kuhn, "Use of elastic neutron scattering in humidity determinations," Atompraxis 5, 133-7 (1959).

R. Le Page, Nuclear Power 4, 104-107 (1959).

M. Ledinegg, "Unstable oscillations in boiling-water reactors," Atomkernenergie 4, 132-5 (1959).

H. Loos, Phys. Rev. Letters 2, 282-283 (1959).

A. Mackinney and R. Ball, Nucleonics 17, 128, 130, 132 (1959).

E. Malamud and A. Silverman, Nuclear Instr. and Methods 4, 67-78 (1959).

N. Moore and J. Huffadine, Nuclear Power 4, 86-89 (1959).

B. Moskowitz, "Experiments on the study of the dynamic behavior of homogeneous reactors with aqueous slurries," Industries Atomiques 3, 54-64 (1959).

P. Murray, Nuclear Power 4, 89-94 (1959).

R. Nathans and A. Paoletti, Phys. Rev. Letters 2, 254-256 (1959).

L. Neel and B. Delepalme, "The Grenoble nuclear research center," Industries Atomiques 3, 34-41 (1959).

Nuclear Eng. 4, 9-10 (1959).

Nuclear Power 4, 102-103 (1959).

Nuclear Power 4, 114-115 (1959).

Nucleonics 17, 100-103 (1959).

H. Palevsky et al., Phys. Rev. Letters 2, 258-259 (1959).

A. Pfau and H. Heinrich, "Combination of ring and conventional scintillation counters for rapid determinations of the specific activity of gamma-emitting isotopes. Part III," Atompraxis 5, 160-9 (1959).

T. Pickavance, Nuclear Eng. 4, 151-156 (1959).

F. Porreca, Nuovo Cimento 11, 283-286 (1959).

W. Rohsenow et al., Nucleonics 17, 150, 152, 154, 157, 158, 159, 161 (1959).

O. Runnalls, Nucleonics 17, 104-111 (1959).

M. Salesse, "Beryllium and zirconium," Industries Atomiques 3, 65-76 (1959).

K. Scharrer and Z. Heilenz, "Method for the quantitative determination of small amounts of strontium in plants and soils," Atompraxis 5, 170-2 (1959).

R. Schmidt and L. Fidrych, Nuclear Power 4, 106-108 (1959).

J. Seetzen, "Present state of the art in nuclear reactor shielding," Atomkernenergie 4, 140-2 (1959).

D. Smidt, "Auxiliary back-up control of power reactors, using enriched compensating elements," Atomkernenergie 4, 129-31 (1959).

K. Stierstadt, "Radioactivity of the atmosphere and wind direction," Atomkernenergie 4 147-50 (1959).

R. Syre et al., "Comparison of the properties of semifinished beryllium products manufactured from metal castings or sintered powder," Rev Met 56, 359-70 (1959).

J. Syrrett, Nuclear Power 4, 95-97 (1959).

J. Thie, Nuclear Sci. and Eng. 5, 75-77 (1959).

M. Thompson, Phil. Mag. 4, 139-141 (1959).

B. Toppel, Nuclear Sci. and Eng. 5, 88-98 (1959).

R. Uhrig, Nuclear Sci. and Eng. 5, 120-126 (1959).

P. Vidal, "Increase of the yield and quantities of crops by irradiation of the seeds," Industries Atomiques 3, 77-84 (1959).

G. Waechter, "Detection and dosimetry of neutrons with the BF_3 counter, "Atompraxis 5, 138-141 (1959).

H. Wilf, Nuclear Sci. and Eng. 5, 137-138 (1959).

W. Zinn, Nuclear Power 4, 109-111 (1959).

2 outstanding new Soviet journals

KINETICS AND CATALYSIS

The first authoritative journal specifically designed for those interested (directly or indirectly) in kinetics and catalysis. This journal will carry original theoretical and experimental papers on the kinetics of chemical transformations in gases; solutions and solid phases; the study of intermediate active particles (radicals, ions); combustion; the mechanism of homogeneous and heterogeneous catalysis; the scientific grounds of catalyst selection; important practical catalytic processes; the effect of substance — and heat-transfer processes on the kinetics of chemical transformations; methods of calculating and modelling contact apparatus.

Reviews summarizing recent achievements in the highly important fields of catalysis and kinetics of chemical transformations will be printed, as well as reports on the proceedings of congresses, conferences and conventions. In addition to papers originating in the Soviet Union, KINETICS AND CATALYSIS will contain research of leading scientists from abroad.

Contents of the first issue include:

Molecular Structure and Reactivity in Catalysis. A. A. Balandin

The Role of the Electron Factor in Catalysis. S. Z. Roginskii

The Principles of the Electron Theory of Catalysis on Semiconductors. F. F. Vol'kenshtein

The Use of Electron Paramagnetic Resonance in Chemistry. V. V. Voevodskii

The Study of Chain and Molecular Reactions of Intermediate Substances in Oxidation of n-Decane. Z. K. Maizus, I. P. Skibida, N. M. Émanuél' and V. N. Yakovleva

The Mechanism of Oxidative Catalysis by Metal Oxides. V. A. Roiter

The Mechanism of Hydrogen-Isotope Exchange on Platinum Films. G. K. Boreskov and A. A. Vasilevich

Nature of the Change of Heat and Activation Energy of Adsorption with Increasing Filling Up of the Surface. N. P. Keier

Catalytic Function of Metal Ions in a Homogeneous Medium. L. A. Nikolaev

Determination of Adsorption Coefficient by Kinetic Method. I. Adsorption Coefficient of Water, Ether and Ethylene on Alumina. K. V. Topchieva and B. V. Romanovskii

The Chemical Activity of Intermediate Products in Form of Hydrocarbon Surface Radicals in Heterogeneous Catalysis with Carbon Monoxide and Olefins. Ya. T. Eidus

Contact Catalytic Oxidation of Organic Compounds in the Liquid Phase on Noble Metals. 1. Oxidation of the Monophenyl Ether of Ethyleneglycol to Phenoxyacetic Acid. I. I. Ioffe, Yu. T. Nikolaev and M. S. Brodskii

Annual Subscription: $150.00

Six issues per year — approx. 1050 pages per volume

JOURNAL OF STRUCTURAL CHEMISTRY

This significant journal contains papers on all of the most important aspects of theoretical and practical structural chemistry, with an emphasis given to new physical methods and techniques. Review articles on special subjects in the field will cover published work not readily available in English.

The development of new techniques for investigating the structure of matter and the nature of the chemical bond has been no less rapid and spectacular in the USSR than in the West; the Soviet approach to the many problems of structural chemistry cannot fail to stimulate and enrich Western work in this field. Of special value to all chemists, physicists, geochemists, and biologists whose work is intimately linked with problems of the molecular structure of matter.

Contents of the first issue include:

Electron-Diffraction Investigation of the Structure of Nitric Acid and Anhydride Molecules in Vapors. P. A. Akishin, L. V. Vilkov and V. Ya. Rosolovskii

Effects of Ions on the Structure of Water. I. G. Mikhailov and Yu P. Syrnikov

Proton Relaxation in Aqueous Solutions of Diamagnetic Salts. I. Solutions of Nitrates of Group II Elements. V. M. Vdovenko and V. A. Shcherbakov

Oscillation Frequencies of Water Molecules in the First Coordination Layer of Ion in Aqueous Solutions. O. Ya. Samilov

Second Chapter of Silicate Crystallochemistry. N. V. Belov

Structure of Epididymite $NaBeSi_3O_7OH$. A New Form of Infinite Silicon—Oxygen Chain (band) $[Si_6O_{15}]$. E. A. Podedimskaya and N. V. Belov

Phases Formed in the System Chromium—Boron in the Boron-Rich Region. V. A. Épel'baum, N. G. Sevast'yanov, M. A. Gurevich and G. S. Zhdanov

Crystal Structure of the Ternary Phase in the Systems Mo(W)—Fe(CO,Ni)—Si. E. I. Gladyshevskii and Yu. B. Kyz'ma

Complex Compounds with Multiple Bonds in the Inner Sphere. G. B. Bokii

Quantitive Evaluation of the Maxima of Three-Dimensional Paterson Functions. V. V. Ilyukhin and S. V. Borisov

Application of Infrared Spectroscopy to Study of Structure of Silicates. I. Reflection Spectra of Crystalline Sodium Silicates in Region of 7.5-15μ. V. A. Florinskaya and R. S. Pechenkina

Use of Electron Paramagnetic Resonance for Investigating the Molecular Structure of Coals. N. N. Tikhomirova, I. V. Nikolaeva and V. V. Voevodskii

New Magnetic Properties of Macromolecular Compounds with Conjugated Double Bonds. L. A. Blyumenfel'd, A. A. Slinkin and A. E. Kalmanson

Annual Subscription: $80.00

Six issues per year — approx. 750 pages per volume

Publication in the USSR began with the May-June 1960 issues. Therefore, the 1960 volume will contain four issues. The first of these will be available in translation in April 1961.

EQUIPMENT FOR A MODERN LABORATORY... A NEW CONCEPT IN DESIGN

Apparatus Drawings Project (ADP)

Sponsored by the American Association of Physics Teachers and the American Institute of Physics under a grant from the National Science Foundation

ADP has been designed to present physics teachers and laboratory workers in the field with **complete** data and drawings concerning **over 30 unique and economical pieces of apparatus** developed in the physics laboratories of some of America's leading colleges and universities.

The equipment described in ADP was developed as up-to-date teaching apparatus for laboratory experiments and lecture demonstrations. The drawings make available to other departments designs for apparatus which would otherwise be difficult to obtain. The reports contained in this series document original equipment which can be duplicated in your shop — **economically** — often by your students.

AN INVALUABLE TEACHING AID!

USEFUL IN RESEARCH!

PLENUM PRESS will publish and distribute the entire series which will cover over 30 different pieces of apparatus. You will be sent 10 reports in the first mailing. Printed on flat sheets (11 x 17, one side) for working convenience, the sheets fit into a durable cardboard case for safe storage.

THE CASE WILL BE SENT TO YOU AT NO EXTRA CHARGE!

Approximately 10 reports will be sent to you each mailing until you have received the complete set. Then (and at no extra charge) you will receive a clothbound (8½ x 11) book which will contain all the material in the reports in handy reference form for your desk or library.

The series of over 30 reports, the attractive cardboard storage case, and the desk-size manual will be sent to you for the single subscription price of only $25.00.

The full-size drawings and the book are not sold separately.

The first ten reports will consist of	Developed at
1. Balmer Series Spectrum Tube	Massachusetts Institute of Technology
2. Magnetic Field of a Circular Coil	Rensselaer Polytechnic Institute
3. Air Suspension Gyroscope	Massachusetts Institute of Technology
4. Resolution of Forces Apparatus	Massachusetts Institute of Technology
5. Simple Mass Spectrometer	Swarthmore
6. Bragg Diffraction Apparatus	Rensselaer Polytechnic Institute
7. Versatile Mass Spectrometer	Dartmouth
8. Driven Linear Mechanical Oscillator	Bryn Mawr
9. Simple Kinetic Theory Demonstration	Princeton
10. Air Suspended Pucks for Momentum Experiments	Massachusetts Institute of Technology

Equipment designed at other leading universities and colleges will be included in future reports.

YOU MAY SEND FOR A SAMPLE PAGE

FOR FURTHER DETAILS, CONTACT MR. CHARLES KNOWLES

PLENUM PRESS 227 WEST 17TH STREET, NEW YORK 11, N. Y.